COMPUTER SIMULATION SYSTEM FOR BRAIN AND CRANIOFACIAL SURGERIES

Takami Yasuda

COMPUTER SIMULATION SYSTEM FOR BRAIN AND CRANIOFACIAL SURGERIES

CONTENTS

写真同士がくっつく恐れがあるため，応急処置として該当箇所に中性紙を挟みこんであります。(2006.6.19)

ACKNOWLEDGMENTS

This work was developed and implemented in the department of electronics at Mie University and in the department of information engineering at Nagoya University. Part of this work was performed in the courses of my pursuit of the MS at Mie University and Ph.D at Nagoya University.

Thanks go to my supervisor, Prof. Jun-ichiro Toriwaki, for his enthusiastic support and meaningful discussions of my studies since I was a doctoral student in Nagoya Univ.. My thanks go to Associate Prof. Shigeki Yokoi who originally gave me a chance to tackle this work when I was a senior at Mie Univ.. At lunch time, he sometimes provided insightful comments that helped me to overcome imminent problems.

I would like to thank Prof. Yasushi Miyake who taught me what the research itself should be, when I was a master course student at Mie Univ.. In this connection I would like to acknowledge the advice and support of Associate Prof. Fumitaka Kimura and Dr. Shinji Tsuruoka.

I wish to thank Associate Prof. Mutsuhisa Fujioka at Dokkyo Medical college, Associate Prof. Hideo Nakajima at Keio University Hospital and Associate Prof. Kazuhiro Katada at Fujita-gakuen University for their valuable advice on medical aspects of the system.

Both a preliminary and a revised version of this dissertation were carefully reviewed by Prof. Noboru Sugie at Nagoya Univ. and Douglas Dickson who is now a graduate student in music at Yale Univ. and one of my best friend in U.S.A..

Thanks are also to Yasuhiro Hashimoto, Yasunori Goto and Ken

Kato for their contributions to the development of the software on the system.

Their friendly companionship in the Lab helped make the work a pleasure.

The support of the Ministry of Education, Japanese Government under Grant-in-Aid for Scientific research (No.61550260, No.61790135, No.63633009, and No.63750348) is gratefully acknowledged.

Finally, my thanks go to my friends and family for encouraging me to accomplish this work.

1. INTRODUCTION

There is no way for medical science to improve it's skill without the most advanced knowledge and technology in each era. We can imagine how much people were surprised, when people could see the inside of the body by x-ray for the first time. X-ray photographs have greatly contributed to the diagnosis and therapy of diseases in the medical field. Although it is very valuable to visualize the inner part of the body without any surgical operations, X-ray images have only 2-D(dimensional) information, since they are generated on the 2-D detector plane such as a photographic film, a fluorescent screen, and an imaging plate by x-rays coming through the body.

In 1973 Hounsfield successfully developed CT(Computed Tomography) to get section images of a 3-D object like the human body[1]. Later he was awarded Nobel prize for the contribution to medical science. The CT image, which shows us a cross section of the patient body like a piece of sausage cut by a knife, has brought an epoch-making leap to the diagnosis and therapy of the present clinic. Namely, imaging spatial location or shape of the disease lesion by observing a sequence of CT images, a medical doctor can diagnose the inside of a patient's body without any surgical operations. The progress of CT machines is so rapidly, and several modalities like x-ray, positron, ultrasonic, MR(Magnetic Resonance), etc. are used for different purposes in hospital. Thanks to the good quality of the CT image by recent CT machines, we can even see very small wrinkles on the brain surface which can not be distinguished by the early ones.

G.T.Herman of the University of Pennsylvania developed a technique to reconstruct the original 3-D object from a sequence of CT images by using computer image processing[2]. His concept is, as it were, that computer may play the role of a medical doctor to imagine the 3-D shape of an object from 2-D CT images and expert knowledge in his mind. It is significant in the sense of

the objectivity and the accuracy of diagnosis that computer can generate the exact shape of the interesting region by calculation. Recently, a few CT machines, which have a function to reconstruct 3-D shapes of organs from a set of CT slices, have appeared in the market. Several researches are now being performed from various directions to use the potential information of CT images not only for diagnosis or education but also for actual clinical therapy planning. In the following of this chapter we shall describe how computer-generated images can be used in order to help medical doctors.

(1) Diagnosis support

It is effective to understand the precise location or the shape of disease lesion for proper diagnosis, if we can successfully process medical images for each purpose. At the present time, the following researches have been done.

(a) Diagnosis of brain disease

Our research group developed a new method to reconstruct the 3-D image of the objects from x-ray CT slices in order to help doctors understand the 3-D informations (location or shape) of the disease by displaying the disease lesion synthesized with other parts such as skull or ventricles[3]. Some studies for diagnosis of the brain disease are also making progress by using an MR Image, which can clearly visualize soft tissues as the brain[4,5]. They employed image processing schemes in order to extract the brain in the head MR images automatically, and displayed it by using CG(Computer Graphics). These studies would be valid especially for understanding the precise form of the brain. The multiplex hologram is one of the best way to get a real 3-D image, so that doctors can discuss the state of the disease surrounding the 3-D holographic image[6].

(b) Evaluation and diagnosis of heart

The 3-D display experiment of MRI of the heart was recently reported[7]. A study to use ultrasonic images for evaluation of the movement of the left ventricle has recently been done in order to diagnose the disease which disturbs normal movement of the heart muscle[8]. In dealing with living heart data, we must take care of the movement of the heart like expansion and shrinking during taking the image information.

(2) Medical treatment planning

It is possible for the 3-D reconstruction of CT images to be applied not only for diagnosis but also for making a plan of various clinical treatments.

(a) Planning for brain surgery

In the field of brain surgery, CT images are important to understand the inner part of the head without actual surgery, when the operation should be done very carefully. We have developed a scheme for 3-D display of skin, skull, ventricles, tumor and suture in order to make a surgical plan before the surgery[3]. Several CG techniques were adopted to realize this function, such as surface construction by triangular patches, translucent display or hidden surface removal.

(b) Planning for craniofacial surgery

It is one of the most challenging research to apply 3-D reconstructed image of x-ray CT to the planning of craniofacial surgery[9-13]. The aim of this kind of surgery is to reform congenital or acquired deformities of the skull. In the actual surgery, first, the skull is cut into small pieces of bony blocks, and then the blocks are moved to achieve desirable shape for a whole skull. Since bony region in CT image can be automatically extracted by the simple thresholding method, it is a good way to use computer for the purpose of image processing of bony area. We have developed a surgical planning system for craniofacial surgery called NUCSS (Nagoya University Craniofacial Surgical-planning System) based on requests from surgeons which has abilities to be used in actual clinic[14].

(c) Planning for orthopedic surgery

Hip joint between pelvis and femur is a suitable part of the body to display its 3-D image by computer, since the hidden part, which is the most important for diagnosis around this section and always invisible, can be seen by computer processes without any operations[15]. If a surgery can be simulated on a graphic terminal according to the scheme doctors actually do, it would be worthy to decide the most proper way of surgery before entering an operation room. Artificial femur is often implanted to patient in this kind of operation. Doctors usually select the most appropriate femur for each patient among several ready-made

ones. CT has made it possible to obtain truly 3-D structure of the inner part of the body noninvasively. This 3-D information can be applied to design custom implants which can be made by NC(Numerical Controlled) machine and would be the best one[16,17].

(3) Medical education

All technologies described above are also valid for education in medical science. Personal computer system which can display rough structure of the inner part of the human body has been developed in order to help young doctors study anatomy[18]. The less hardware costs, the more precise structures could be stored in the computer memory for education in near future.

In the following two chapters of the paper(chapter 2 and 3), we describe a computer system for brain surgical planning and diagnosis. The outline of the process in the system is introduced in chapter 2. Input images, computer and graphic terminal used here are also mentioned.

Chapter 3 explains the details of processings. The techniques for displaying surfaces from volume data consist of applying a border detection algorithm to CT images, fitting geometric primitives to the detected borders, and rendering these primitives using conventional surface-rendering algorithms. Border following is applied to the binary representation obtained using simple thresholding on each CT image in order to extract a set of contours of interest regions. Connecting the contours on adjacent slices by a set of polygonal patches, the 3-D surface can be constructed as a polyhedron covered by a mesh of polygons. Section 3.2 mentions these processes.

The CT value itself is sometimes important for diagnosis, so that three kinds of cross section images with gray tones corresponding to CT numbers are generated as discussed in section 3.3.

Several rendering techniques for assisting diagnosis and surgical planning are presented in section 3.4 and 3.5, respectively.

In section 3.6, experimental results of this system are presented. Displaying gray values(CT numbers) on any cross section with the surface image such as the skull, the ventricle and disease lesion has been proved to be effective for understanding the 3-D brain structure. Translucent or windowing display of the skull is considered to be suitable for planning surgery.

In the latter two chapters (chapters 4 and 5), we describe another computer system, called NUCSS(Nagoya University Craniofacial Surgical-planning System), which supports medical doctors to make a plan especially for craniofacial surgery. The overview of NUCSS is presented in chapter 4.

Section 4.2 and 4.3 explain how to display the skull and the face from a set of CT images. Since it is necessary to display the skull as fast as possible during the planning stage, an accelerated projection method is proposed to generate the image on a screen. Furthermore, filtering techniques are applied to improve the quality of generated images. Prediction of soft tissue alterations caused by moving bony structures is considered to be valuable not only for surgeons but also for patients. We implemented the function to roughly predict the patient's post-operative face for the first time.

Interactive manipulative techniques that allow simulating the process of surgery are developed and described in chapter 5. The functions now available are to cut, translate, rotate and reverse bony regions according to the instructions given by a surgeon.

Geometrical information concerning the degree of deformity in the shape of the skull is sometimes necessary for surgeons to make a precise surgical plan. Measurement functions implemented in our system are presented in section 5.4.

Experimental results of planning a surgery and prediction of soft tissue alterations are shown in section 5.5. Surgeons have already used this system to obtain desirable surgical plans in about 10 cases.

2. A SYSTEM FOR COMPUTER AIDED BRAIN SURGICAL PLANNING AND DIAGNOSIS - OUTLINE

2.1 INTRODUCTION

This and the following chapter present a software system for three dimensional (3-D) display of brain CT images developed to help medical doctors in interpreting CT images, in diagnosing, and in planning therapy or surgical operations[1-3]. The aim of the system is to provide facilities for planning and estimating the effects of surgical operations in the field of brain surgery. To achieve the desired ability of the system, we need to solve two major problems: how to extract 3-D information from 3-D pictures (a set of 2-D CT slices), and how to present the information to observers.

For the former problem, conventional image processing techniques are utilized such as thresholding, border following, and filtering. All of these algorithms are available as a FORTRAN subroutine library stored in our computer file[4,5]. However, since fully automated extraction of medically significant objects, such as organs or disease lesion, is still rather difficult, interactive determination of objects to be displayed are employed in the system at the present time.

The latter problem of display is solved by resorting to computer graphics techniques. Though ordinary computer graphics mainly use well-defined numerical data for display, for medical images we must deal with "raw image data" such as CT slices gathered from a living body. Therefore, special displaying methods should be developed for helping doctors to perceive the 3-D internal structure of the brain recorded on CT images. Such methods include: reslicing along an arbitrarily oriented plane, reconstruction of surfaces of soft tissues and bones (skull), shaded display of reconstructed surfaces, generation of the translucent surface, and windowing the skull surface to observe

inside the brain.

In an X-ray CT image, two different types of information are contained: morphological information represented by borders of objects or by spatial relations among several different objects, and the gray value (i.e. value of the CT number) attached to each picture element (pixel). Since both are important for medical usage, we need methods to display both of them effectively. Our solution is to display these two kinds of information simultaneously in the same picture plane by mapping related gray values onto any cross section observed in a presented picture.

2.2 OUTLINE OF SYSTEM FUNCTIONS

A system we discuss here consists of two major parts. One is to extract the region of interest such as the skull, soft tissues, or diseased parts. The other is to display these objects.

(1) Extraction

We use 2-D image processing techniques to extract each region, since the CT data consists of a 2-D image sequence. Simple thresholding and border extraction of 2-D images are used to detect skull, skin and hematoma regions in brain CT images. These regions are easily distinguished from other areas in an X-ray CT. For example, CT values of the skull are higher enough than those in other organs. Hematoma or tumors also have higher CT numbers than surrounding soft tissues, though there are some cases in which the gray values on and near disease lesion borders shade off gradually and edges are not clear, thereby extraction of regions becoming difficult. In such a case, we extract regions to be processed by an interactive procedure.

(2) Display

The general processing flow to display 3D images in this system is shown in Fig.2.1. Several approaches as follows are adopted since both a surface image and a density (CT value) image should be displayed for better understanding of the state of diseases.

Surface image: (1) Extraction of border points.
(2) Construction of a 3-D surface.
(3) Calculation of shading values on the surface.

Density image: (1) Reslicing to produce a new section plane
(2) Mapping to give the plane CT value

(3) Image data used in the experiment

Original data is a set of brain X-ray CT images consisting of parallel slices, with the resolution of 256 x 256 pixels. We reduced them to 128 x 128 pixels for the convenience of system implementation on a mini-computer. Slice interval is 5 mm and pixel size is 2 mm for 128x128 resolution.

We use the following two sets of images offered by Fujita-Gakuen University Hospital(Fig.2.2).

data 1: hematoma. The number of slices is 18. Hematoma exists in the 5th. through the 15th. of 18 slices.
data 2: tumor. The number of slices is 18. Tumor exists in the 8th. through the 10th. slice.

(4) Computer and graphic display device

64KW main memory and a raster type display GRAPHICA M-305S. The resolution of the display is 512 x 320 dots and the memory for one dot is 15 bits (5 bits are assigned to Red, Green and Blue, respectively).

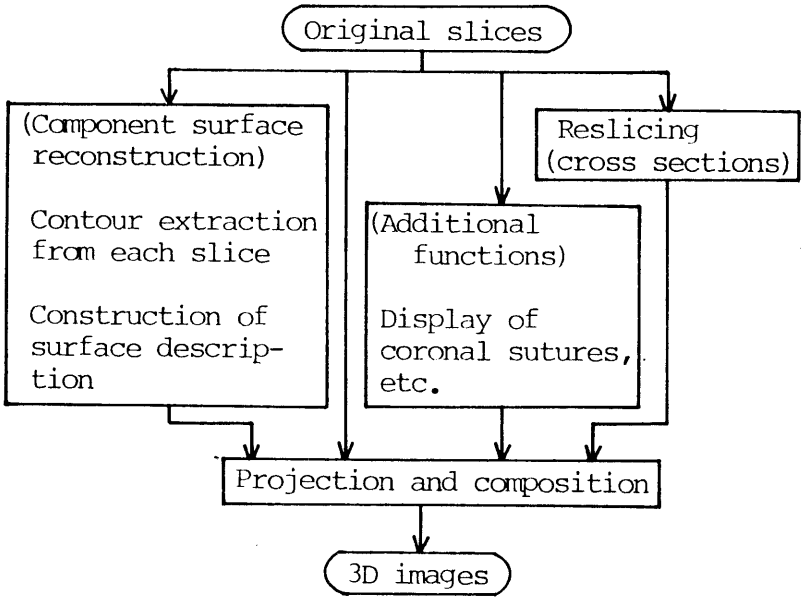

Fig.2.1 The processing flow.

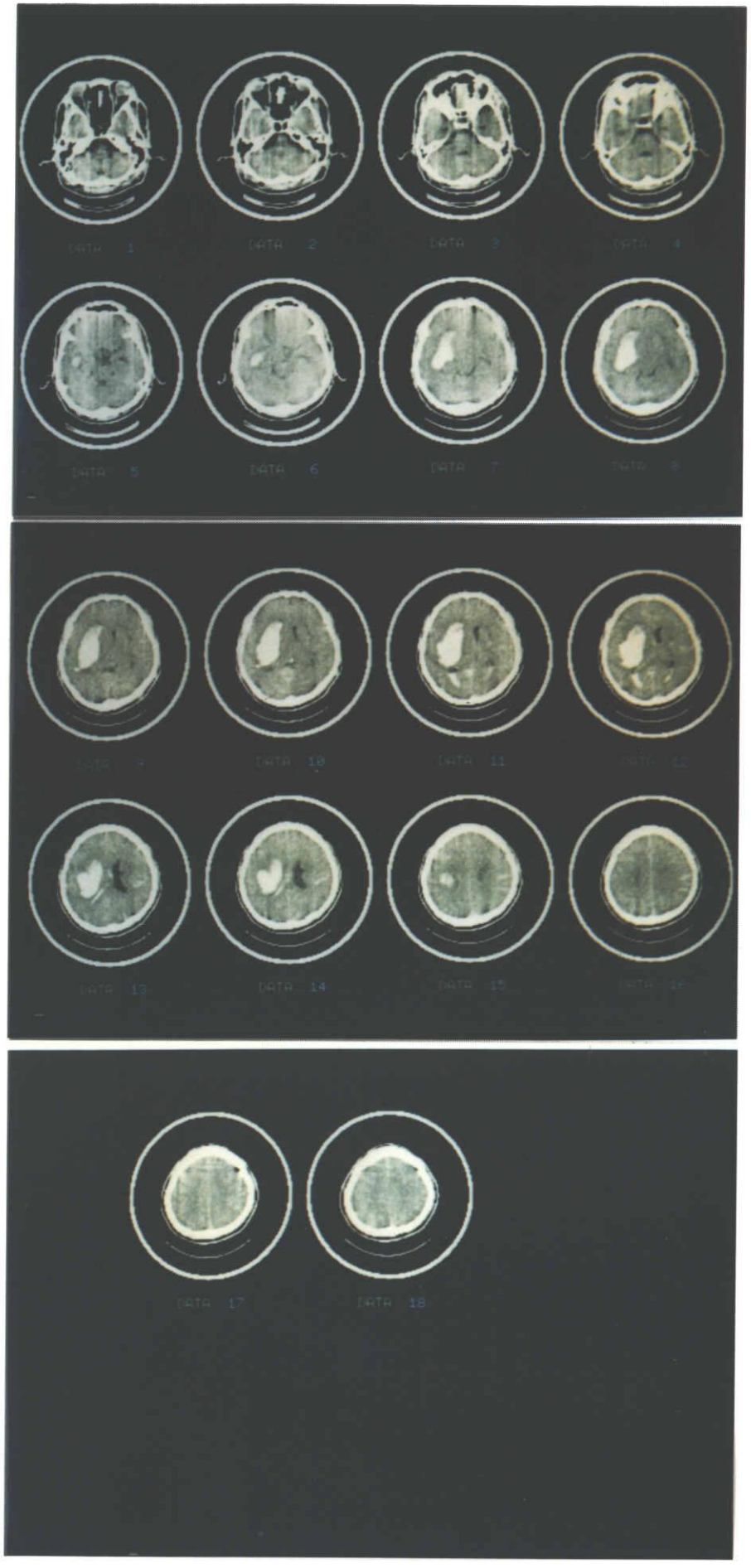

Fig.2.2(a) Original slices of data 1 (hematoma).

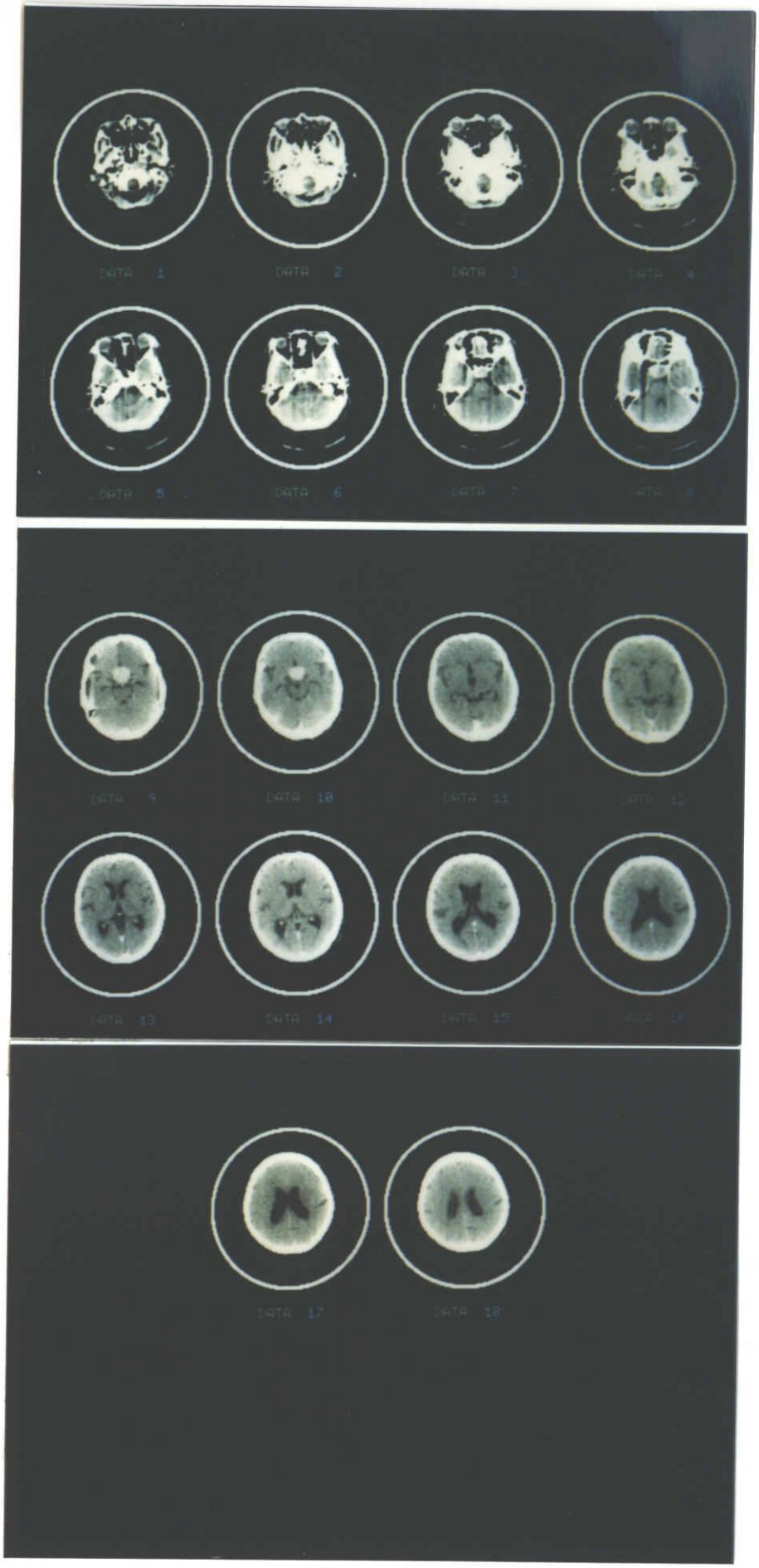

Fig.2.2(b) Original slices of data 2 (tumor).

3. IMAGE PROCESSINGS FOR BRAIN SURGICAL PLANNING AND DIAGNOSIS

3.1 INTRODUCTION

Since the brain is the most mysterious part of the human body, the surgery and the diagnosis of this organ should be prudent enough. Furthermore the brain surgery is dangerous and should not be tried many times. From this point, doctors have to diagnose the disease as precisely as possible, and make the most suitable plan for the surgery. Although images taken by CT machines can help doctors to make the strategies for medical care, it is sometimes difficult to understand the 3-D shape or the location of the disease lesion, since a CT slice itself is a 2-D image. Computer can produce 3-D images from a set of CT slices, and they would be useful for this purpose.

In this chapter we discuss the 3-D image generation schemes for diagnosis or surgical plan of brain diseases. We have developed a simple method to reconstruct 3-D surface images from a set of borders. The borders of the interesting region such as the skull are extracted automatically from original CT slices by using image processing techniques. We also prepare an interactive extraction scheme for the organ whose border is difficult to specify automatically. In order to represent the border points, we developed "Cylindrical Coordinate Expression" described in 3.2.2. The 3-D surface can be reconstructed by connecting neighbor triangular patches made by three border points. We developed another method to make 3-D object from 2-D borders called "Border Sweeping" presented in 3.2.2 for the object whose shape is too complex to make triangular patches.

Original CT values are important for the diagnosis, too. We developed a function to generate new cross sections with CT values from original slices. These sections are a vertical plane, a tilted plane and a vertical cylinder. We can observe the distribution of CT values on these cross sections with sur-

face images such as the skull. The details of the schemes to generate each cross section and a complex of different sections and surfaces are explained in 3.3. and 3.4, respectively.

Section 3.5 describes a simple simulation system for brain surgeries. In the actual surgeries, small part of the skull is opened to observe the inside of the brain. The most important thing is to find the best position of the skull to be removed. The region to be opened should be decided by considering the two major factors: dangerous area inside the brain and the relative location of the disease to the skull. In order to help doctors to decide the best part of the skull to be cut, we prepared a skull display function which has a "window" from which we can observe the disease lesion. It might be also useful to offer doctors translucent display of the skull surface, since they could observe a disease lesion from any viewing directions through the translucent skull.

3.2 3D SURFACE CONSTRUCTION

The process to generate surface images of 3-D objects includes 3D surface construction and rendering. The construction process is divided into two steps: border extraction and surface reconstruction.

3.2.1 Border extraction

3-D objects are reconstructed from a set of 2-D CT slices. Therefore borders of the region in question should be extracted on each cross section, i.e. each slice. In this stage, we can use either of automatic extraction and interactive one, if necessary.

(1) Automatic extraction: The CT number of bone regions is much higher than that of other tissues. Therefore the skull border can be extracted automatically by simple thresholding and border following procedures using ordinary 2-D picture processing techniques once the adequate threshold value is found by a suitable threshold selection algorithm[1].

(2) Interactive extraction: The above method cannot be applied to a region whose CT number is not distinguished clearly from that of neighboring tissues. Use of the anatomical knowledge of medical doctors is necessary to extract such regions exactly. At present, interactive procedure is used in our system. Viewing each CT slice on a graphic terminal display, doctors input the borders of the object in question by using the hair cursor. We use this mode for ventricles, tumors and hematoma lesions in a brain CT image.

3.2.2 Surface reconstruction

In this section, the procedure to reconstruct a 3-D surface from a set of borders extracted by the above method is shown. Two methods are employed for this purpose according to the features of each tissue.

(1) Cylindrical coordinate expressions and triangulation: This procedure consists of two steps: transformation to the Cylindrical Coordinate System(CCS) representation from the Euclidean coordinate system expression, and generation of triangular patches as surface elements. CCS is suitable for representing 3-D surfaces of relatively compact objects like the upper part of the skull. After converting to CCS representation, the surface is reconstructed by triangular facets made by connecting three neighboring sample points in CCS. Details of these processes are described as follows:

Suppose that all slices are situated in z direction as in Fig.3.1, before the transformation process. For each slice at $z=z_j(j=1,2,\cdots)$, sampling points are extracted at suitable sampling angles defined by the interval angle θ, center point and starting angle position. The sampling angle θ on one slice corresponds to that on the other slices. Distance r_{ij} from the center point to a border point at the angle θ_i on the slice $z=z_j$ is stored in a memory called r-buffer. If no border point is detected at some sampling angle, we use linear interpolation of neighboring r values to get a hypothetical r value for that sampling angle. The r-buffer value is reentered when a new border point is found if the new point is farther from the center than

was the point previously stored in the r-buffer. After this process is completed for all sampling angles on all slices, the r-buffer contains information on the utmost border location. The r-buffer is described as $r_{ij} = f(\theta_i, z_j)$, where i is the number of the sampling angle coordinate and j is the slice number in CCS (Fig.3.1).

The surface reconstruction process is accomplished by connecting the neighboring points in the r-buffer as follows. For any given point (r_{ij}, θ_i, z_j) in the r-buffer, two triangular tiles can be defined whose vertices are $[(r_{ij}, \theta_i, z_j), (r_{i+1,j}, \theta_{i+1}, z_j), (r_{i,j+1}, \theta_i, z_{j+1})]$ and $[(r_{i,j+1}, \theta_i, z_{j+1}), (r_{i+1,j}, \theta_{i+1}, z_j), (r_{i+1,j+1}, \theta_{i+1}, z_{j+1})]$. The whole surface is constructed by a set of these tiny tiles (Fig.3.2).

The r-buffer method is one of the easiest ways to reconstruct 3-D surfaces since the exact correspondence of sampling angles for all slices makes it a simple problem. On the other hand, objects that this method can be applied to are limited to the ones that have relatively simple shapes. For more complicated objects, the triangulation algorithm developed by Christiansen and Sederberg [2] is employed. In this method, there is no need to determine the relation between border points on adjacent slices. It can automatically generate the most suitable triangular patches connecting two neighboring slices.

(2) Border sweeping: When the border shapes are too complicated, such as the case wherein the cross section of an object is multiply connected, the above two methods no longer can create suitable triangle patches. The procedure called "border sweeping method" will never fail to construct 3-D shapes once a set of borders on each slice is extracted even in such a case as described above[3]. It can construct 3-D objects as a stack of boards which are generated by shifting the extracted borders upward and downward by half of the interval between the slices. Two boards produced by this method are shown in Fig.3.3. The board consists of two parts - the side and the top. The side is made by triangular patches which connect border points of the two sweeped borders. The top is made by painting the inside of

the upper sweeped border. The shape of objects generated by this method is stairlike, and looks artificial, though it is robust in the sense that it works well for any 3-D shapes. The ventricles are displayed by applying the border sweeping method to manually extracted contours (as described in 3.2.1(2)). It is difficult to get them automatically.

3.3 DENSITY IMAGE GENERATION

Though the surface image constructed from the extracted borders in CT slices is helpful for diagnosis, the CT number itself sometimes contains important meaning. For this reason, CT values are also rendered by putting them on cross section planes. We call such image a density image. Cross section planes which are tilted or vertical to the original slice are used as the density image. These new cross section planes are produced from a set of original slices[4-6]. We call this procedure "reslicing" since new cross sections of the different direction from original slices' are calculated from a set of given slices. A vertical cylinder is also utilized as the density image for an example of curved surfaces.

3.3.1 Vertical cross section

Fig.3.4 illustrates how to reslice original images to obtain a vertical cross section. A new section L_R can be located at any position and in any direction. Both the center line l_c and the angle θ from the x-axis specify the position and the direction of the cross section to be produced. Now we consider the intersecting line between the cross section and one of the original sections. Let us call this intersecting line l_k for the k-th slice. The number of pixels on the line is the same as that on an edge of a square which is the original slice, since we want the quality of the new slice to be the same as that of the original one. For the i-th pixel on the line l_k, it's x- and y-coordinates (x_i, y_i) are obtained by

$$x_i = (i - n/2)\cos\theta + c_x \qquad (3.1)$$

$$y_i = (i - n/2)\sin\theta + c_y \qquad (3.2)$$

where n is the number of pixels on l_k and (c_x,c_y) are the x and y coordinates of the center line l_c, respectively. Unfortunately, it is rare that (x_i,y_i) exactly coincides with one of the original pixels. Thus, linear interpolation technique is used to obtain the CT value of a new pixel. That is, the value of the pixel (x_i,y_i) is calculated by the interpolation of those of four pixels surrounding the pixel (x_i,y_i). After that this value is assigned to (x_i,y_i). We call it "mapping" to put the value on the new section by the method described above. We should also interpolate the value in z-direction to get the same spatial resolution as in the horizontal cross section.

3.3.2 Tilted cross section

Tilted cross sections can be similarly resliced. In this case, two kinds of tilted cross sections are considered:

(a) tilted cross section based on a line parallel to the y-axis, and
(b) tilted cross section based on a line parallel to the x-axis.

These sections are defined by the coordinates of the base line (S_x,S_y,S_z) and the angle θ from the original slice(Fig.3.5). One reason we use these two kinds of tilted sections is that it is rather simple to construct them once we rearrange the original set of CT image sequences for this purpose. Another is that according to our medical sources these two sections are enough for a proper diagnosis. Reconstruction will become much more complex in a system whose main memory cannot afford to store whole 3-D data, if any other tilted section is required.

The number of slices to intersect the desired tilted section decreases as the tilted angle approaches 0° or 180°. Thus the quality of the produced image becomes poor since only few points on the original slices are available for the reconstruction. To overcome this defect we keep the sampling interval d on the new slice equal to that of the original image. Fig.3.6 shows the relation between sampling points on a tilted section and original slices. The coordinates of the i-th sampling point (x_i,y_i,z_i) for the two cases mentioned above are given as

follows:

case (a):

$$z_i = S_z + (i - n/2)\sin\theta \quad (3.3)$$

$$x_i = S_x + (i - n/2)\cos\theta \quad (3.4)$$

y_i : same as the original slice

case (b):

$$z_i = S_z + (i - n/2)\sin\theta \quad (3.5)$$

$$y_i = S_y - (i - n/2)\cos\theta \quad (3.6)$$

x_i : same as the original slice

We use the four-point interpolation again along the tilted plane to produce an image of good quality. The process for the case (a), for example, is shown in Fig.3.7. Interpolated value f(**P**) for a sampling point **P** is determined by four neighboring values according to the following equation:

$$f(\mathbf{P}) = f(\mathbf{A})(1-\alpha)(1-\beta) + f(\mathbf{B})\alpha(1-\beta) + f(\mathbf{C})(1-\alpha)\beta + f(\mathbf{D})\alpha\beta . \quad (3.7)$$

3.3.3 Vertical cylinder

A vertical cylinder is defined by the coordinate (C_x, C_y) of the center axis C and a radius R (Fig.3.8). We reslice the surface of this cylinder by extracting sampling points in the form of CCS along a circle that is the intersection of the cylinder and the slice. R-buffer, in this case, stores interpolated CT values instead of distances from the center point of the circle, because we can easily obtain the position of triangles geometrically from C and R. The x and y coordinates of the i-th sampling point on an arbitrary slice is determined by

$$x_i = R\cos(2\pi(i-1)/n) + C_x \quad (3.8)$$

$$y_i = R\sin(2\pi(i-1)/n) + C_y \quad (3.9)$$

where n is the number of sampling points on a slice. We also use the interpolation in the z-direction for the improvement of image quality.

3.4 DISPLAY FOR DIAGNOSIS

Some concrete 3-D informations such as the location, shape or saturation of diseases are important for diagnosis, because original slices are 2-D images and until now medical doctors have had to reconstruct 3-D images in their mind's eyes. One of the best ways to understand 3-D information is to observe some combination images consisting of density images and surface images. Intensity (or brightness) calculation and density "mapping" on a surface are necessary to display these images. It should be noted that the hidden surface problem (see 3.4.2) is one of the most important problems to overcome in displaying objects.

3.4.1 Projection

Parallel (orthogonal) projection is used for all projection in this system since the projected image is not distorted and it is performed more easily than the perspective (central) projection. For surface images, three vertices of each triangular tile are projected onto the projection plane. The brightness of the tile on the plane is determined by Lambert's cosine law:

$$I = C_1 + C_2 \cos \theta \tag{3.10}$$

where C_1 and C_2 are suitable constants and θ is the internal angle between the surface normal and the direction to the light source(Fig.3.9). The surface normal is found by the vector product of the two vectors which are directed from one vertex to the other two neighboring vertices. This value is given to the triangular area determined by the projected three vertices. A 3-D surface image is constructed after we project all triangles onto the plane in the same way. Hidden surface removal is easily performed by considering the scalar product between the direction of the viewer **V** and the surface normal **N**. If this value is positive, the viewer can see the surface, and otherwise not, that is,

$$\mathbf{N} \cdot \mathbf{V} > 0 \quad : \quad \text{visible} \tag{3.11}$$

$$\mathbf{N} \cdot \mathbf{V} < 0 \quad : \quad \text{invisible} \tag{3.12}$$

where both **N** and **V** are unit vectors.

For density images, we have to determine a painting region ($\Delta x, \Delta y$) on a projection plane for one projected point P. The density value of the point P is mapped (or given) to the whole region($\Delta x, \Delta y$). If the size of that region is not sufficient, undesirable gaps might appear in the density image. If the size is too large, the quality of the mapped image becomes poor. Thus we determine the size as follows. First, three neighboring points including the desired point P are projected onto a projection plane. Then, the two lengths of edges of the circumscribed rectangle that includes the projected three points are used as ($\Delta x, \Delta y$) in Fig.3.10.

3.4.2 Image composition

Arbitrary composition of original slices, surface images and density images is available. However, there are some cases that a density image interferes with some parts of a surface image or another density image. We should avoid to display such regions. The processing is simple in the case of displaying the skull surface under an original slice, because it is enough to say that nothing higher than the slice is projected.

In displaying a tilted cross section together with a skull surface and a slice, some parts of the skull and the slice are eliminated by the cross section. Both the skull and the slice are divided into two parts by the cross section. The eliminated part is decided by the relation between the normal vector **N** of the cross section and the viewing vector **V**. Let us assume $F(\mathbf{P}) = 0$ is the cross section itself, where **P** is any point on the skull or the slice. Then an arbitrary point **P** is displayed, if $F(c\mathbf{V}) \cdot F(\mathbf{P}) < 0$, and not displayed otherwise, where c is a sufficiently large constant. Thereby, one can observe the density image without being disturbed by a slice or the skull since the parts of the skull and the slice which are nearer to the viewer are eliminated. $F(\mathbf{P})$ is determined for the two cases of the tilted cross sections in 3.3.2 as follows.

case (a):

$$F(\mathbf{P}) = -x \tan\theta + z + S_x \tan\theta - S_z$$

$$= \mathbf{N_1}\cdot\mathbf{P} + d_1 = 0 \qquad (3.13)$$

case (b):

$$F(\mathbf{P}) = y \tan\theta + z - S_y \tan\theta - S_z$$

$$= \mathbf{N_2}\cdot\mathbf{P} + d_2 = 0 \qquad (3.14)$$

where $\mathbf{N_1} = (-\tan\theta , 0 , 1)$

$\mathbf{N_2} = (0 , \tan\theta , 1)$

$d_1 = S_x \tan\theta - S_z$ (3.15)

$d_2 = -S_y \tan\theta - S_z$. (3.16)

Fig.3.11 illustrates the image composition in the case (b).

To display a vertical cylinder with the skull surface and a slice, we also eliminate some parts of the skull and the slice. Two kinds of image compositions are available for a vertical cylinder:

(c) composition of a vertical cylinder, the outer part of which is eliminated, the skull surface and a slice.
(d) composition of a vertical cylinder, the inner part of which is eliminated, the skull surface, a slice and a vertical cross section.

We will show the elimination process for each case.

Case (c) The part of the skull surface higher than the slice under consideration is omitted first, because the skull surface is cut by the slice. Also, the part of the cylinder lower than the slice is not displayed, since this part is under the slice and invisible. The cylinder is constructed by triangular tiles which have densities (or CT values) to be mapped by the procedure described in 3.3.1. We should decide which tiles are visible before mapping their densities. Suppose **N** and **V** are the surface normal vector of a tile and the viewing vector, respectively. Then, the tile is visible if $\mathbf{N} \cdot \mathbf{V} > 0$, and invisible if $\mathbf{N} \cdot \mathbf{V} < 0$.

Case (d) The vertical cross section divides the skull surface

and the slice under consideration into two parts. We first omit the frontal (or viewer's) part of the skull and the slice in order to show the inner part of the brain. The slice and the vertical section are displayed by mapping densities over each plane. We should not render some parts of each plane which are inside the cylinder. Fig.3.12 and Fig.3.13 give a top and an upper view of the relation between the skull surface and each sections(a slice, the vertical cross section and the vertical cylinder).

The elimination process by the vertical cross section for the skull and the slice is performed like that of the tilted cross section described above. The vertical cross section including a point $\mathbf{C}(C_x,C_y,C_z)$ is expressed as follows:

$$F(x,y,z) = - x \tan \theta + y + C_x \tan \theta - C_y. \qquad (3.17)$$

Let us assume again that **V** is the viewing vector and c is a sufficiently large constant. Then a point **P** on the slice or the skull is displayed, if $F(c\mathbf{V}) \cdot F(\mathbf{P}) < 0$, and otherwise not.

Some parts of the slice and the vertical cross section are omitted since they are inside the cylinder. The slice is cut according to the following rule:

the point $\mathbf{P}(P_x,P_y)$ is displayed if $(P_x - C_x) + (P_y - C_y) > R$, and otherwise not.

where (C_x,C_y) and R are the the center position and the radius of the cylinder, respectively.

The density value is mapped on the cylinder, if and only if the condition described below is satisfied.

$$\mathbf{N} \cdot \mathbf{V} < 0 \qquad (3.18)$$

where **N** is the surface normal of the cylinder and **V** is the viewing vector.

The dark curve in Fig.3.12 is the part of the cylindrical surface to be rendered.

3.5 DISPLAY FOR SURGICAL PLANNING

One of the most important decisions in surgical planning is choosing the exact area of the skull which will be opened for the operation. The region chosen should be the most appropriate for each patient. This system has a function to help surgeons to decide the most suitable operative area by displaying 3-D images including diseased regions with the skull and density images(original CT images). They can get the information about the location of the disease area relative to other regions such as the skull or coronal sutures in displayed images, and simulate the operation before the actual surgery. Two functions (1)windowing and (2)translucent display are available in display of the skull for this purpose. We will show the details of each function in the following sections.

3.5.1 Skull windowing display

In the actual brain surgery, one part of the skull is opened and the operation is performed through that skull "window". The skull surface is generated by the "CCS and triangulation" method described in 3.2.2. We can make a 3-D image of the skull which has a window by eliminating triangular tiles in the specified area of the skull surface, so that diseases can be observed through the window.

The window can be specified by z and θ coordinates in CCS such as (z_H, z_L) and (θ_R, θ_L) in Fig.3.14.

The skull windowing display might generate ambiguous images wherein the distance from the diseased area to the window is obscured. An original slice, in such a case, is useful for indicating the distance from the skull surface to the disease. We added the lowest slice of the image where the disease was observed. The time and memory-consuming process of removing hidden surfaces can be expedited by displaying the lowest slice, diseased tissue, skull surface, and the top slice in this order.

3.5.2 Translucent display

It is not useful to create a skull window for observing the interior tissues before the optimal window has been determined, since one might not be able to see the disease through the window from some directions. Displaying the skull and the top slice translucently is one of the ways to observe the interior tissues from an arbitrary direction. We adopted Newel's method[7] for translucent display. That is,

$$I = (1 - t) I_b + t I_f \tag{3.19}$$

where

I_b = intensity of objects behind the other object closer to the observer,

I_f = intensity of the surface of the closer object (to be displayed translucently),

I = total intensity,

t = transparency coefficient,

$$\begin{cases} 0, & \text{if transparent.} \\ 1, & \text{if opaque.} \end{cases}$$

This method is simple, but generates useful images for understanding the spatial arrangement of disease lesions[8,9,10].

3.6 EXPERIMENTAL RESULTS

Figures 3.15 to 3.21 are several examples of pictures generated by this system. Fig.3.15 shows the skull surface with horizontal and vertical cross sections with CT values on them. Two kinds of tilted cross sections are added in Fig.3.16. Fig.3.17 shows vertical cylinder cross sections displayed using the two methods described in 3.3.2. The same original images including tumor was used here.

A ventricle surface reconstructed by border sweeping method is shown in Fig.3.18.

Figures 3.19 to 3.21 are the results of preliminary experi-

ments for 3-D display to help surgical planning. In Fig.3.19, one can observe a tumor or hematoma through the skull window as described in 3.5.1. The lowest slice is useful to understand the depth of the diseased part in the brain in Fig.3.19(b). The smooth shading method was adopted here to render the skull surface, and the coronal suture is also added to the skull surface so that the location of skull area to be removed will be better understood[11]. By displaying the skull surface translucently, one can observe the disease from any direction in Figs.3.20 and 3.21.

Computation time was 7 minutes (Fig.3.15) to 15 minutes (the case including translucent display) to generate images from original CT slices. These times include data conversion processes to make CCS surface data from original slices. FORTRAN was used for the program of our system, except small parts of I/O routines written in assembler language. Rather long computation time at the present stage is mainly due to the limited ability of the computer used here, hence it will be reduced considerably by improving the program and the computer itself, and by utilizing special hardware. See 2.2 (3) and (4) for images and computer systems used here.

3.7 CONCLUDING REMARKS

A system for displaying 3-D images of human brain structure by reconstructing it from CT image sequences has been developed. The system has the following functions:

(1) It generates cross-sectional images along an arbitrary plane and generates a cylindrical surface reconstructed from a given set of CT slices as well as the coronal or sagittal section images.

(2) Together with the above mentioned cross-section images, the system also displays shaded images of component figures such as the skull, the ventricle and some kinds of disease lesions (e.g. hematoma, tumor, etc.). These components are extracted by interactive procedures or fully automatic methods using pattern

recognition techniques.

(3) In order to observe parts of the brain hidden by the skull image, the system provides two types of display methods. One is to eliminate part of the skull so as to make a window for viewing inside the skull. Another is to display the skull as a translucent surface.

This system is expected to be useful especially for surgical planning and education in medicine. Both the display of gray values (CT values) on an arbitrary cross section and the additional display of the skull and the ventricle with cross-sectional images were remarkably useful for understanding 3-D brain structure. Using a window in the skull and shaded images of disease lesions were also helpful for simulation of surgical operations.

The objectives of this study performed about five years ago were 1)to find useful methods for completely utilizing 3-D information currently available in CT image sequences for medical diagnosis and treatment, and 2)to develop the methods to generate such images, rather than to make a practical system immediately. Computation time will be reduced remarkably by using recent computer systems which are more than ten times faster than ours. In most of modern CT system this type of 3-D image generation is becoming popular and widely available as their optional functions. This implies practical significance of 3-D image display we discussed. In order to realize and to take full advantage of more intelligent display systems, methods should be developed for fully automated extraction and 3-D projection of medically significant images.

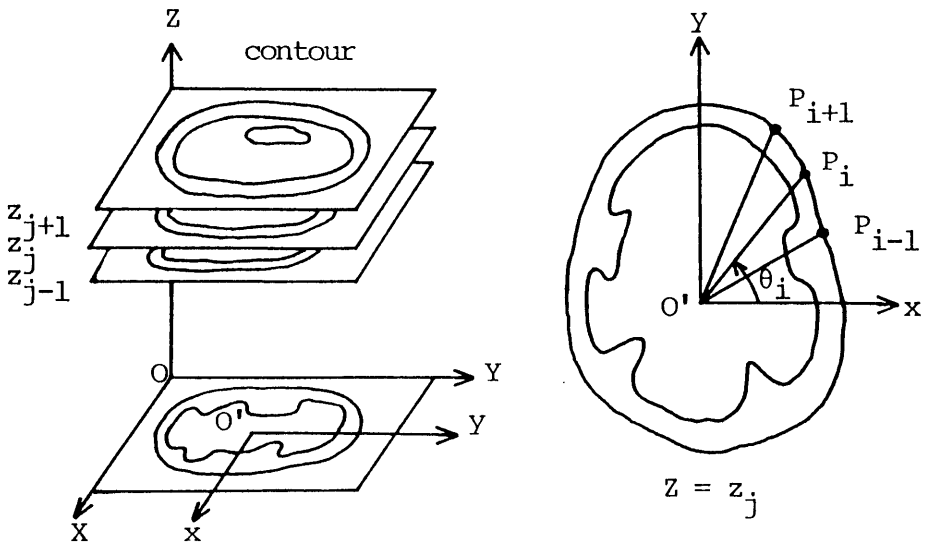

Fig.3.1 The cylindrical coordinate system (CCS).

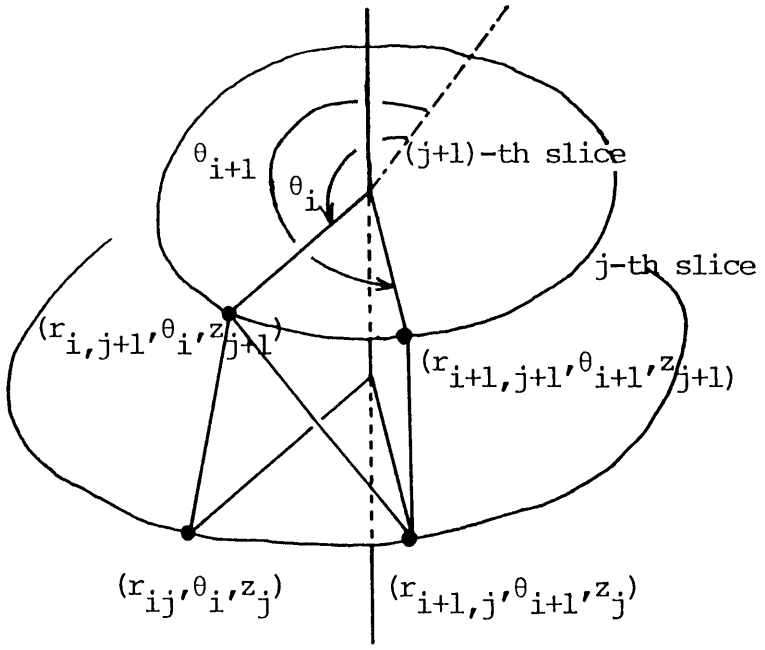

Fig.3.2 Reconstruction of the skull surface by CCS.

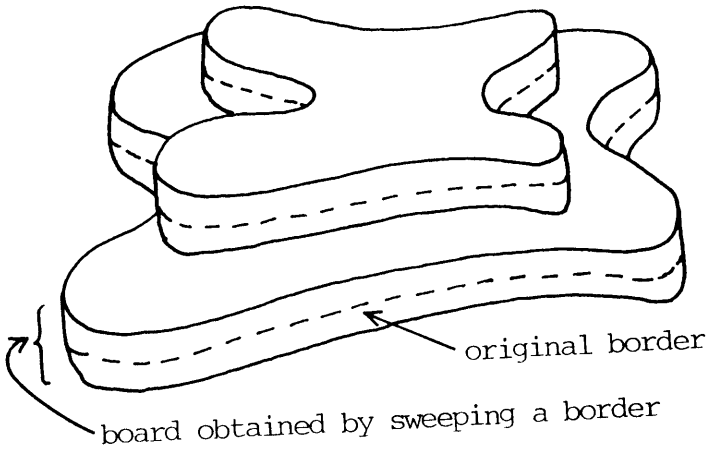

Fig.3.3 Reconstruction by border sweeping.

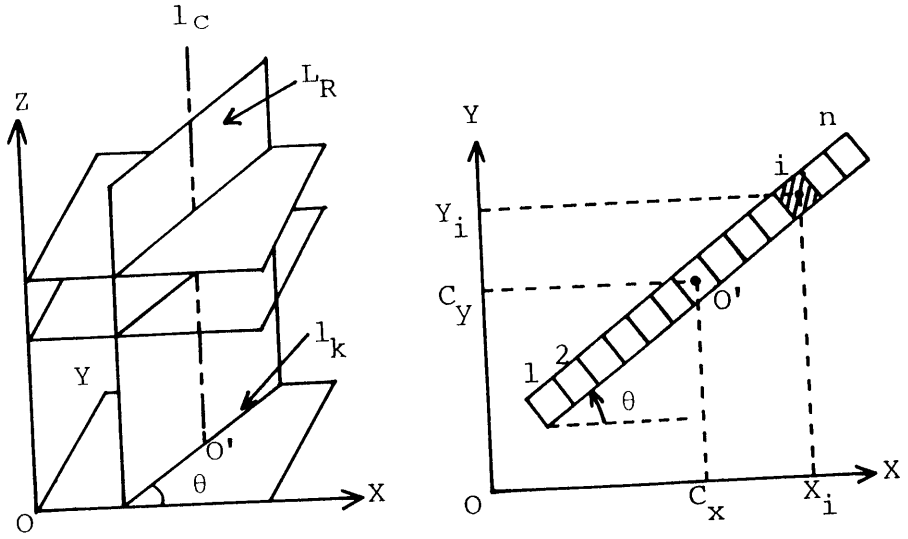

Fig.3.4 Reconstruction of a vertical cross sectional image.

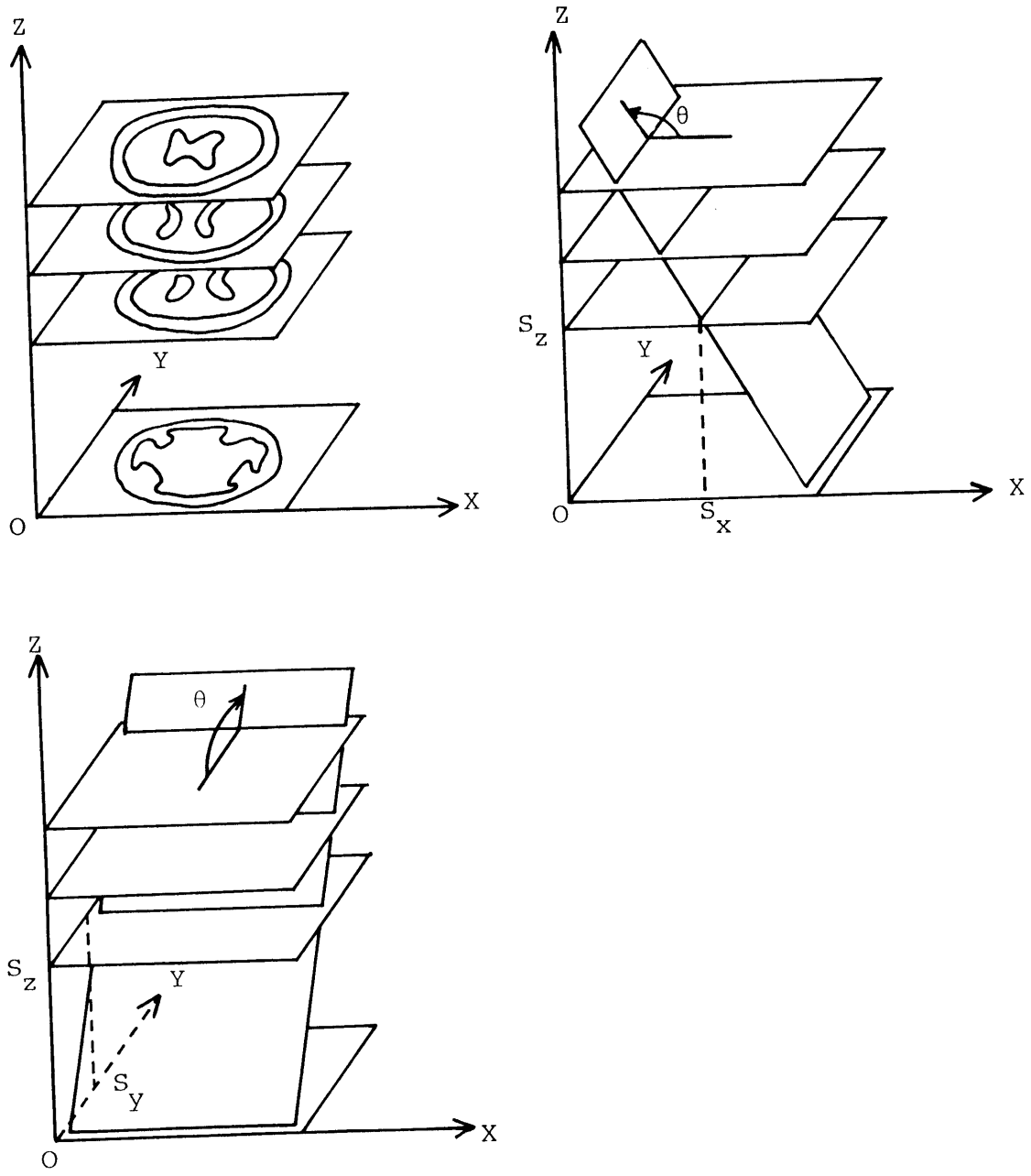

Fig.3.5 Generation of tilted cross sectional images.

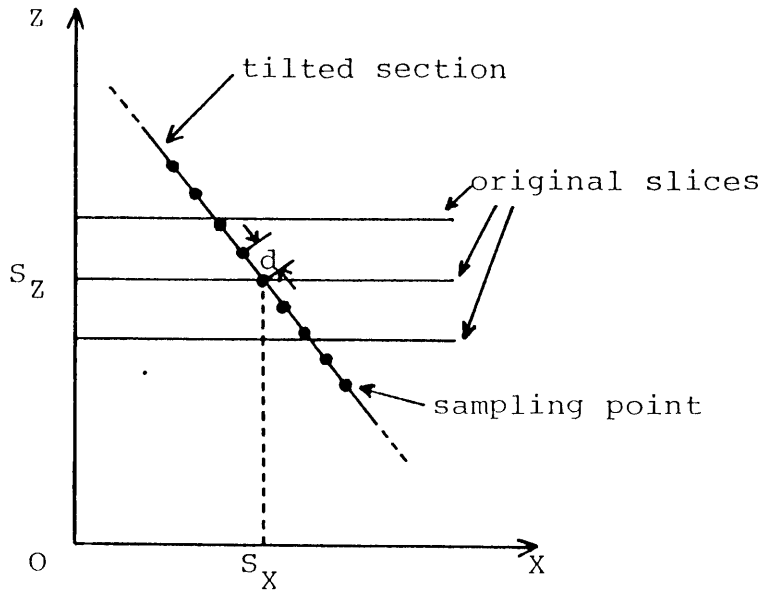

d: sampling distance which is the same as original slices'.

Fig.3.6 Sampling points on the tilted section.

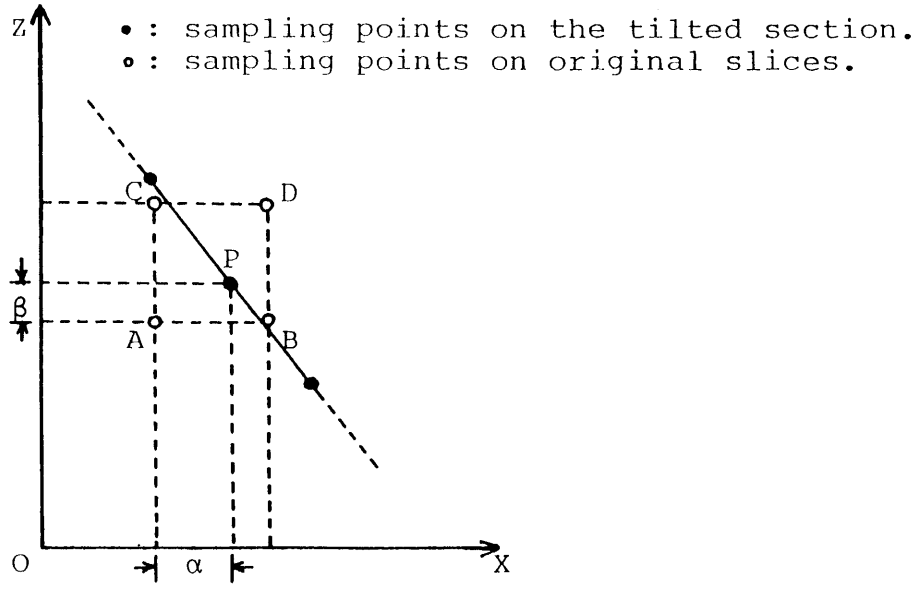

Fig.3.7 Four-point interpolation.

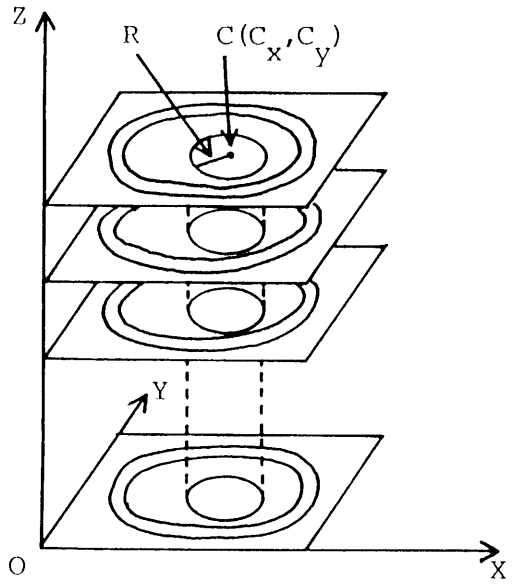

Fig.3.8 Specification of cylindrical surface.

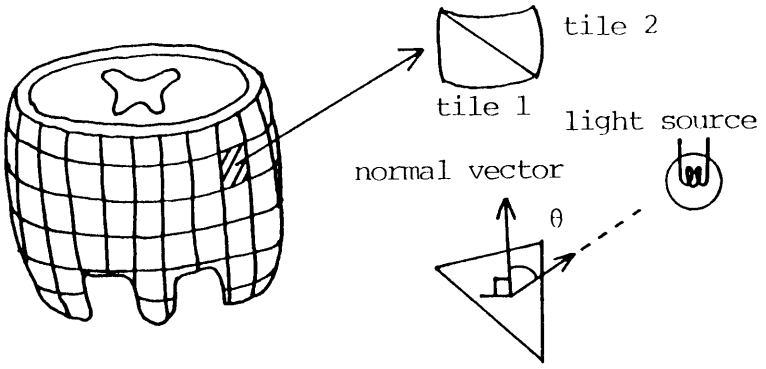

Fig.3.9 Projection of a 3-D surface for display.

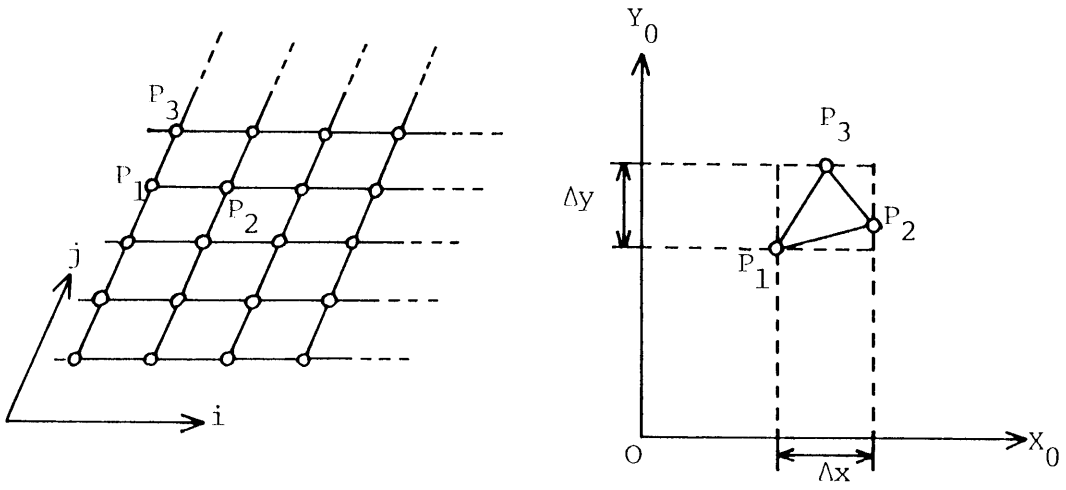

Fig.3.10 Projection of density values.

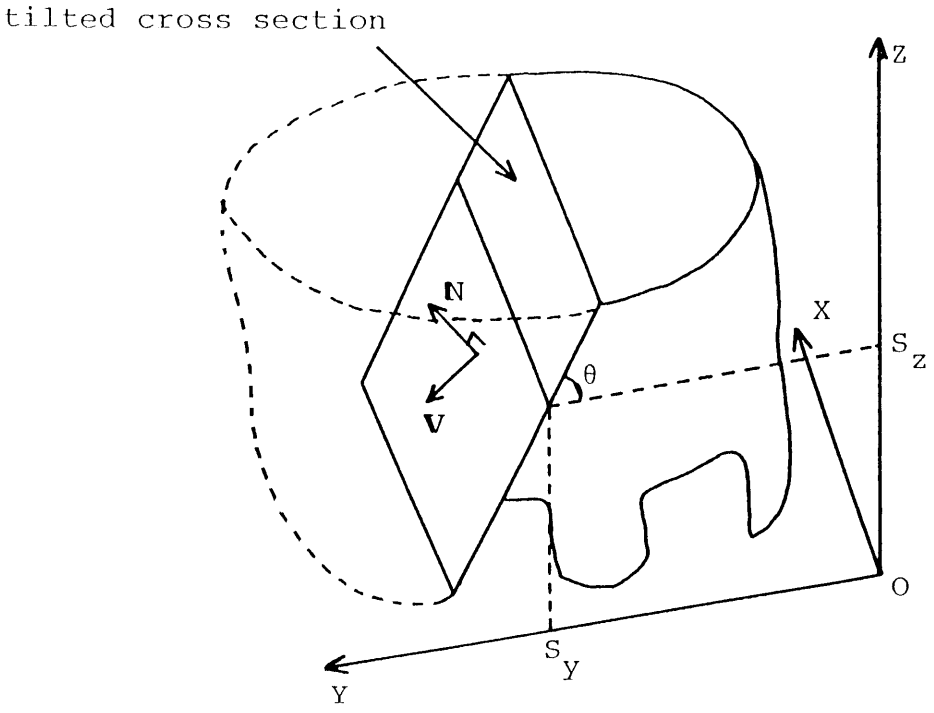

Fig.3.11 Image composition of the case (b).

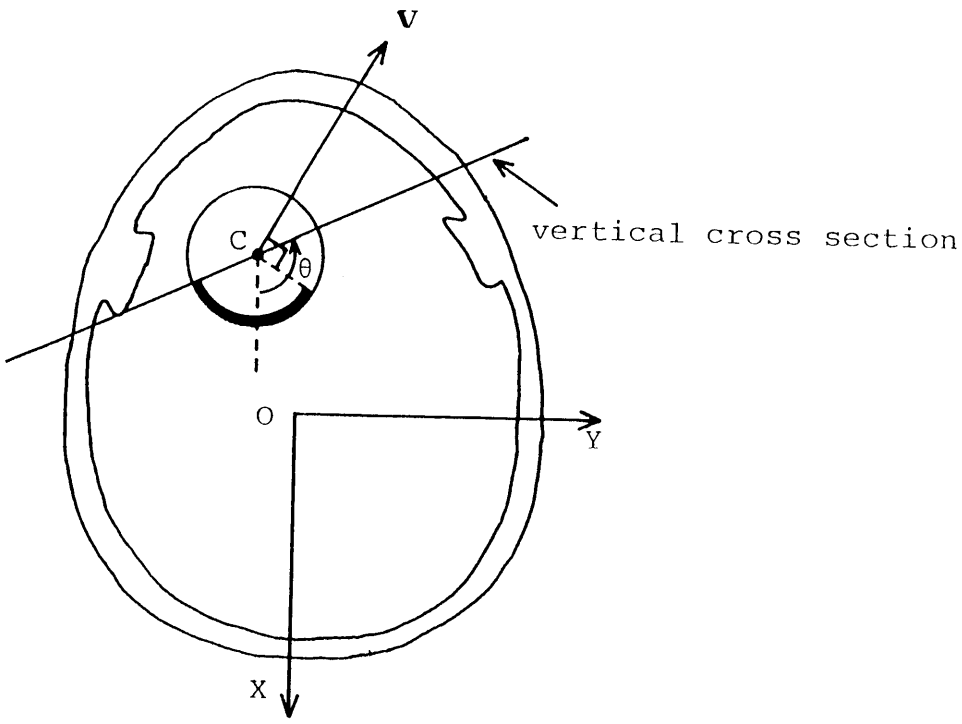

Fig.3.12 Top view of the relation between each sections.

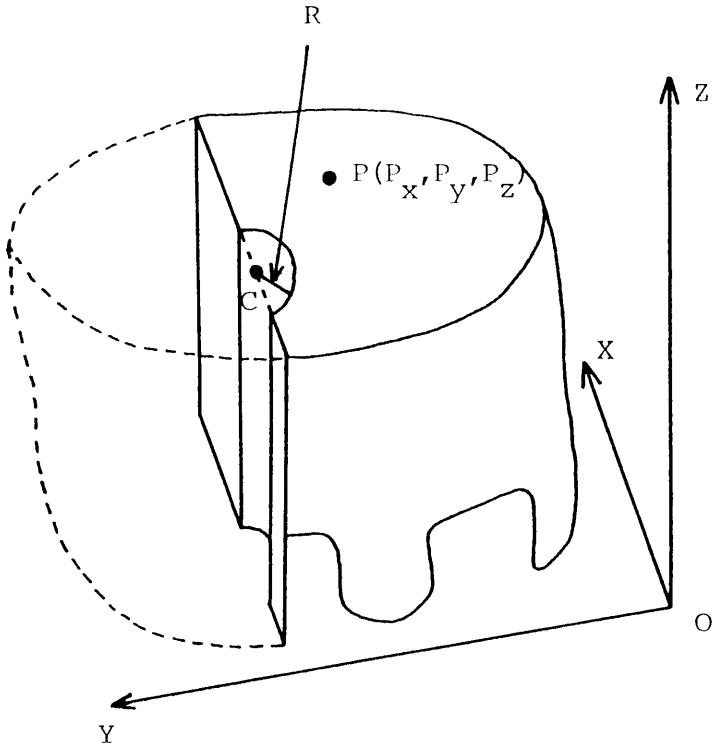

Fig.3.13 Upper view of the relation between each sections.

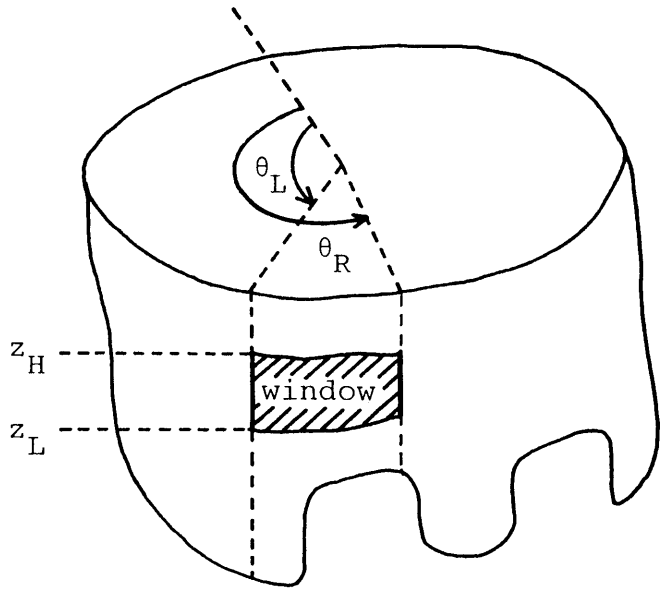

Fig.3.14 Specification of the window.

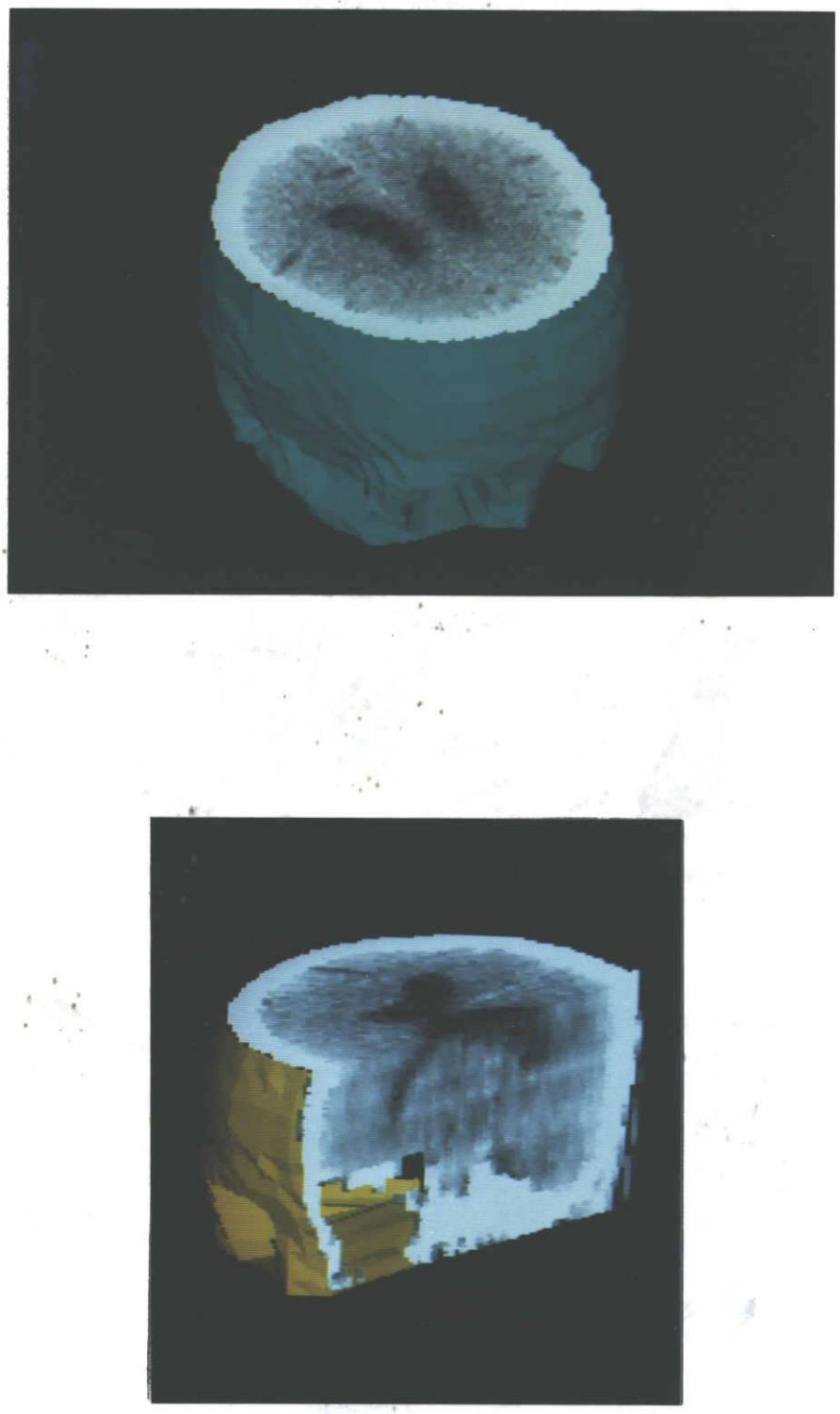

Fig.3.15 Displayed images (skull, vertical cross section and original slice).

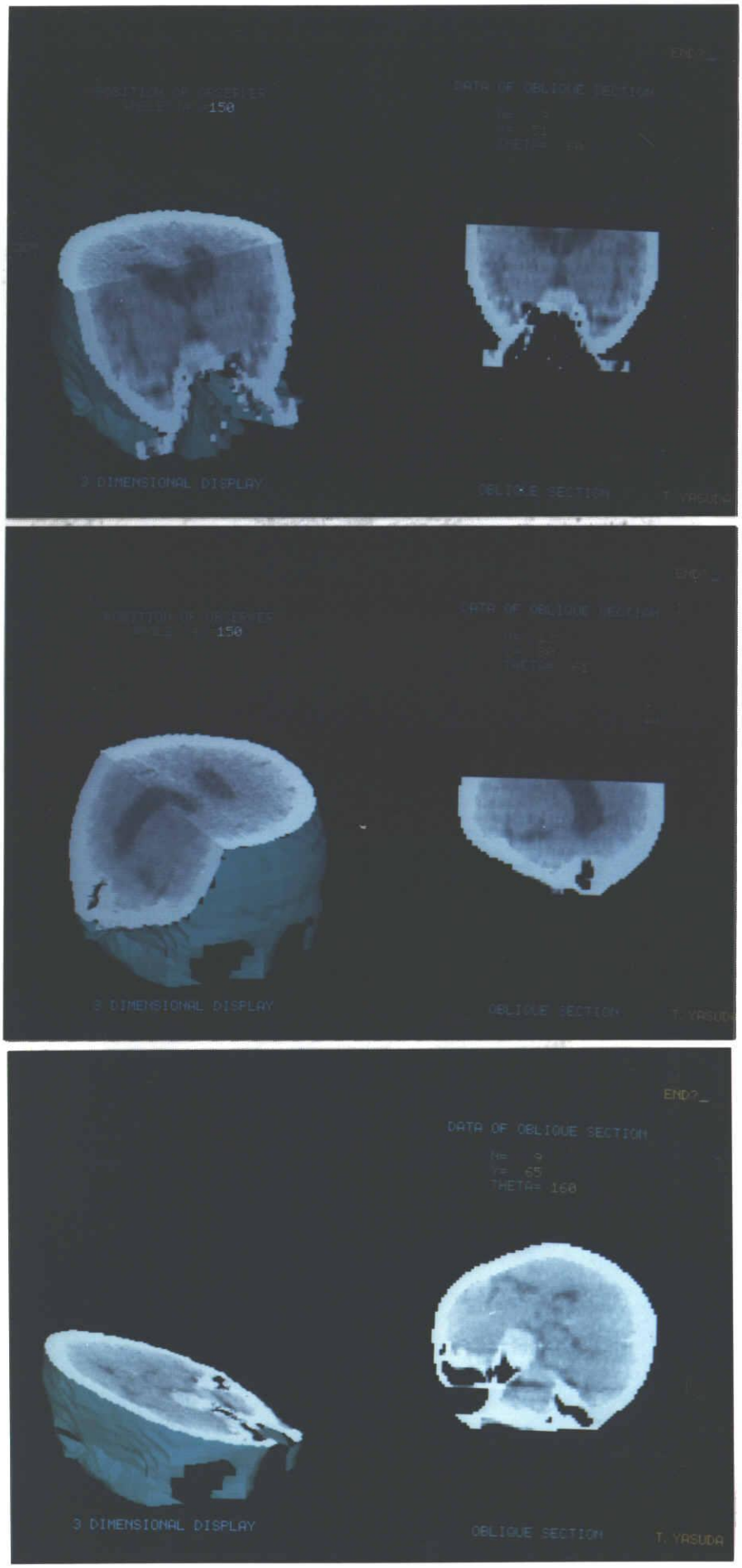

Fig.3.16 Displayed images (skull, tilted cross section and original slice).

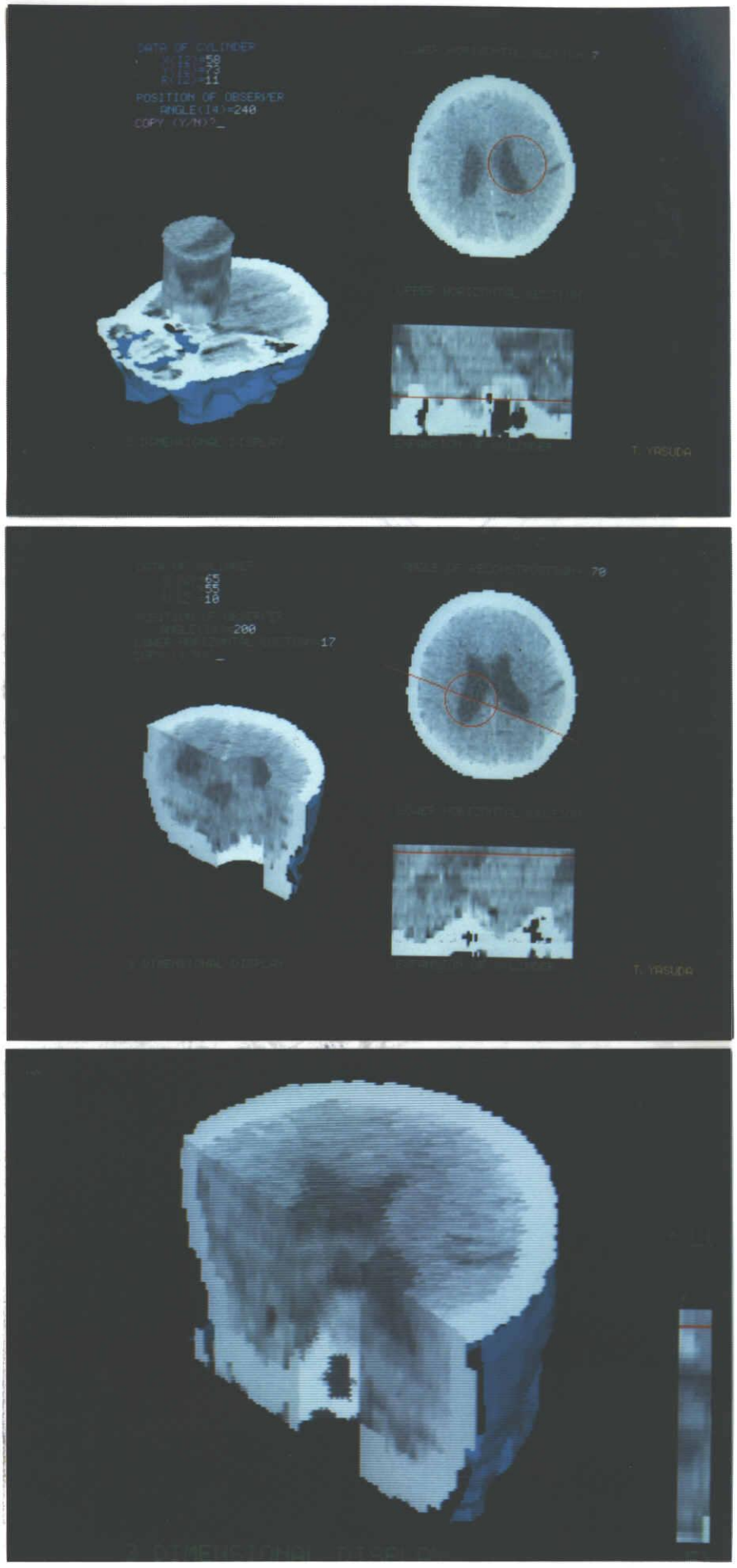

Fig.3.17 Displayed images including the cylindrical surface.

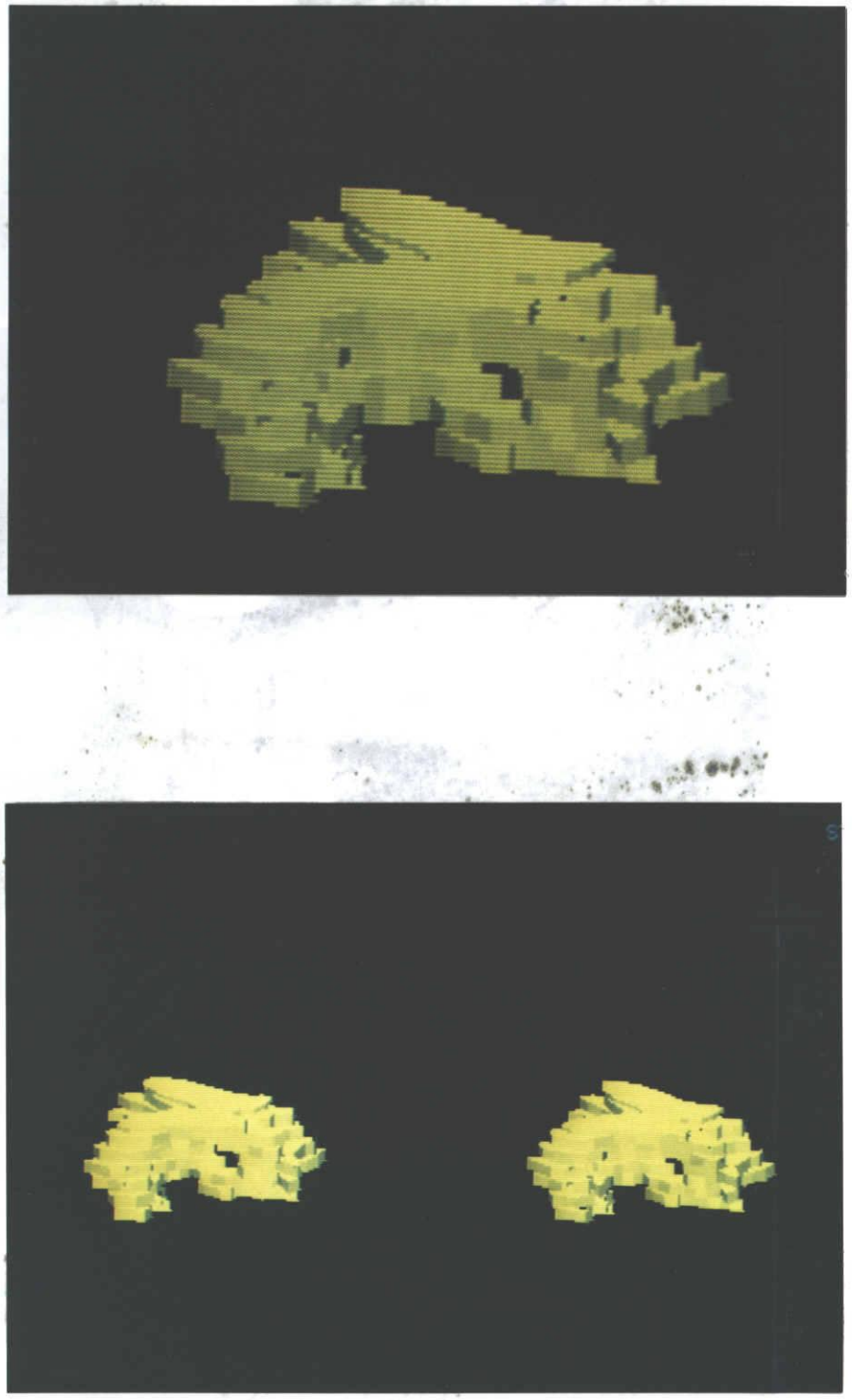

Fig.3.18 Ventricles reconstructed by border sweeping.

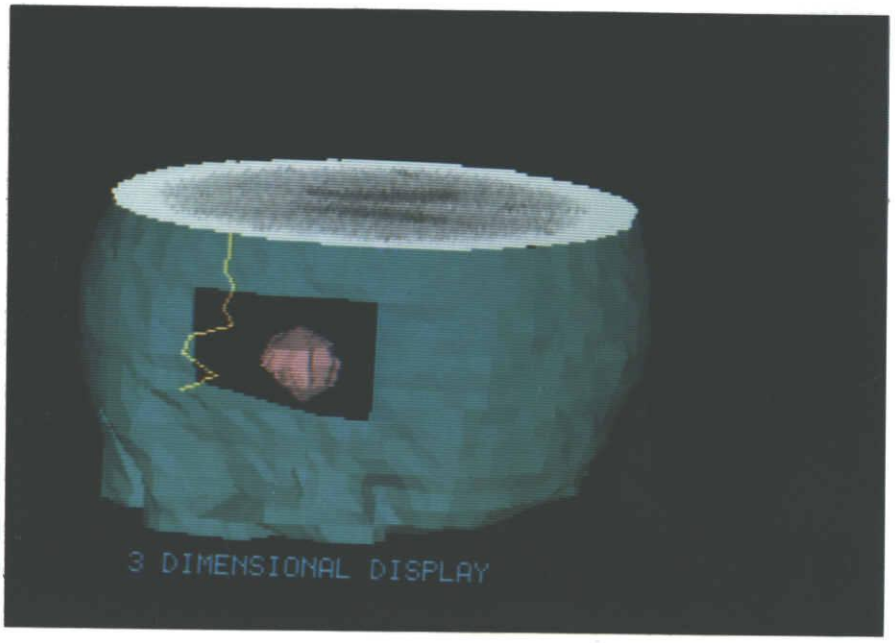

(a)

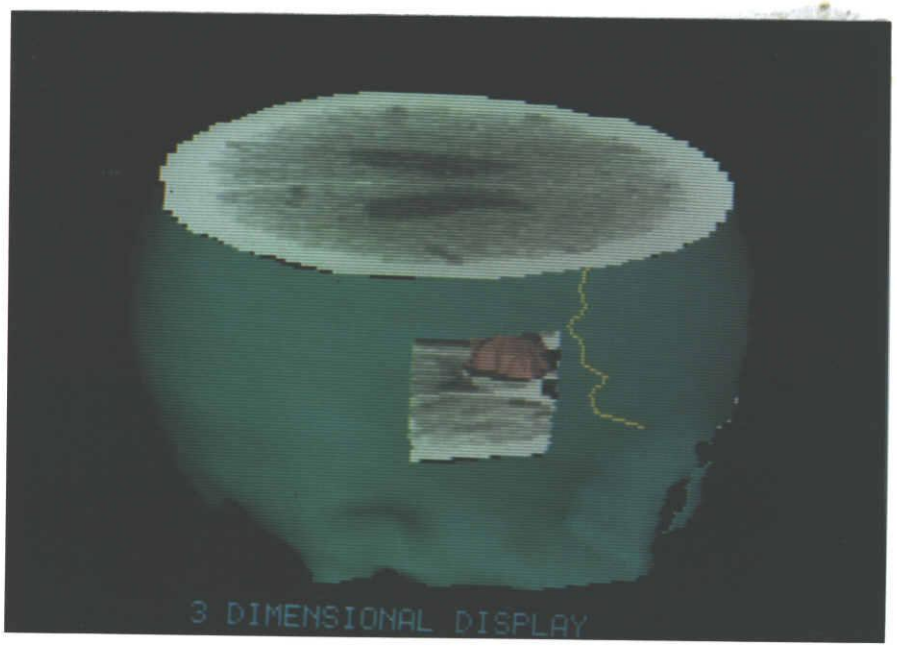

(b)

Fig.3.19 Disease lesion observed through a window on the skull. Coronal sutures and original slices are also accompanied. ((a),(b): tumor , (c),(d): hematoma.)

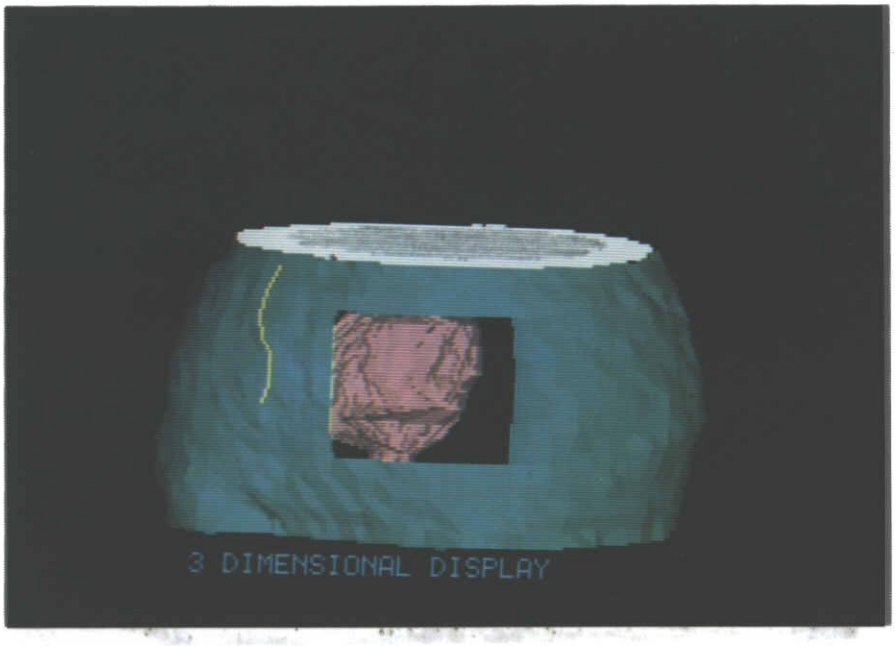

(c)

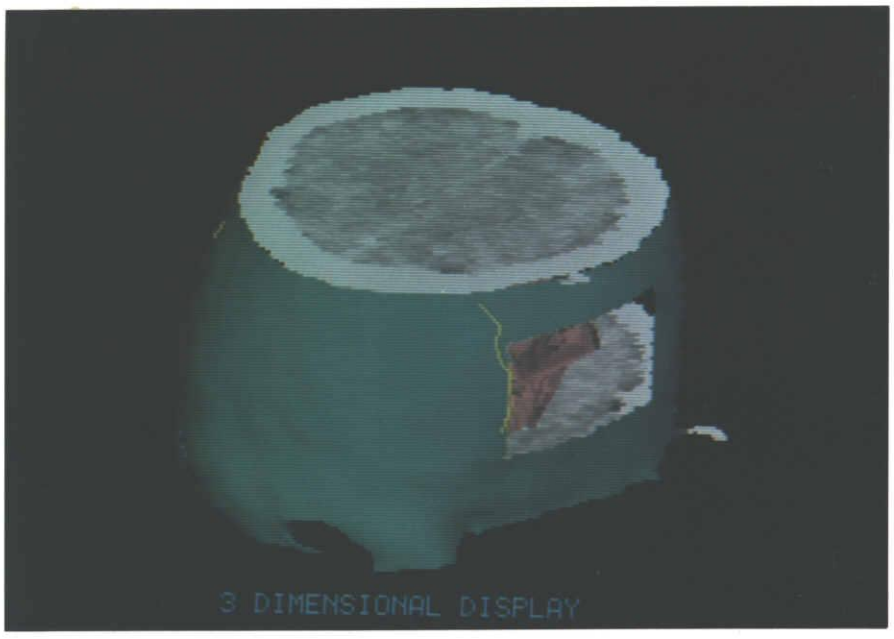

(d)

Fig.3.19 Disease lesion observed through a window on the skull. Coronal sutures and original slices are also accompanied. ((a),(b): tumor , (c),(d): hematoma.)

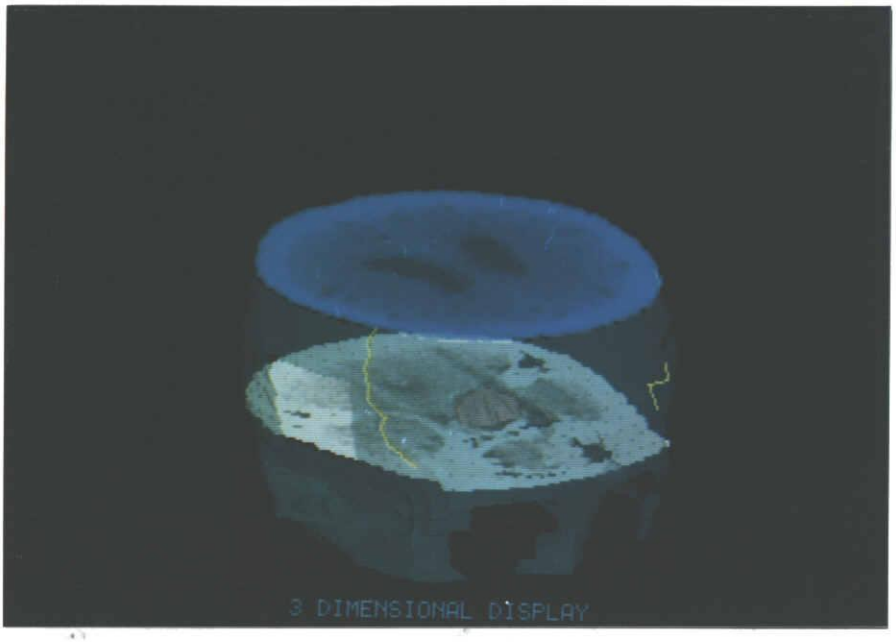

(a)

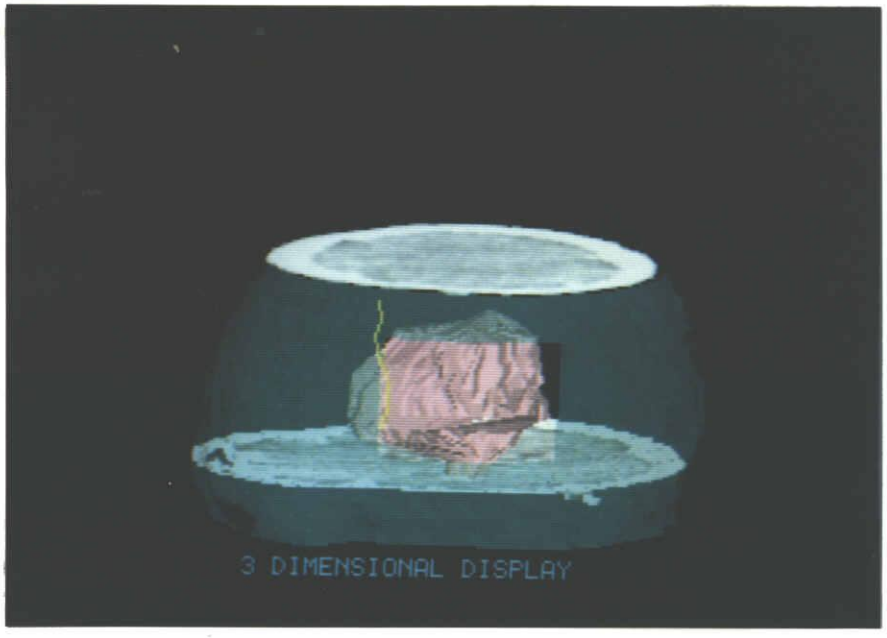

(b)

Fig.3.20 Translucent display of the skull. Tumor and hematoma can be observed through the skull surface in (a) and (b), respectively.

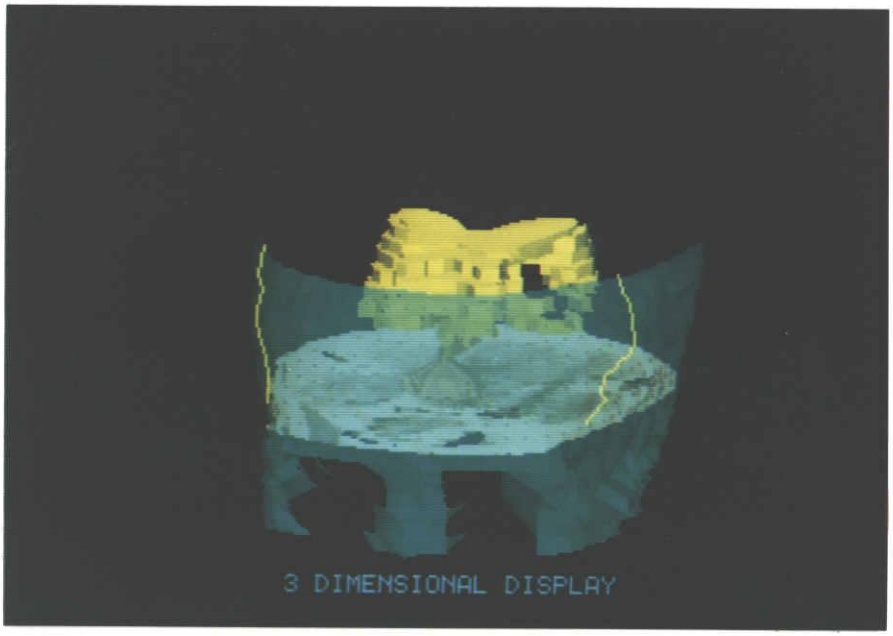

Fig.3.21 Ventricle and tumor observed through the translucent skull.

4. COMPUTER SYSTEM FOR CRANIOFACIAL SURGICAL PLANNING "NUCSS" - OVERVIEW

4.1 INTRODUCTION

Various kinds of techniques have been reported for reconstruction of three dimensional(3-D) features of body tissues from 2-D tomographic images(slices). The quality of these reconstructed images has been remarkably improved since recent CT devices have offered better quality of tomographic images. Surgical planning in brain or craniofacial surgery based upon computer-generated 3-D images is one of the most promising clinical applications of such 3-D reconstructed images. We have already described a system for planning of brain surgery in chapter 3. We will present a planning system for craniofacial surgery in this and the next chapters. The main objective of the craniofacial surgery is to reform inherent or acquired deformities of the skull by cutting the skull to separate small pieces or bone blocks and rearranging them to achieve desirable shape for a whole skull. This is meaningful especially when the volume of the skull is too small for normal brain growth. In performing an individual operation, the most suitable surgical approach must be determined for each patient. Since, until the present time, this decision has been made using a sheet of a 2-D sketch image, that is, by cutting or rearranging the sketch paper, surgeons have not been able to consider the post-operative 3-D shape of the skull and soft tissues, except imaging it from rearranged 2-D bone blocks.

A few studies with techniques of computer graphics and image processing have been recently reported for 3-D simulation of the craniofacial plastic surgery using CT images. Vannier et. al. developed a system for evaluating deformities of the skull by using 3-D displayed images, and have used the system clinically [1]. Herman evaluated the volume of bone graft and the amount of graft resorption[2]. Tuy et. al. simulated bone removal operations[3]. Brewster estimated the reformed skull shape by

using the symmetric transformation[4]. Fellingham developed a planning system which has a function to cut some bone regions from a side view[5]. Although these systems can help surgeons to make surgical plans which are relatively simple,they do not have enough functions for routinely encountered complex craniofacial surgery planning.

NUCSS(Nagoya University Craniofacial Surgical-Planning System) has been developed as a practical planning system for craniofacial operations based on requirements and suggestions by plastic surgeons. The processing flow of this system is shown in Fig.4.1. It provides the following functions: (1)generation of 3-D images, (2)calculation of the distance between two points on a 3-D image, (3)surgical planning on a side view of the skull, (4)bone cutting in arbitrary angles, locations and shapes, and (5)rough prediction of the post-operative face though the 3-D reconstruction of the skin surface. In the next chapter, we will present in detail these functions now available in NUCSS with experimental results.

Features of NUCSS are roughly divided into two major parts:- image generation and planning.

(1) 3-D IMAGE GENERATION

Organs or tissues of the human body can be seen as 3-D images reconstructed from a sequence of 2-D slices. Since this system mainly deals with the skull,bone regions are extracted from each slice of x-ray CT images by the thresholding technique before 3-D image generation.The gradient shading method is applied to the extracted skull which has been expressed as a set of voxels for generating shaded 3-D images on a graphic terminal[6],[7]. We also apply filtering operations on the depth buffer, which is used for the method described above, to improve the quality of generated images. Such a 3-D skull image may be constructed at any stage of the pre-, the under-, and the post-operation stage. Also, a post-operative face image is roughly predicted and generated based on the decided surgical plan.

(2) SURGICAL PLANNING

Slices are modified according to the surgeon's instructions by cutting, moving and joining pieces of bones to make the simulated post-operative slices.

a) Planning on a side view: After displaying the side view of the skull,the most suitable surgical plan can be decided interactively by drawing bone-cutting lines on the side view image, and then shifting, rotating and reversing the bone pieces cut by these lines. Doctors can simulate several possible plans to select the best one, studying 3-D properties of these plans comparatively and testing their relevancy by observing 3-D skull images resulting from the assumed plans at arbitrary directions.

b) Cutting and moving bone blocks in an arbitrary direction: After displaying the skull observed from an arbitrary direction, vertices of the cutting region are input on the graphic terminal by the interactive mode, and then the region is moved to any location.

Details of these functions will be shown in the following sections.

4.2 SKULL IMAGE GENERATION

4.2.1 Fundamental method

3-D images are obtained through four processes in this system, which are region extraction,shape expression,projection, and brightness calculation[8]. Details of these processes are as follows.

Skull or soft tissue regions can be automatically extracted from each original slice by a simple thresholding procedure. Since extracted images of organs are simply represented in the form of the voxel data, each voxel is projected on the display(projection) plane by using the parallel (orthogonal) projection. The projection is performed by calculating the depth (the distance between the voxel and the projected plane). The hidden surface removal is accomplished by storing the

nearest depth for each pixel on the projected plane. The buffer for recording the depth is called the depth buffer.

In our experiment, the extracted result is expressed as a set of voxels V(I,J,K), which lies at the point (I,J) on the K-th slice. Each V(I,J,K) has the value "1" or "0" as follows.

$$V(I,J,K) = \begin{cases} 1, & \text{if the point}(I,J,K) \text{ is in the bone region.} \\ 0, & \text{otherwise.} \end{cases} \quad (4.1)$$

Only the voxels which has the value "1" are projected on the display plane(Fig.4.2). The screen coordinates(x,y,z) of the projected voxel is calculated, and the depth(z) is stored in the depth buffer (z-buffer) Z(x,y) which is the same size of the screen, that is,

$$Z(x,y) = z. \quad (4.2)$$

This process is applied to the all "1" voxels. The nearest one is selected and stored in the Z buffer when more than one voxels are projected on the same location(x,y). The Z buffer expresses the skull surface after the projection process is completed.

Brightness on the displayed image is found by using the gradient shading method[7] applied to the depth(Z) buffer.

4.2.2 Accelerated projection method

Quick response is required in order to make a surgical planning on a graphic terminal. Surgeons might check his plan by a 3-D image on the screen from various directions. The voxel projection consumes larger part of the time required for the 3-D display. Therefore, it is effective to reduce the projection time as much as possible.

cube. In the original method proposed by Herman et. al., all of these six faces should be projected on the screen when a voxel was displayed on the graphic terminal[8]. After his proposal, various new methods have been reported in order to reduce the time for the projection[9-11]. Artzy pointed out that only three faces should be considered, since at most three faces can be

seen if the projection direction is fixed [9]. Herman proposed a new algorithm which needed none of the Z buffer and the comparison of z value, since the voxel projection order was fixed as the farther voxel from the viewer was projected earlier than the nearer voxel(back-to-front algorithm)[10]. Frieder showed that it was enough to project only the center point of the voxel, iff the size of the voxel was the same as the resolution of the image plane [11]. He also reduced the calculation process for the projection by using tables in the back-to-front algorithm.

In order to compare this with our new method, we will explain his algorithm briefly. The transformation from (I,J,K) to (x,y,z) is given by the equation (4.3)

$$\begin{pmatrix} x \\ y \\ z \end{pmatrix} = \begin{pmatrix} L_1 & L_2 & L_3 \\ M_1 & M_2 & M_3 \\ N_1 & N_2 & N_3 \end{pmatrix} \begin{pmatrix} I \\ J \\ K \end{pmatrix} + \begin{pmatrix} I_0 \\ J_0 \\ K_0 \end{pmatrix} , \qquad (4.3)$$

where the 3 X 3 matrix is the transformation matrix, and translation on the display plane is represented by the term (I_0,J_0,K_0). Three products $L_3 \cdot K$, $M_3 \cdot K$, and $N_3 \cdot K$ are calculated once for each slice, since K is fixed for a slice. Other six products $L_1 \cdot I$, $M_1 \cdot I$, $N_1 \cdot I$, $L_2 \cdot J$, $M_2 \cdot J$, and $N_2 \cdot J$ are stored in six one-dimensional arrays for all I and J, and read from them using I or J as the index, if necessary.

We have developed a much faster projection method which reduces the number of the product, and needs no array, therefore saving the searching time.

Assuming $L_3 \cdot K$, $M_3 \cdot K$, and $N_3 \cdot K$ have been already found for the K-th slice, these values on the next slice are calculated as follows.

$$L_3 \cdot (K+\Delta K) = L_3 \cdot K + L_3 \cdot \Delta K \qquad (4.4)$$

$$M_3 \cdot (K+\Delta K) = M_3 \cdot K + M_3 \cdot \Delta K \qquad (4.5)$$

$$N_3 \cdot (K+\Delta K) = N_3 \cdot K + N_3 \cdot \Delta K \qquad (4.6)$$

where ΔK is the length of the voxel in the K direction. Thus

there is no multiplication and only one addition can produce the desired values, once $L_3 \cdot K$, $M_3 \cdot K$, and $N_3 \cdot K$ are found.

A similar approach is used for I and J directions. This procedure then can calculate all elements of the transformation matrix only by addition operations, after the initial values and the increment amounts have already been found by nine multiplies. Frieder's method, on the other hand, needs 9 X N multiplications for the original image whose size is N X N X N. N^3 multiplications might be necessary, if no tables are used.

4.2.3 Improvement of the image quality

The skull surface image is produced by using the gradient shading method[7] applied to the Z buffer. This method has the defect of suffering from some bumpy shapes on a generated object due to the essentially angular shape of individual voxels, but it is a rather simple procedure to find brightness of the images expressed by the Z buffer. Chen et. al. proposed the normal-based contextual shading in order to reduce this kind of bumpy shapes[12]. This method estimates the normal vector of the skull surface by the relation of the neighboring voxels in order to decide the brightness of the point. Although the image quality by this algorithm is rather good, it requires much time due to the 3-D procedure.

2-D filtering techniques to smooth the Z buffer may be effective to eliminate small bumpy noise without losing essential shape features of the displayed object. The variable weight filter is proposed for this purpose, and compared with the following three kinds of smoothing filters with the mask size of 3X3 or 5X5 pixels, and their iterative applications.

(1) variable weight filter[13]: The output value at a pixel (i,j) is given by the weighted sum of the input pixel values in the neighborhood of (i,j), where the weight values for neighboring points depend on the differences between the depth values at the pixel (i,j) and at its neighbors.

$$g_{ij} = \sum_{m=-1}^{1} \sum_{n=-1}^{1} \{ (W_{mn} \cdot Z_{i+m,j+n}) / W_{mn} \} \qquad (4.7)$$

where

Z_{ij} : input value at (i,j)

g_{ij} : output value at (i,j)

W_{mn} : weight.

The weight W_{mn} is defined by

$$W_{mn} = W(d_{mn}) = \begin{cases} 1, & \text{if } d_{mn} \leqq a, \\ 0, & \text{if } d_{mn} \geqq b, \\ 1/2 + 1/2 \cos\{(d_{mn}-a)\pi/(b-a)\}, & \text{otherwise,} \end{cases} \quad (4.8)$$

where

$$d_{mn} = Z_{i+m\ j+n} - Z_{ij} \quad (4.9)$$

$a = 2.0$

$b = 5.0$.

(2) edge-preserving filter[14]: Divide the neighborhood of the pixel P into a few subregions and find the subregion where the variance of the input densities is minimum. The output value at P is obtained by averaging input densities in this subregion.

(3) median filter[15]: The median value in 3 X 3 neighboring pixels is used for the output of the center pixel.

Comparison of these filterings can be seen in Fig.4.3. According to the visual evaluation by medical doctors, the median filter and the variable weight filter were considered to be effective for improvement of understandability of the bone structure.

4.3 PREDICTION OF THE FACE SHAPE

In craniofacial surgery, it is important, not only for doctors but also for patients (and their families), to know how their faces will be changed by the operation. However, it is not easy to predict the precise shape of the post-operative face, since muscular changes resulting from the surgery cannot be found by a simple way. We implemented the function to roughly predict the patient's post-operative face by considering only the bone and the exterior tissue. This function has been developed only for

relatively simple surgery of brachycephaly at the present time, since it strongly depends on the individual operative strategy. The operation for correction of brachycephaly includes moving the anterior part of the skull forward to expand the volume of the skull. The predicted post-operative face is constructed by computer from the skull reformed according to the selected operation plan. The outline of this function is as follows.

(1) According to the decided plan,the skull is cut and moved with the attached soft tissues, i.e. brain, skin, etc. This process is illustrated in Fig.4.4. Ocular globes(or eye balls) should be detected in the planning stage to determine the region which will not be moved during simulated operations, since eye balls are not moved in real operations. Automatic detection of globes is difficult by using CT values alone because the difference of CT values between the eye region and other soft tissue regions is not so large as to respond well to the simple thresholding technique. Therefore, we detect the ocular globes on a slice by a semi-automatic procedure partially supported by interactive help of the operator.

The operator specifies by the crosshair the center point (X_e,Y_e) and the radius R_e of an ocular globe on a typical slice containing it displayed on the graphic terminal. For each slice, we test the following conditions to determine whether an globe exists on it or not.

Condition(a): All CT values in a circle with the center point (X_e,Y_e) and the radius R_e on the slice lie in the range of those of soft tissues (Fig.4.5(a)).

Condition(b): Find the first encountered pixel which is in bony region. Then the Y coordinate of this pixel Y_b is greater than Y_e (Fig.4.5(b)), by scanning all pixels whose X coordinates are X_e from the anterior part of the face on a slice.

We consider that an eye ball exists if and only if both of two conditions are satisfied. Ocular globes might not appear even if one of the conditions holds alone as shown in Fig.4.6. This

process is applied to both right and left eye ball regions so that we may detect existence of globes, and not move soft tissues on such slices.

(2) New slices are reproduced in a computer by using the planning data shown in Fig.4.7.

(3) Since gaps may remain on the skull surface after cutting and moving bone blocks at the planning stage, we should use a rendering technique to smoothly connect soft tissues on adjacent slices. In our system, "Cylindrical Coordinate Expression"(CCE) technique is employed for reconstructing the surface of soft tissues(face). CCE uses CCS described in 3.2.2 in order to specify a point in 3-D space. This technique was improved to be useful in generating a 3-D object surface from a set of CT slices. The linear interpolation of the surface data between two adjacent slices is also used to smooth the reconstructed post-operative surface(Fig.4.8).

Although the CCE generates good shapes of the face and shoulders, a hole may appear at the top of the head if the input CT slices do not cover the upper part of the head. In order to overcome this difficulty, "Polar Coordinate Expression"(PCE) technique was developed for reconstructing the surface of the face. This method is suitable especially for the upper part of the head. The PCE can generate natural shape of the head by connecting the surface around the top of the head. We then combine advantages of CCE and PCE in order to reconstruct more natural shape of the human head and face, since the CCE is much superior for generating the face and shoulders. On the other hand, the voxel type expression of 3-D objects from 2-D CT images is also recommended for this purpose. In section 5.5, we compared these methods to predict the shape of the post-operative face.

The method described here cannot estimate the precise shape of the soft tissue, since it does not take into account the material properties of the soft tissue. However, we can assume that the thickness of the soft tissue over the skull is approximately constant especially for the surgery of the upper

part of the head. From this point of view, we have received the reputation by surgeons that our method is useful enough to present the rough shape of the post-operative soft tissue for the surgeries of the upper part of the head.

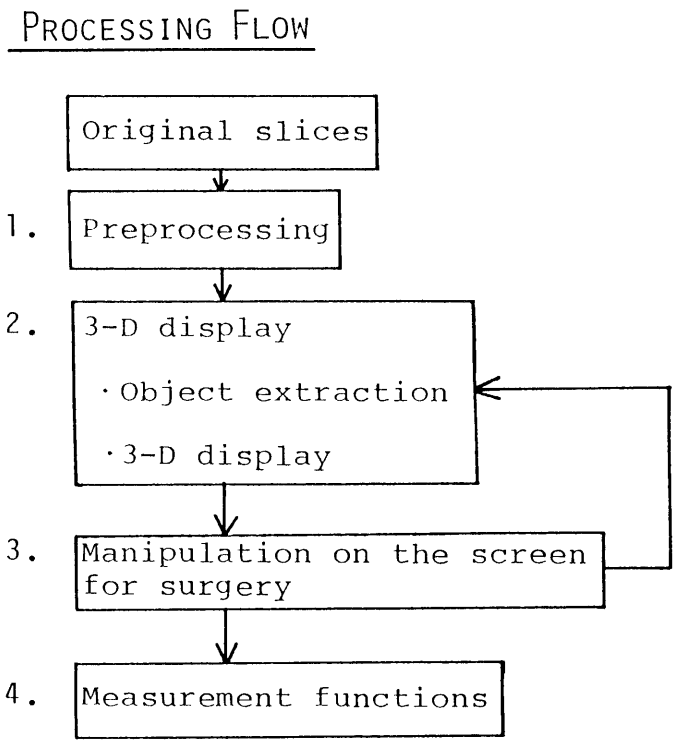

Fig.4.1 Processing flow of NUCSS.

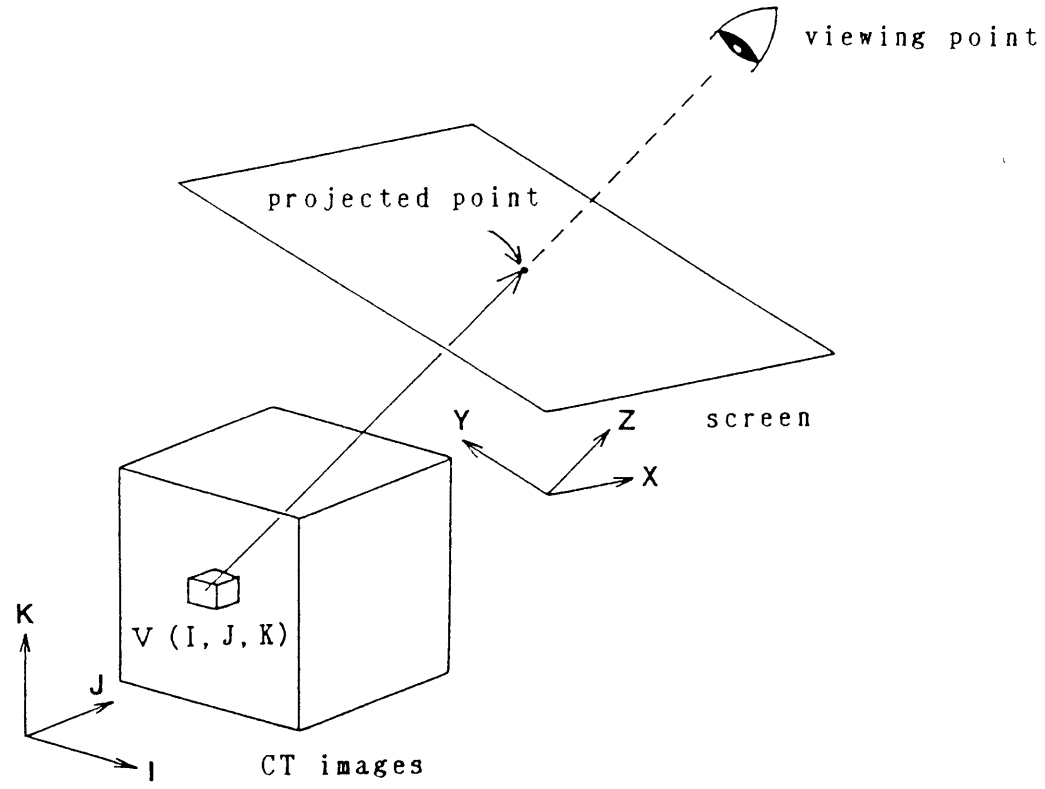

Fig.4.2 Voxel projection.

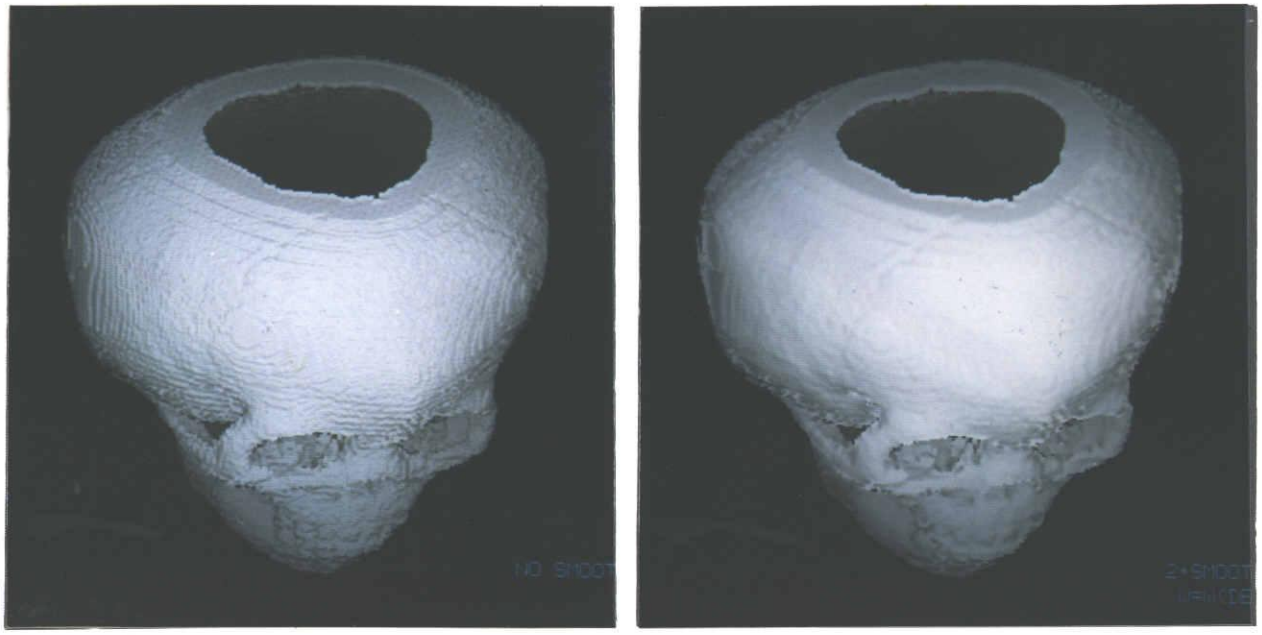

(a) No filtering (b) Variable weight filtering

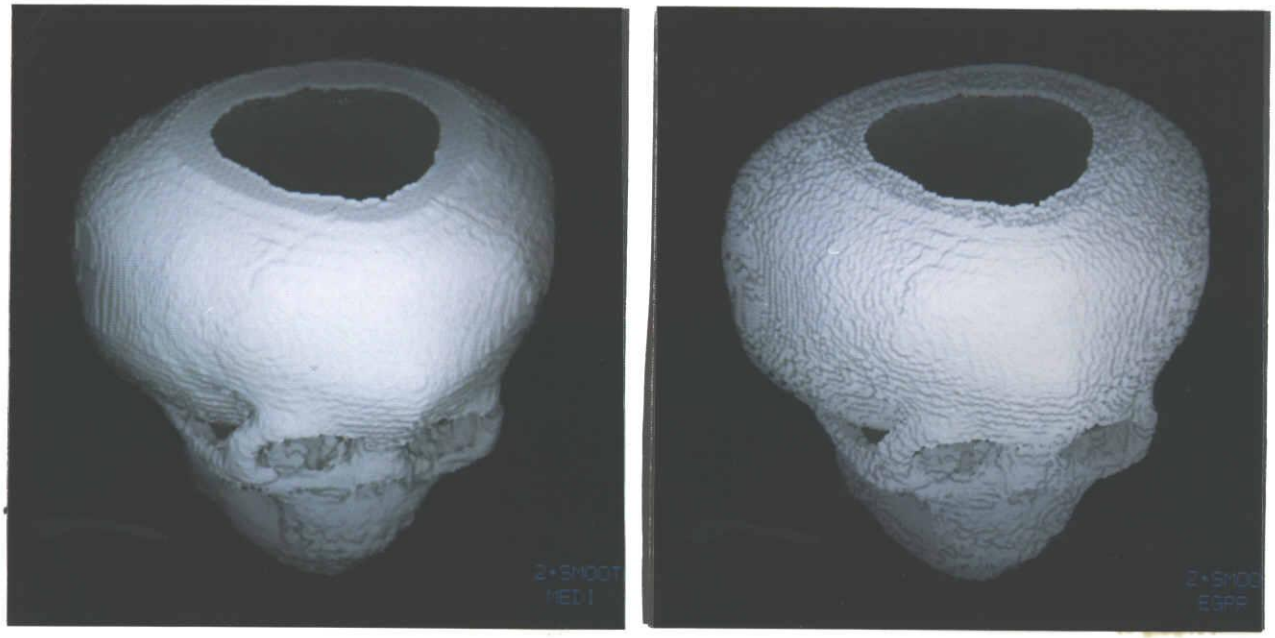

(c) Median filtering (d) Edge-preserving filtering

Fig.4.3 Comparison of images generated by using three kind of filters.

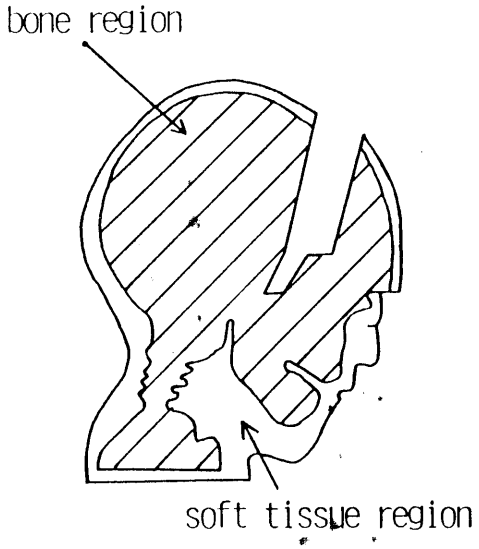

Fig.4.4 Shift of a bone block with soft tissue.

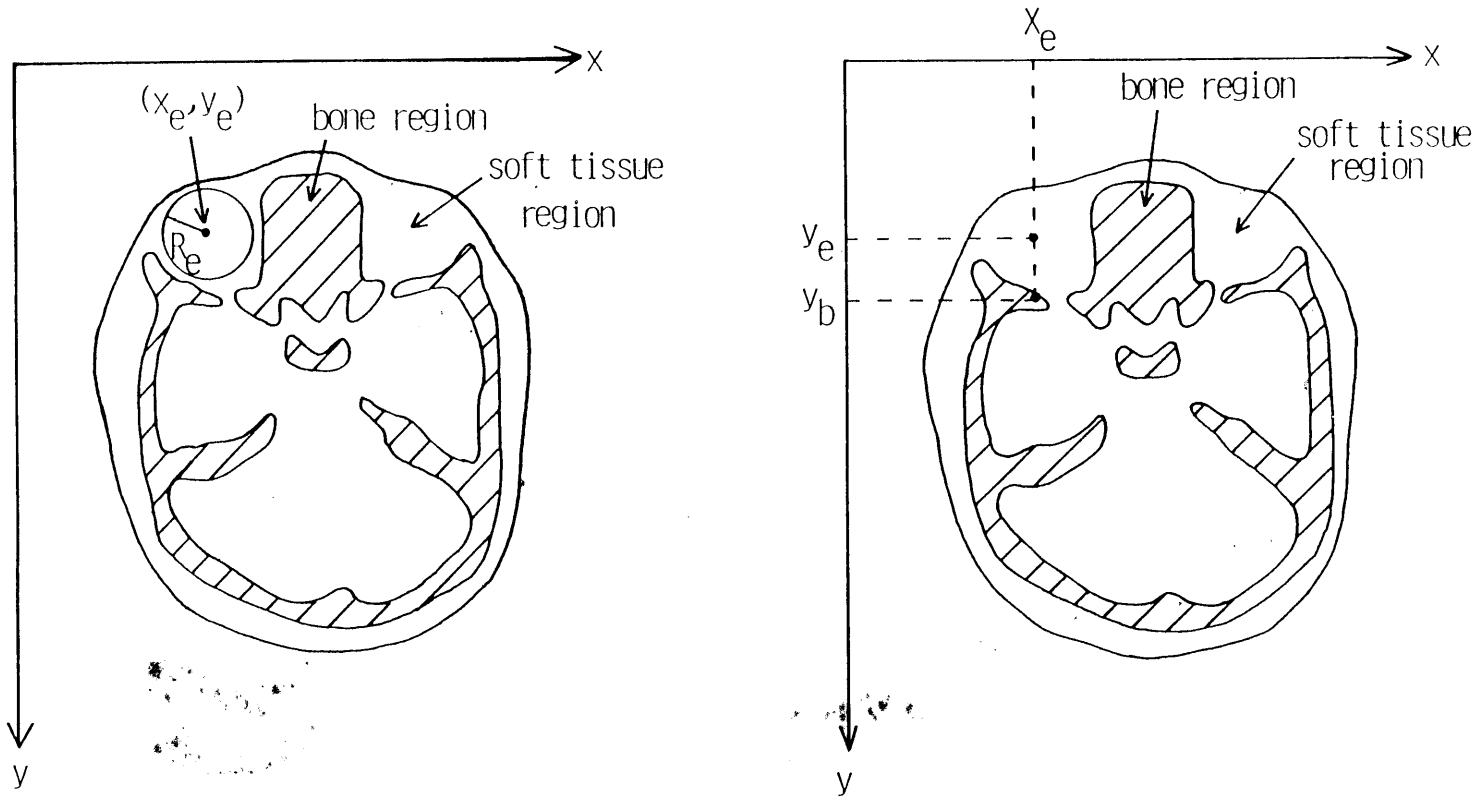

(a) Condition (a) (b) Condition (b)

Fig.4.5 Conditions for detecting ocular globes on a slice.

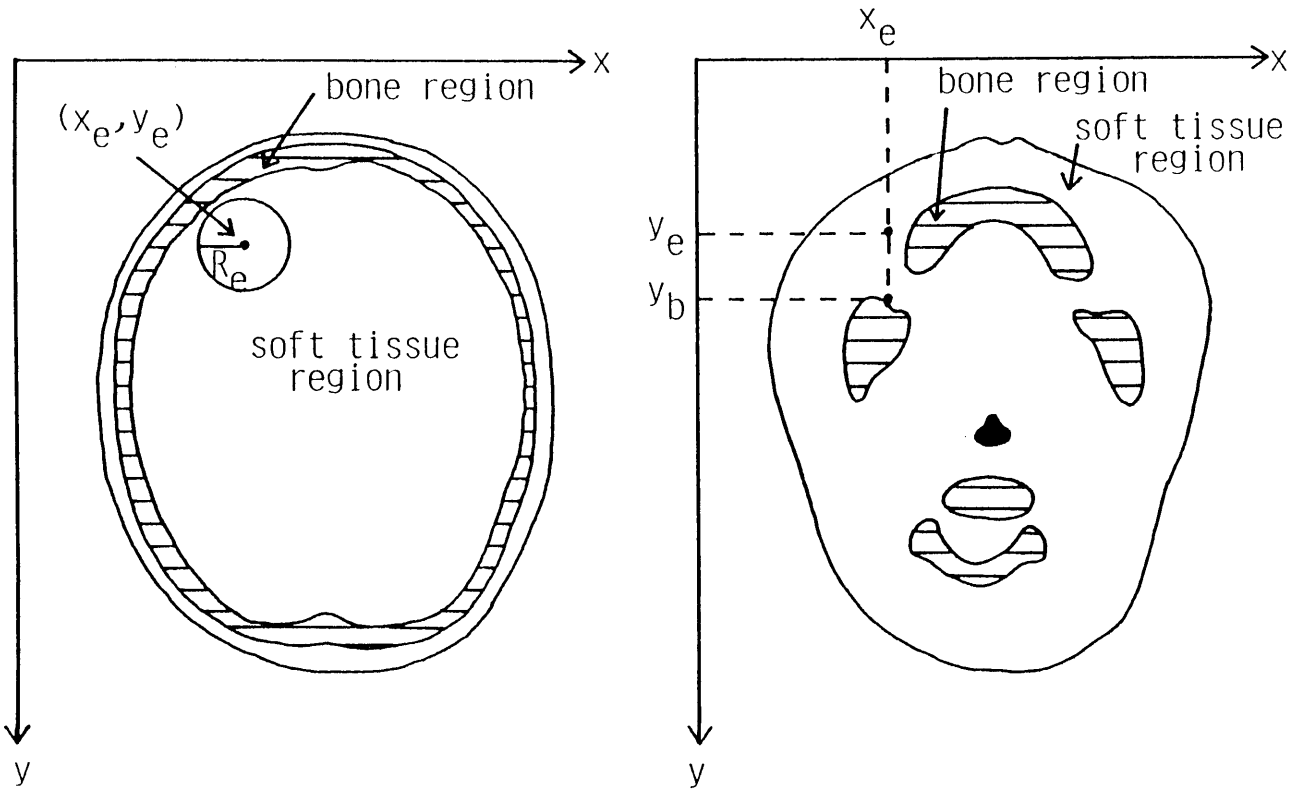

(a) Failure case using the condition (a)

(b) Failure case using the condition (b)

Fig.4.6 Failure cases using a single condition.

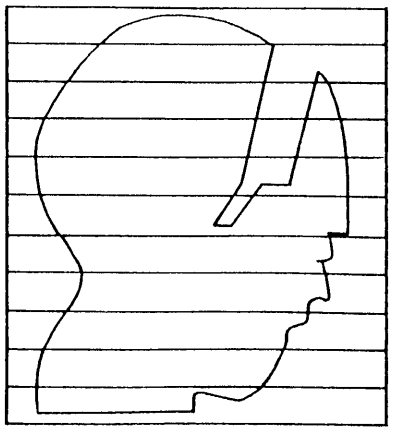

Fig.4.7 Generation of new slices after the shift of bones.

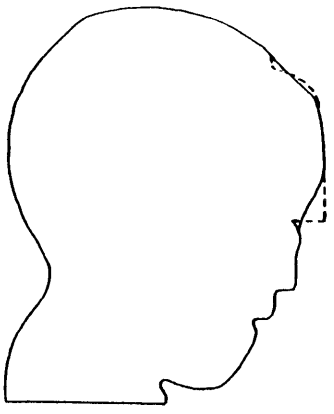

Fig.4.8 Surface smoothing in a 3-D image of head.

5. SURGICAL PLANNING BY NUCSS

5.1 INTRODUCTION

In this chapter, we will describe functions to make a surgical plan in NUCSS. Most of the surgical plans can be made on the 3-D skull image of the lateral view. NUCSS has been developed to simulate the procedure of the planning method which is actually used by doctors. The basic principle in this system is to interact with the object through its depiction in the view space, transform the user-specified manipulative operation in the view space to one in the object space, and then carry out the operation in object space.

The procedure to manipulate the 3-D skull on the lateral view of the skull is described in section 5.2. Another simulation scheme for osteotomies
is introduced in 5.3. We prepared some measurement functions to confirm the decided plan by NUCSS. Section 5.4 describes this function. Actual clinical applications are shown in 5.5.

5.2 PLANNING ON THE SIDE VIEW

At the present time, most planning of craniofacial surgery is made by surgeons using a lateral view of the skull in an ordinary x-ray image. After tracing the skull silhouette on a paper from the x-ray film, they cut the paper into small pieces and rearrange a set of pieces according to their plans (Fig.5.1). It is difficult in this method to understand 3-D features of the post-operative skull shape from the paper model. Our system NUCSS, on the other hand, can generate 3-D images observed from arbitrary directions to examine the validity of plans made on the graphic terminal instead of a paper model [1,2]. This function is applicable only to the operation in which bone blocks are cut symmetrically with respect to the sagittal plane. Nevertheless,this kind of cutting is sufficiently useful for most craniofacial surgeries.

The details of this planning procedure is as follows. First, the skull of the patient viewed from the side is displayed on the graphic terminal. Then a doctor draws the planning curve as a guideline for reforming a distorted skull. According to the planning curve, the cutting lines are stored in the system as a list of all border pixels located on the given planning curves. All border pixels are assigned their labels so that each bone block defined by its border pixels may be identified and manipulated separately. For example, we can move these blocks to any location by specifying the block to be moved and then giving the position of destination. Shift, rotation, reverse movement and arbitrary sequence of them are available for moving. All processes described above are selected by the hair cursor from the menu displayed at the bottom of the screen. Mathematically each step of block movement is represented by a transformation matrix of the 3-D affine transformation and a sequence of movements is described by the products of matrixes corresponding to an individual movement. Thus, the final state of a block is easily found even after a long sequence of movements given interactively by a user.

After the plan which seems to be the most suitable for the patient is determined on the side view of the skull, the feasibility of the plan should be confirmed carefully from 3-D viewpoints for guaranteeing the safety of the actual surgery. Our system can generate an arbitrary 3-D view of the skull after the bone blocks were moved according to the plan.

It is desirable that planning on the side viewed skull image described above can be easily applied to any viewed image, since the initial reference image should not only be the side viewed one, but also images viewed from various directions. In our system, surgeons can make a surgical plan by selecting the most suitable direction for cutting each bone. Therefore, they can cut a bone block from any angle according to the real movement of the electric surgical knife. The final plan is decided by combining several plans decided from different directions. The planning processes are shown in section 5.5.

5.3 CUTTING AND MOVEMENT OF AN ARBITRARY SHAPE OF BONE BLOCKS

The function described in the last section is applicable only for operations which cut the bone by planes vertical to the screen. Although this is useful for simulation of most craniofacial surgery, it is still not adequate for operations which requires other types of cutting, because it exclusively requires symmetrical bone cutting. We developed another function to deal with bone cutting operations different from those presented in section 5.2. Here the cutting bone block can have an arbitrary shape and thickness, and hence the system can be applied for the operative planning which includes asymmetrical bone cutting[3]. Therefore the new function can be used not only for craniofacial surgery but also for brain surgery in general, since it is possible to simulate opening the skull arbitrarily according to the location of the diseased parts in the brain. We will show the process of this function in detail.

5.3.1 Interactive specification of the cutting bone

Assuming that the shape of the bone block to be cut is an arbitrary polygon with finite thickness, vertices of the polygon are input sequentially on a 3-D skull image. The skull with this polygon can be observed from all directions to examine the shape and the location of the removal region. In order to superimpose the region precisely on the skull, all the world coordinates of pixels on the polygon contour should be calculated from the screen coordinates and stored in the system because they are invariant regardless of viewing angle.

Contour points of the cutting region are marked on the skull utilizing the transformation from the world coordinate to the screen coordinate. This contour line may become discontinuous, if a viewing direction different from that used for defining the removal region is chosen. For such parts of discontinuity, new points are inserted by linear interpolation to connect the line smoothly.

5.3.2 Removal of the specified skull region

The removal region is decided slice by slice. Since there might be few cases that the stored contour point exists on a slice, we first find the contour point which is on one of the original slices. For an original slice **S** on which the contour point is missing, we find the pair of the contour points such that by connecting them a line segment intersecting the slice **S** is generated. Then the contour point on the slice **S** is determined by the intersecting point between the line and the slice **S**. Let us denote a sequence of contour points by $C_1, C_2, ---, C_m$, the Z coordinates of these points by $Z_1, Z_2, ---, Z_m$ and the Z coordinate of the slice by Z_S as shown in Fig.5.2. The point pair C_i and C_{i+1} should satisfy the following condition:

$$(Z_i - Z_S)(Z_{i+1} - Z_S) < 0 \qquad (5.1)$$

where $1 < i < m$ and $Z_{m+1} = Z_1$.

Then the X and Y coordinates X_K and Y_K of the contour point on a slice whose Z coordinate is Z_S are determined by the interpolation of the X and Y coordinates using X_i, Y_i and X_{i+1}, Y_{i+1}, respectively, of the points found above. Namely,

$$X_K = (X_i \mid Z_{i+1} - Z_S \mid + X_{i+1} \mid Z_i - Z_S \mid) / \mid Z_{i+1} - Z_i \mid , \qquad (5.2)$$

$$Y_K = (Y_i \mid Z_{i+1} - Z_S \mid + Y_{i+1} \mid Z_i - Z_S \mid) / \mid Z_{i+1} - Z_i \mid . \qquad (5.3)$$

For all pairs of the contour points satisfying the condition (5.1), the interpolated contour points are determined by Eq.(5.2) and (5.3). This gives all contour points on the slice $Z=Z_S$. The world coordinates of a point on the user specified contour are determined using the z-buffer and the viewing direction. The point is not necessarily on a slice. Therefore, the contour point on a slice should be found by eq.(5.2) and (5.3).

The removal process is carried out by extracting all pixels in the removal bony area on each slice. Assume, for instance, that contour points K_1 and K_2 are found on the slice $Z=Z_S$ as shown in Fig.5.2. The locations of these points are determined by CCE as (r_1, θ_1) and (r_2, θ_2), respectively. We decide the removal

region by these coordinates as illustrated in Fig.5.3. First, we calculate the maximum and the minimum radii R_{max} and R_{min} for the removal area as follows:

$$R_{max} = \max (r_1, \theta_1) + \Delta_1, \quad (5.4)$$

$$R_{min} = \min (r_2, \theta_2) - \Delta_2, \quad (5.5)$$

where Δ_1 and Δ_2 are suitable constants selected beforehand so that R_{max} and R_{min} cover the whole bone region. Second, we remove all pixels within this area. The pixel $P(r_P, \theta_P)$ should be removed, if and only if the following conditions are satisfied:

$$\text{Condition:} \quad \theta_1 < \theta_P < \theta_2 \quad \text{and} \quad R_{min} < r_P < R_{max}. \quad (5.6)$$

By applying this process to all slices, the removal region is eliminated from the displayed 3-D image of the skull.

5.4 MEASUREMENT FUNCTION

Geometrical information concerning the degree of deformity in the shape of the skull is sometimes necessary for surgeons to make planning of craniofacial surgeries more precise[4,5]. We developed a function to find the distance between two points specified on a displayed skull image. After displaying a skull image from a suitable angle, a user interactively (i.e. by crosshair) inputs two points on a skull image which are the end points of the distance he wants to know. Values of X and Y coordinates of the two points are determined in the screen coordinate system when he inputs them, and Z coordinates are obtained from the Z buffer table generated at the display stage in the form of Z=f(X,Y). The distance is calculated using the world coordinates of the two points which are transformed from the screen coordinate system. Similarly, the distance between two points along to the object surface can be measured in our system.

The angle for the rotation of a bone block is important in reconstructing natural shape of the head. Therefor, our system

displays the angle for the rotation, when a bone block is rotated on the graphic terminal.

As an estimation of the decided surgical plan, the volume of the inner part of the skull is most important. We calculate the change of the volume between pre-operation and simulation in order to verify the plan. In the case of an actual surgical plan which a surgeon decided, the volume of pre-operation (918 cm^3) would be enlarged to 1137 cm^3 after the operation. The numbers of these volumes are considered as reasonable compared to surgeon's experiences.

5.5 EXPERIMENTAL RESULTS

In this section, we will show several examples of applications. Two kinds of X-ray CT image sequences given below were used as the input data.

image I: 512 x 512 pixels x 100 slices with the slice interval of 2mm. The pixel size in the plane of section is 0.7mm

image II: 512 x 512 pixels x 50 slices with the slice interval of 4mm. The pixel size in the plane of section is 0.7mm.

The resolution is reduced to 256 x 256 before the process for saving computation time and memory[2]. Original slices are shown in Fig.5.4.

The process of surgical planning by this system is shown in Fig.5.5. First, the side view of the skull is displayed on the graphic terminal(Fig.5.5(a)). Second, the command for bone cutting is selected from the menu shown at the bottom of the screen, and according to a doctor's plan, the cutting line is input on the skull interactively by hair cursor(Fig.5.5(b)). Third, several manipulations are applied to each bone block. In Fig.5.5(c), for example, the anterior bone block is shifted backward after rotating 90 degrees and the posterior block is reversed after being moved to the upper left. This plan can be

checked by a 3-D image of the reformed skull observed from any direction a user requires. One of the images for the examination is shown in Fig.5.5(d). An example of clinical application is shown in Fig.5.6. For more complex surgeries, several planning from different directions can be combined. Fig.5.7 shows the process of planning for a complex surgery. Another result of the planning of a complex surgery is shown in Fig.5.8. Input data used here is the "image I" described above. For the image generation, we used the gradient shading method[6] after smoothing the Z buffer by the variable weight filter.

Fig.5.9 shows examples of cutting a polygonal shape bone block. The removal region specified by vertices of an arbitrary polygon is seen on the skull image in Fig.5.9(a). The location and the shape of this region may be checked from another viewing point (Fig.5.9(b)). The 3-D shape of the skull with the decided cutting area removed like the real operation can be observed from different directions as shown in Fig.5.9(c),(d). "Image II" was used as the input data and the depth coding was employed to generate images for this function.

The predicted face images using CCE are given in Fig.5.10. For comparison, pre-operative, predicted and post-operative face images are shown in upper left, lower left and lower right, respectively. The skull shapes of the pre-operation, simulation and the post-operation for this case are shown in Fig.5.11. Here we used the method for extracting the ocular globes described in section 4.3. The faces generated by CCE, voxel expression, and PCE-CCE are compared in Fig.5.12. The PCE-voxel combined method can present the face shape more precisely than any other method, where PCE is used for the upper part of head and voxel is used for the lower part of head and the face (Fig.5.13). Figs.5.14 and 5.15 show clinical applications of this scheme. We used "image I" as the input data here.

The system was implemented on FACOM M-380 and 382, and the program was coded in FORTRAN 77. It took about 1 minute for generating an image in Fig.5.5, 30 seconds for an image in Fig.5.9, and 10 seconds for an image in Fig.5.10. The graphic terminal

display used here is GRAPHICA M-1008,whose resolution on the screen is 1024 x 1024 dots, and color information of each dot is stored in the corresponding 24 bits memory of which 8 bits each are assigned to Red,Green,and Blue components. Generated images are projected on a 512 x 512 plane and then magnified to 1024 x 1024 for displaying.

5.6 CONCLUDING REMARKS

A new 3-D CT image display system called NUCSS has been developed for craniofacial surgical planning. NUCSS is now possible to find the best surgical plan before actual operations by interactively manipulating a displayed skull image on a graphic terminal. According to the decided plan, the post-operative face shape can be automatically predicted and displayed as a 3-D shaded image.

Finally, the major problems for future studies are summarized as follows.

(1) From a set of successive CT slices, 3-D images are generated as precisely as possible. We understood 2-D filtering techniques applied to Z-buffer could be effective to improve the quality of the displayed 3-D image produced by using the gradient shading method. This scheme can be used for any voxel type images. For 3-D image generation in the future, the quality of the resulting image should be much more sophisticated, and the required time for generation should be much more reduced.

(2) Surgical planning by NUCSS can be applied to most of the actual craniofacial surgery at the present time. We also have already used our system in an orthopedic surgery of the hip joint[7]. However, some new functions are expected to be developed to cope with more complex surgeries and for better interface between a surgeon and NUCSS. Planning scheme from one viewing direction does not work well enough for some of the recent complex surgeries. Furthermore, from one viewing direction, it is still difficult to specify the exact location where the bone block should be moved. We are now developing new functions for solving these problems in NUCSS[4].

(3) The prediction of the post-operative face shape according to the decided plan in NUCSS is performed by considering only the bone and the exterior tissues. It will be necessary to consider muscular changes resulting from the surgery in order to predict more precise shape of the post-operative face in the future.

(4) Although we did not discuss efficient object representations for voxel-based images, it is important for rapid display and data compression in the actual usage of our system [8]-[12].

Furthermore we are now planning to improve functions in our system to cope with more complex craniofacial surgery and operations in a wider range of fields. Measurement functions to obtain quantitative information such as brain surface and measures of deformity should be added in the future. This system will be also used for a variety of surgeries, such as orthopedic surgery, surgery for cancer in the skull, or cosmetic surgery. It might be available even for the scientific investigation (forensic medicine) of police by predicting the face shape from a corpus delicti.

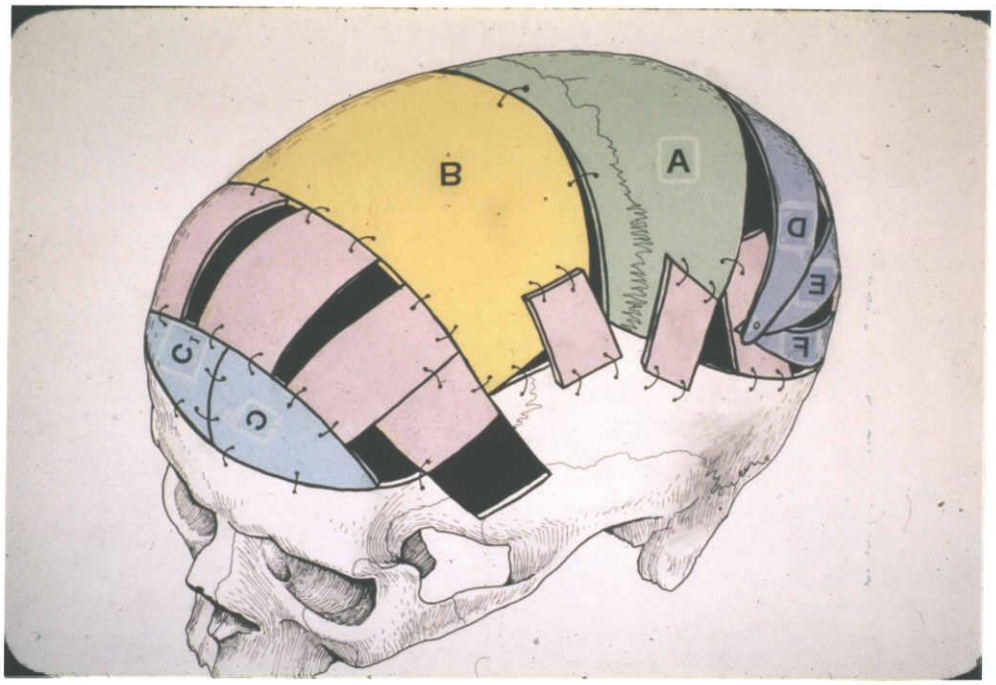

Fig.5.1 Sketches for a craniofacial surgery and reconstructed bony blocks.

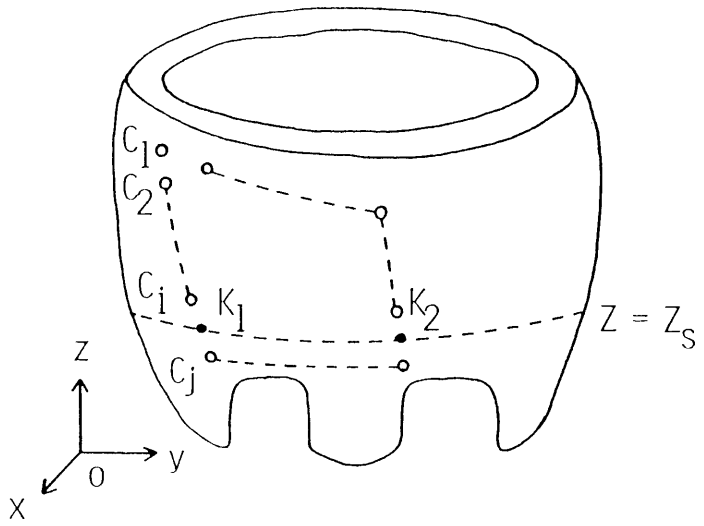

Fig.5.2 Determination of contour points on the slice $z=z_s$.

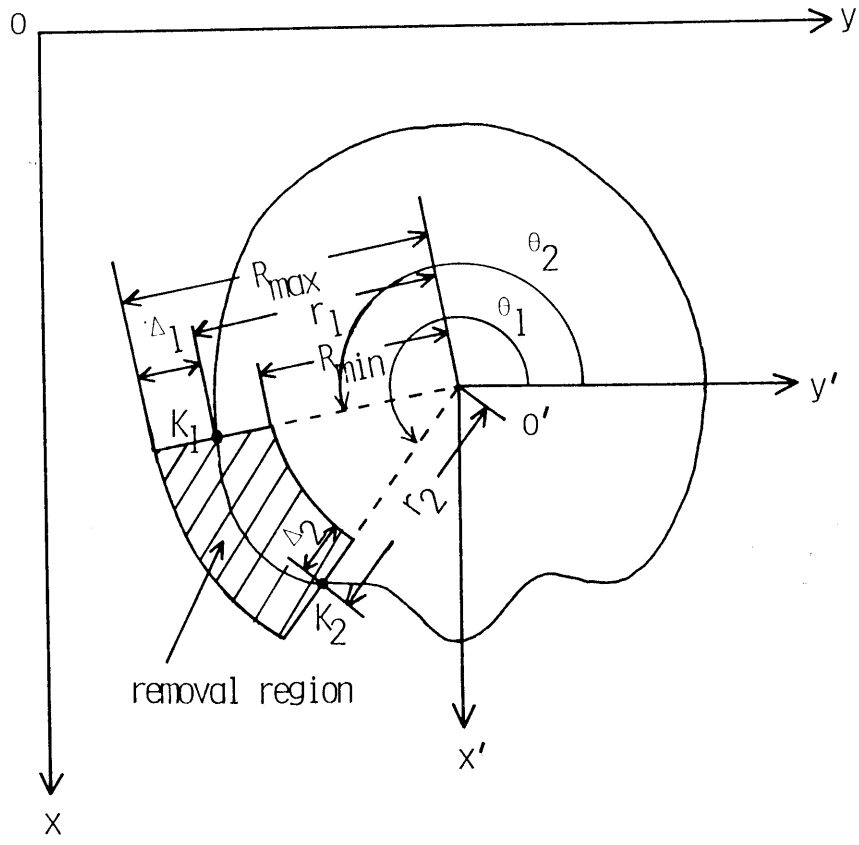

Fig.5.3 Removal region on a slice.

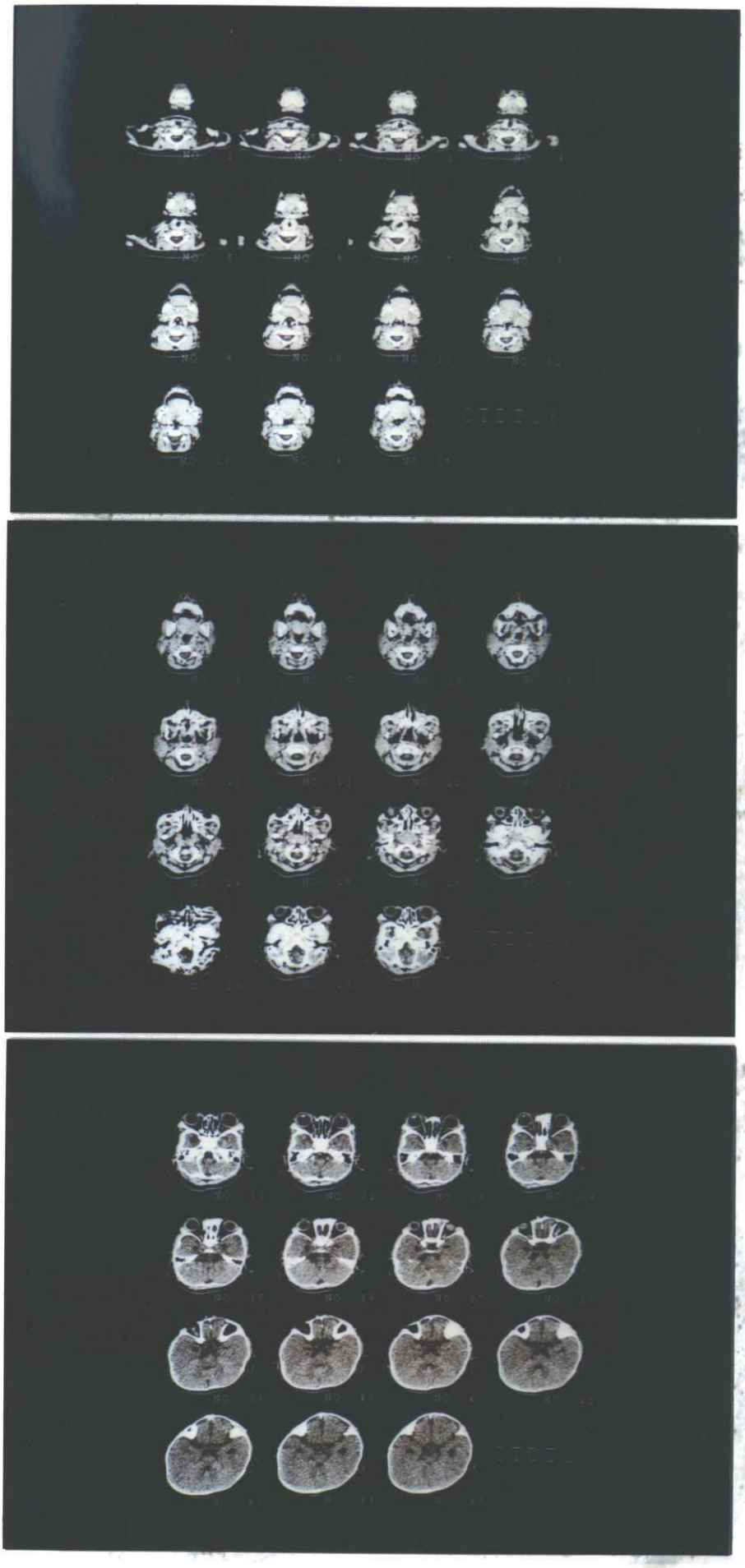

Fig.5.4 An example of original slices.

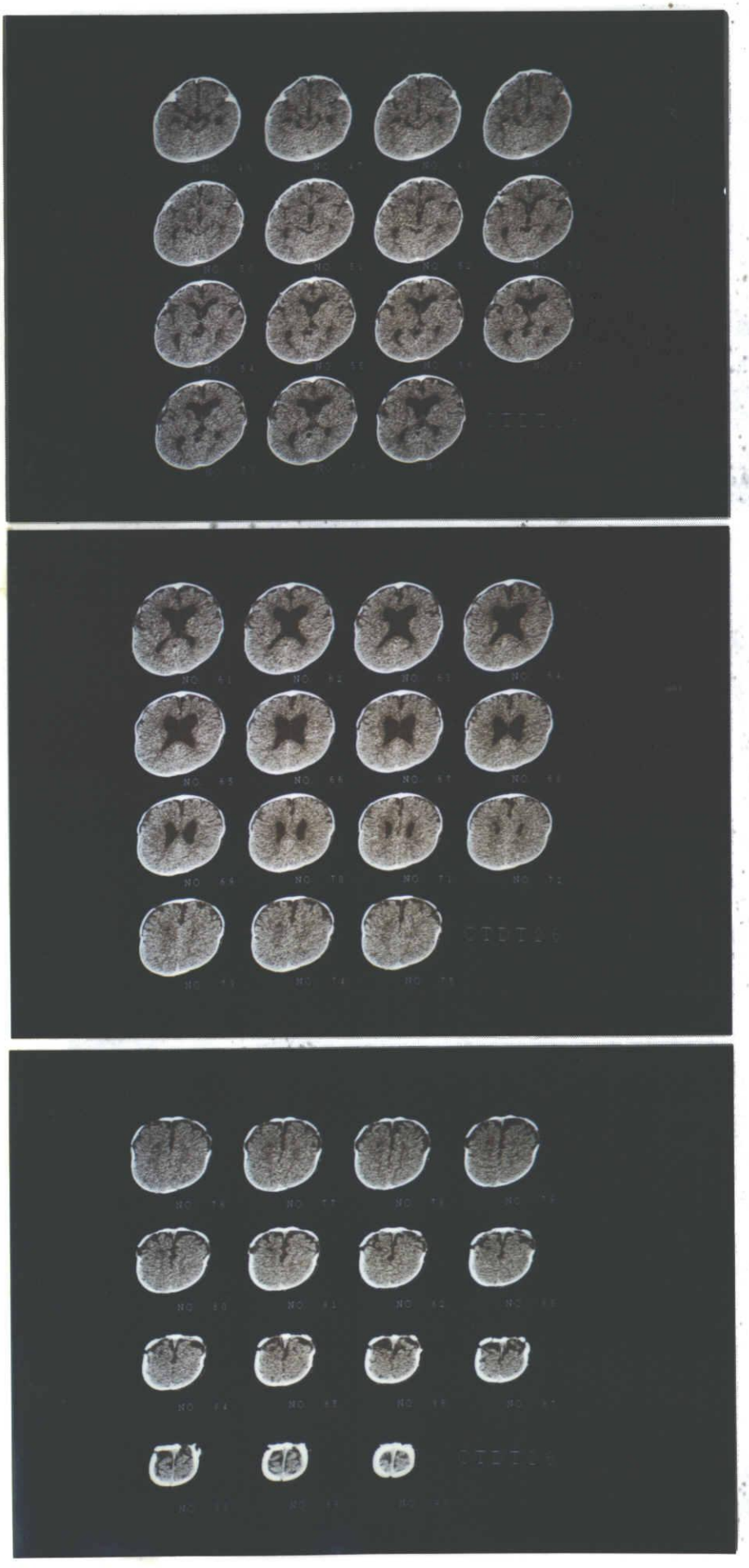

Fig.5.4 An example of original slices.

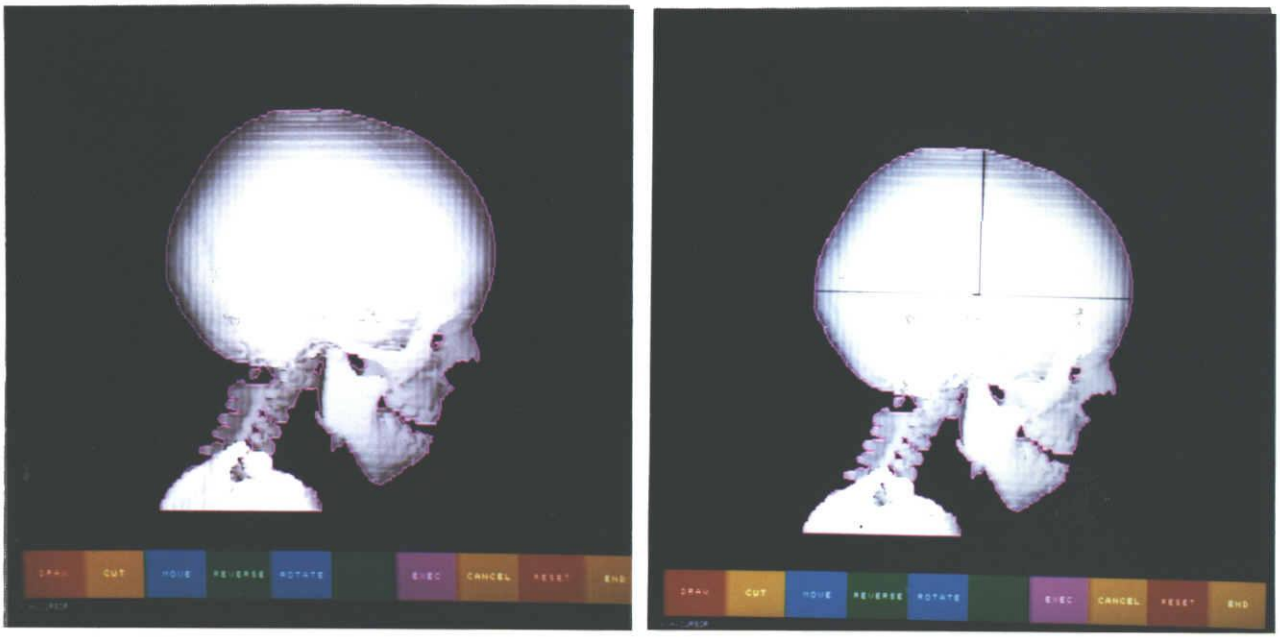

(a) Side view (b) Input cutting lines

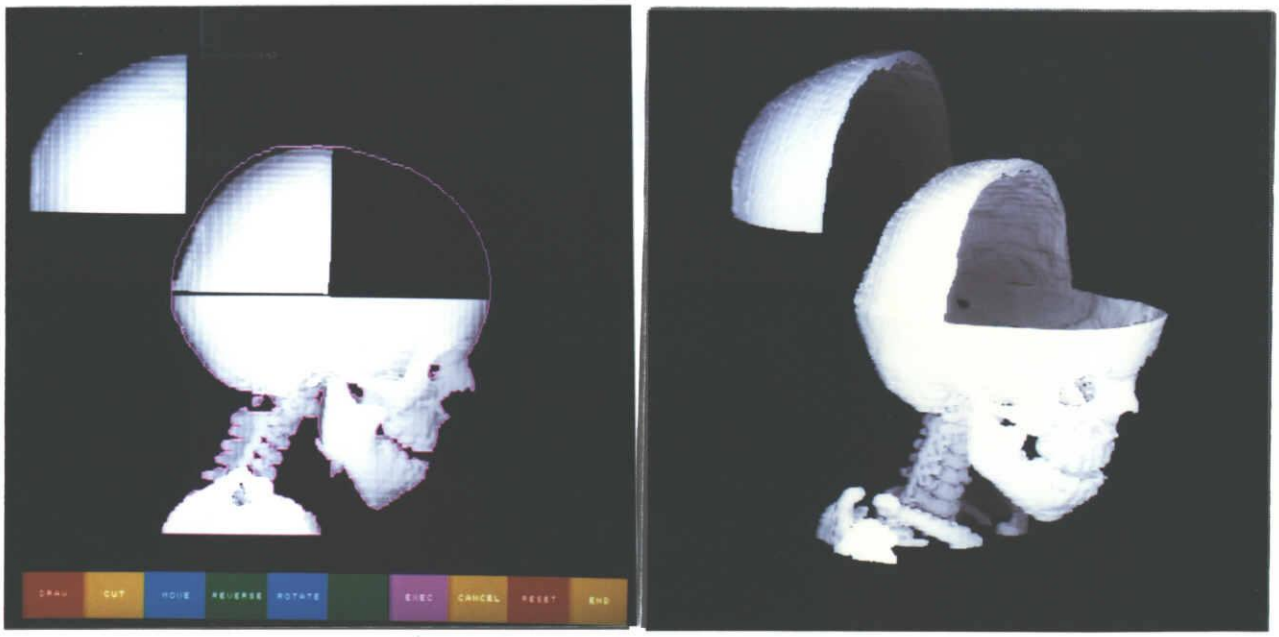

(c) Moved and rotated blocks (d) 3-D display

Fig.5.5 Surgical planning on the lateral view.

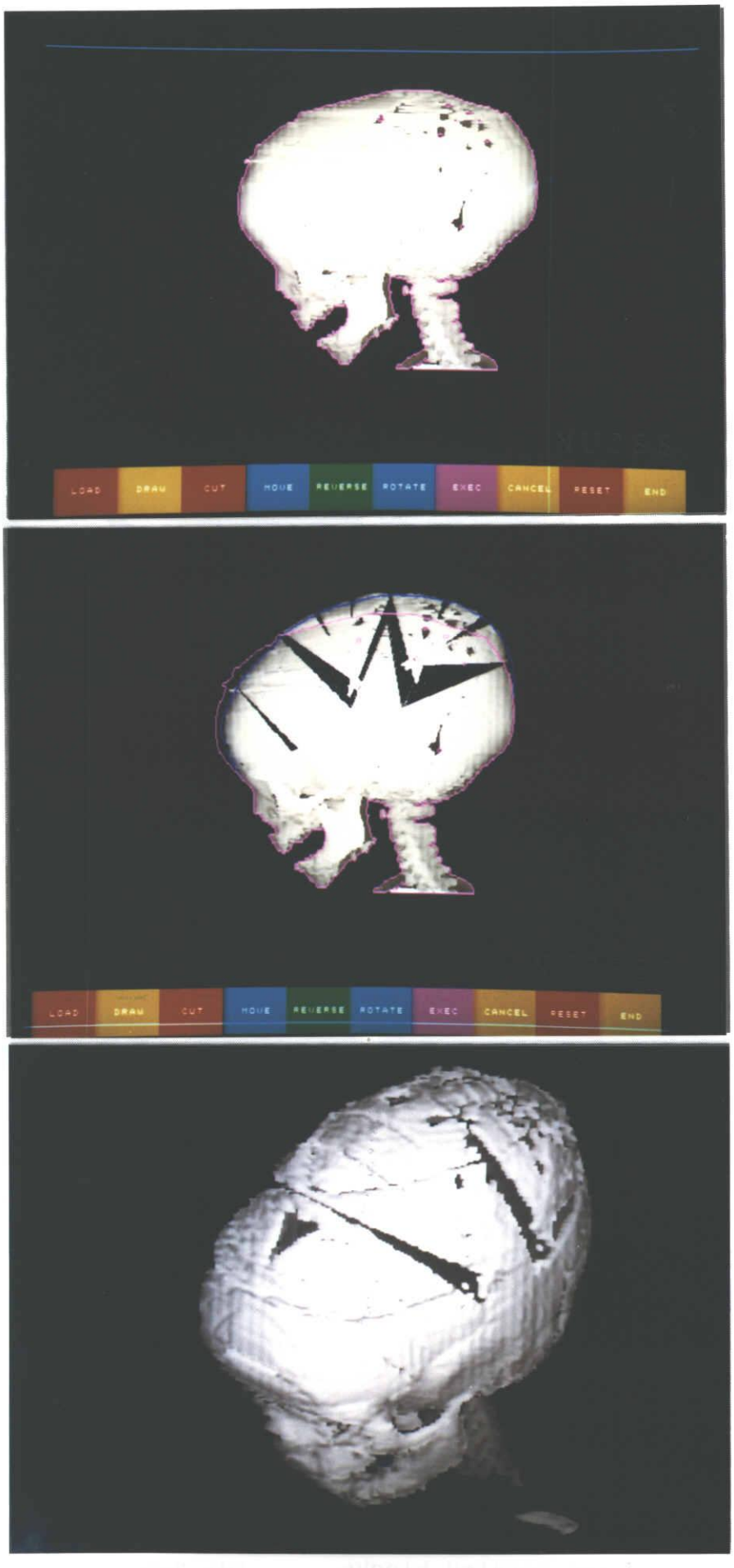

Fig.5.6 An example of clinical application.

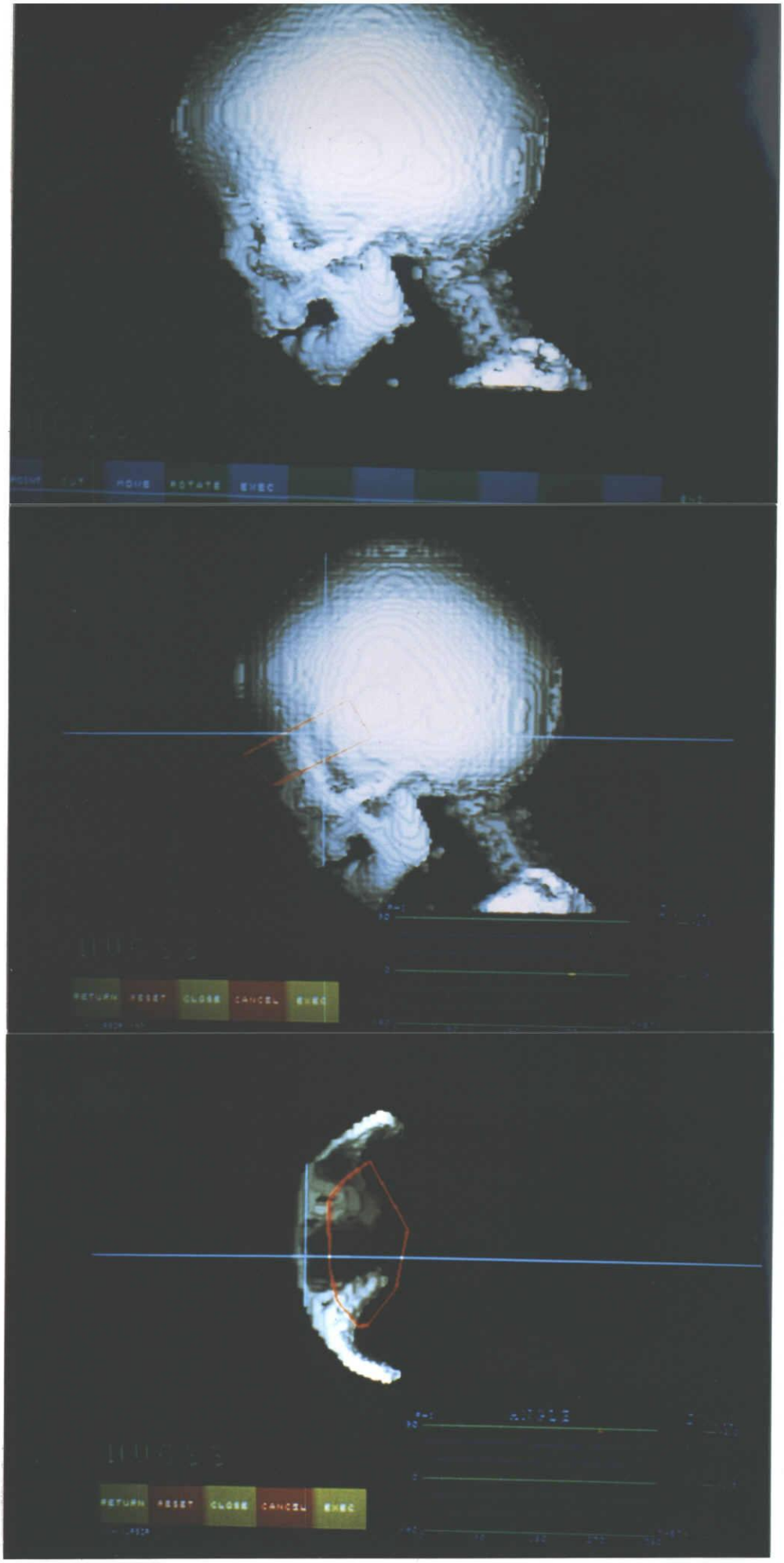

Fig.5.7 An example of the plan for a complex surgery.

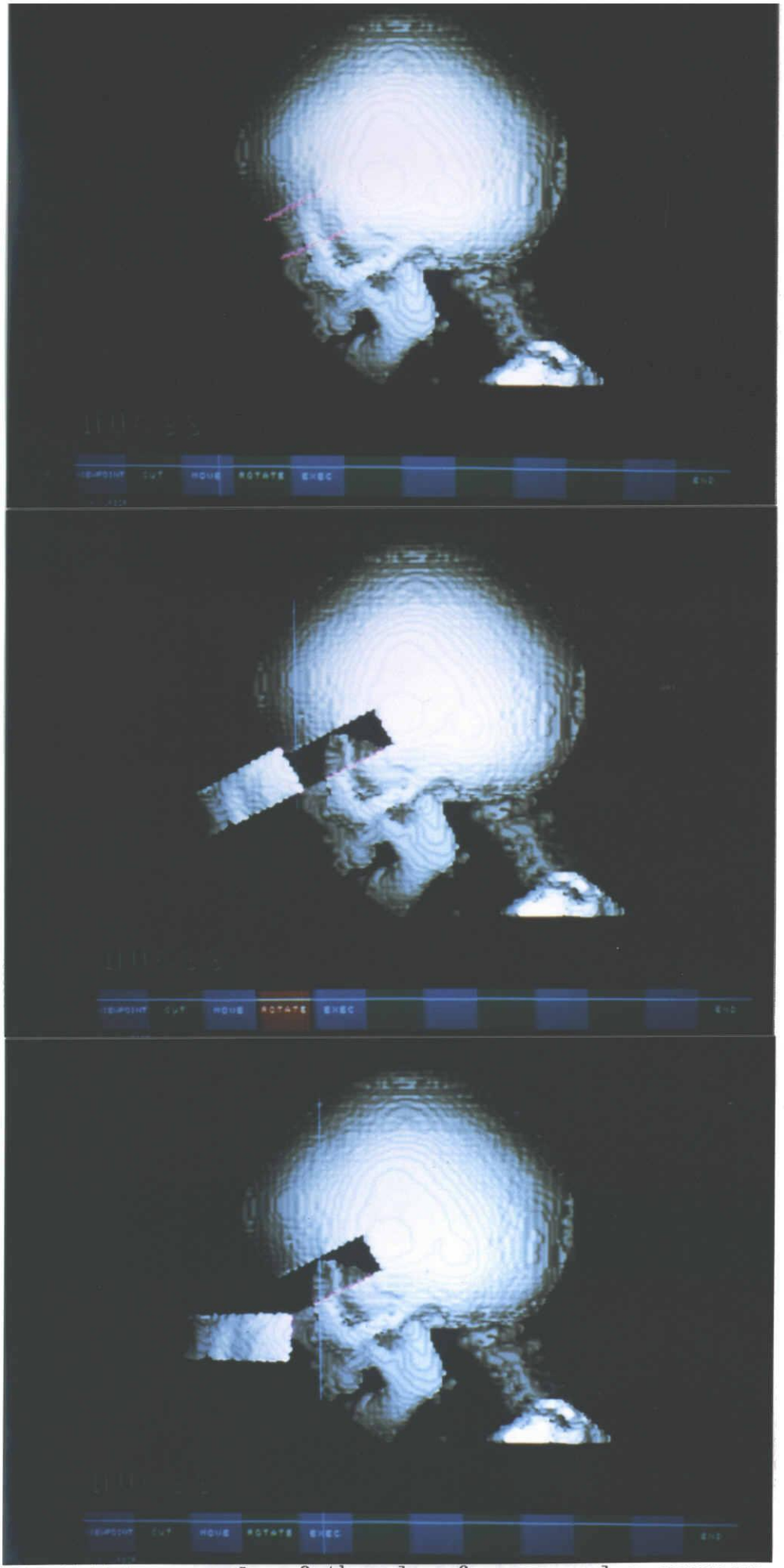

Fig.5.7 An example of the plan for a complex surgery.

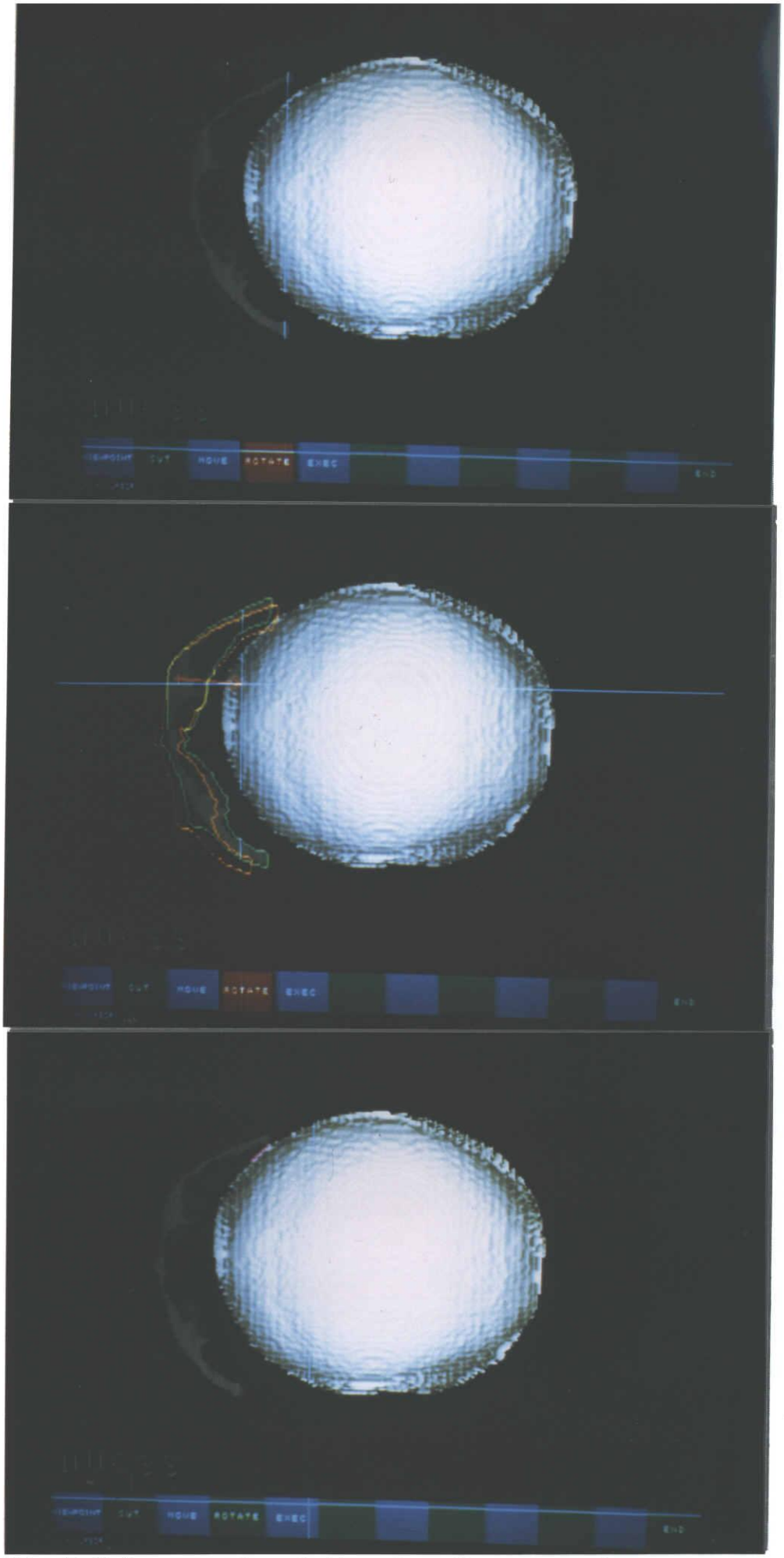

Fig.5.7 An example of the plan for a complex surgery.

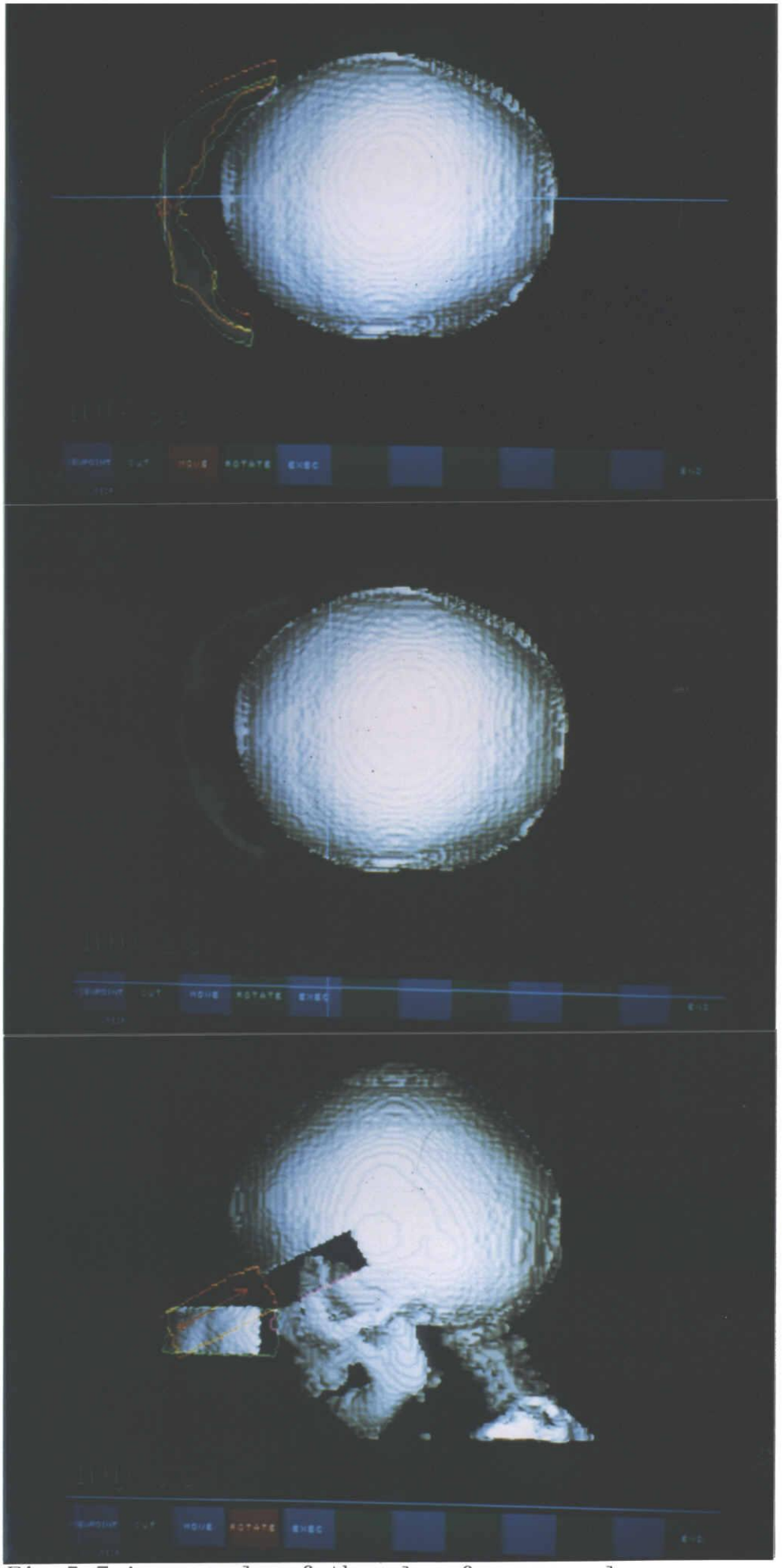

Fig.5.7 An example of the plan for a complex surgery.

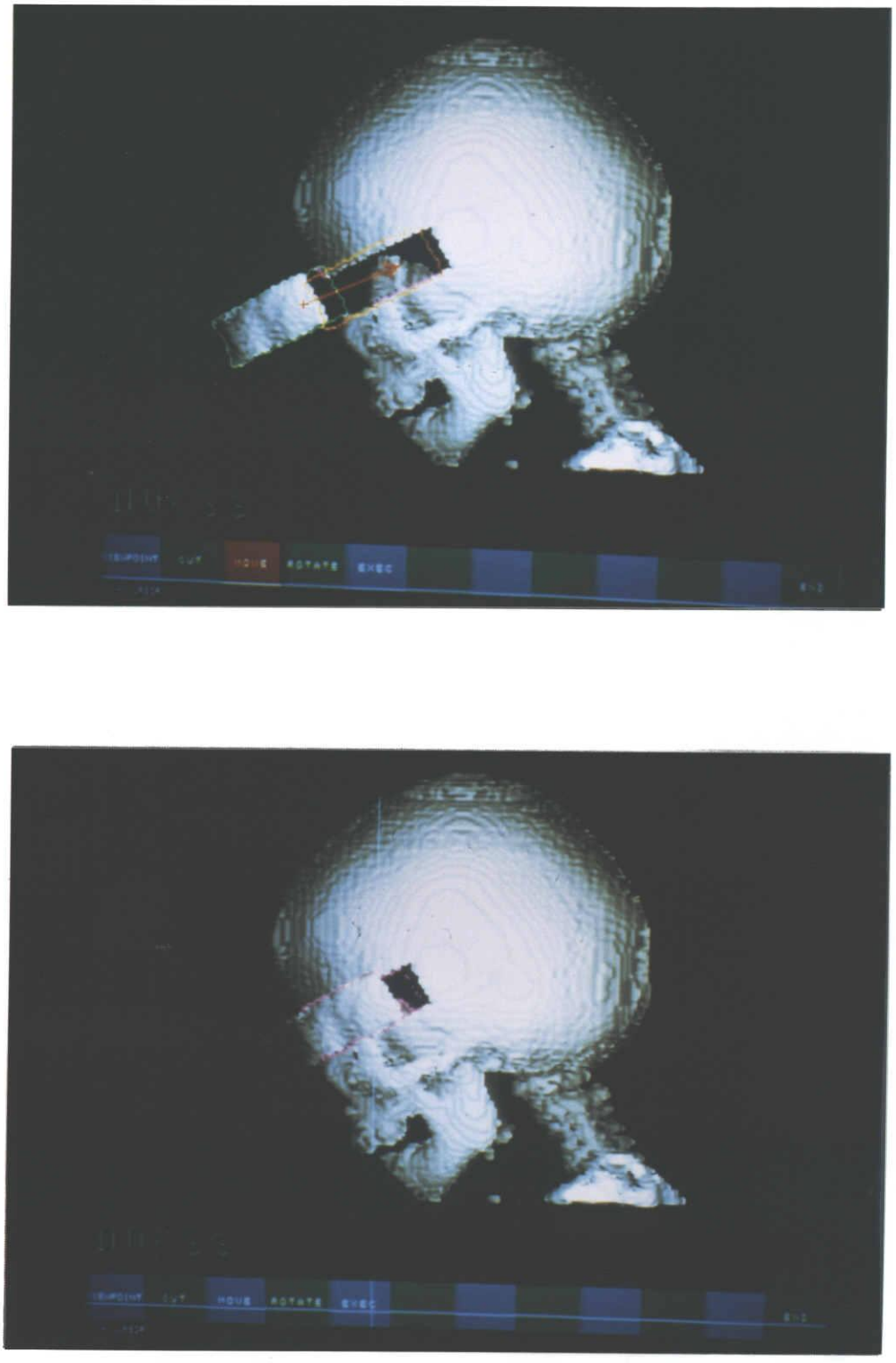

Fig.5.7 An example of the plan for a complex surgery.

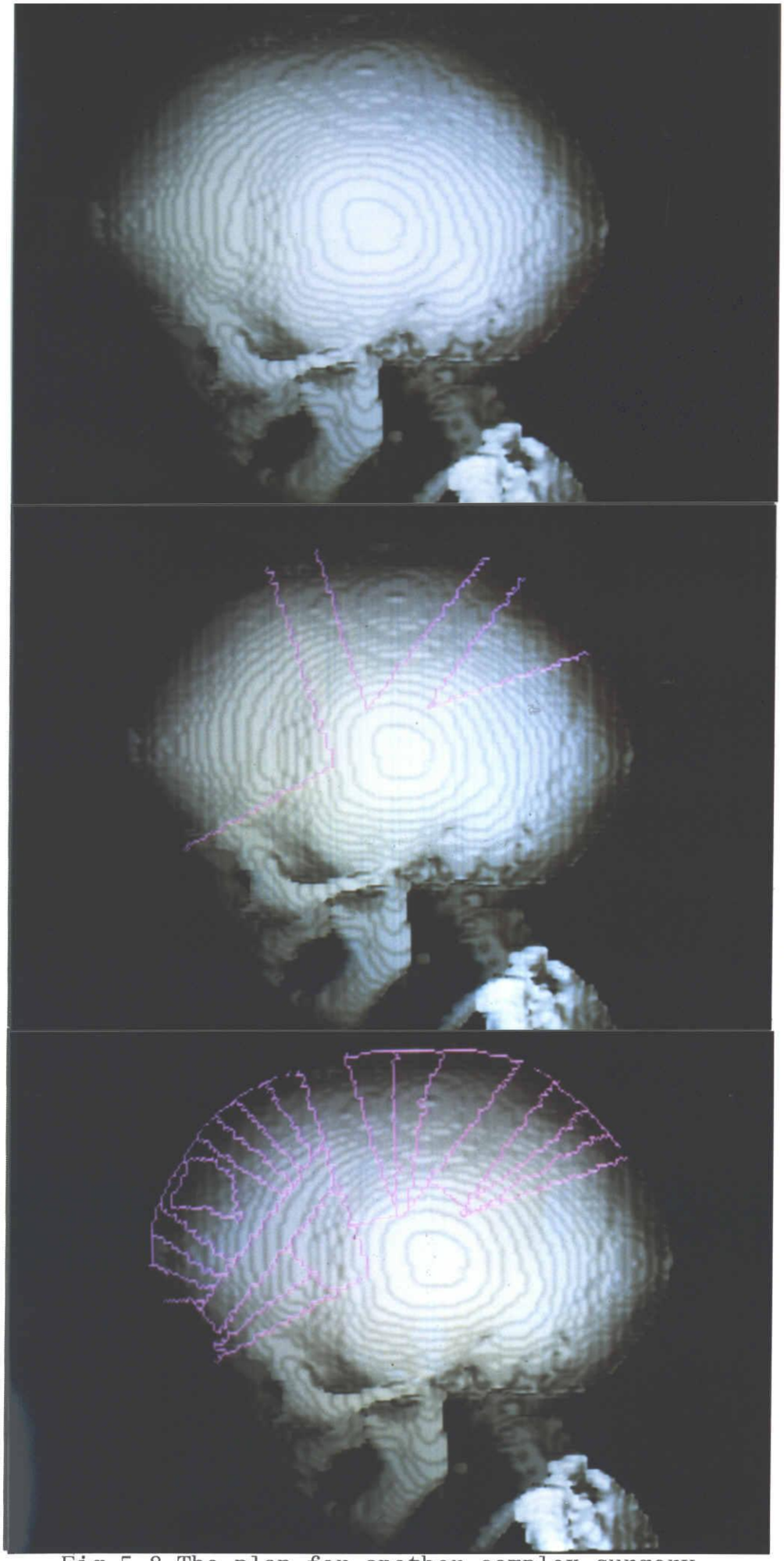

Fig.5.8 The plan for another complex surgery.

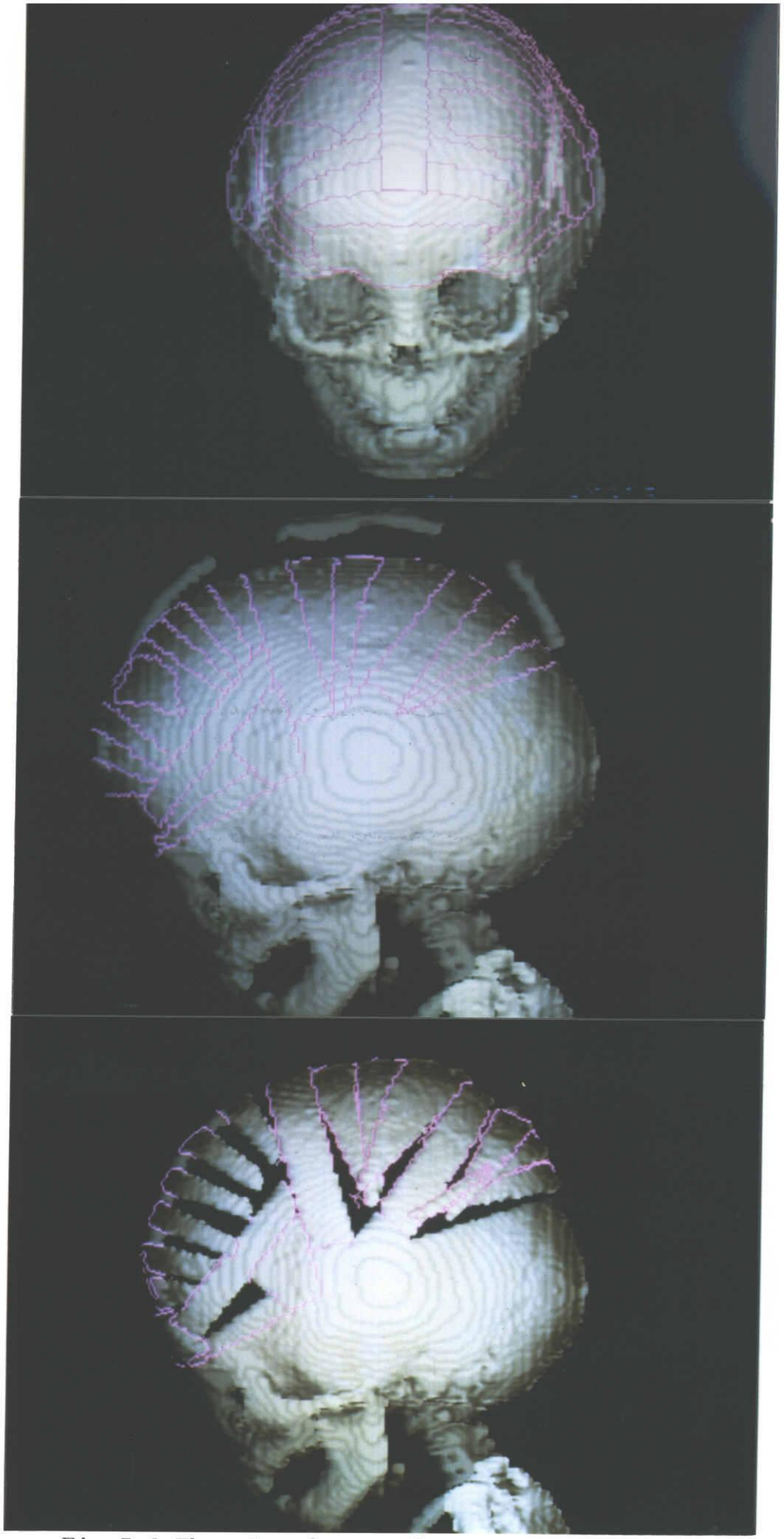

Fig.5.8 The plan for another complex surgery.

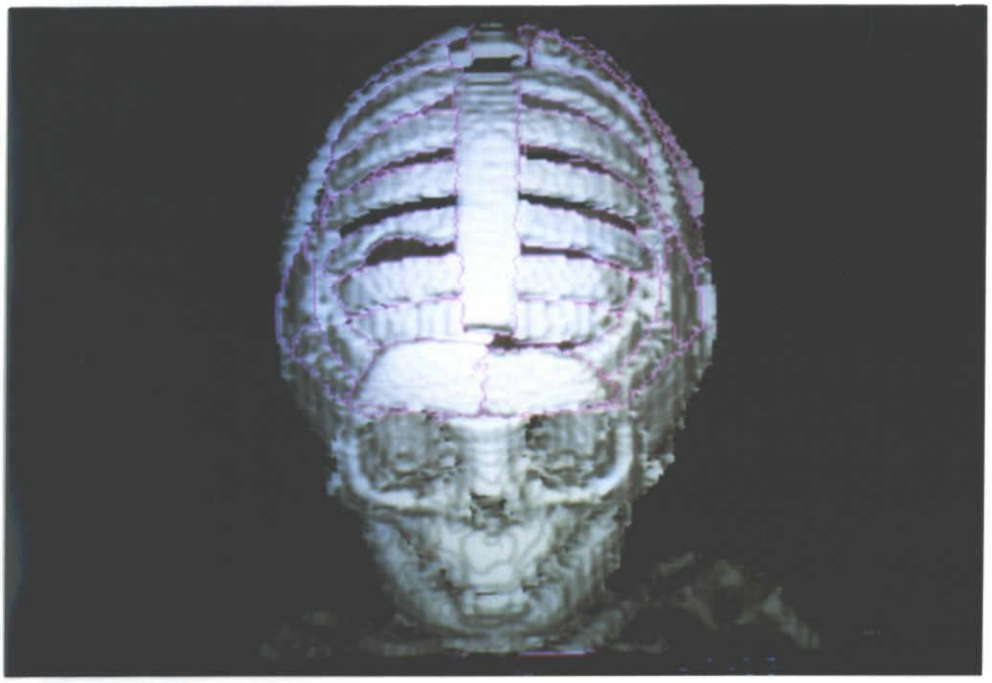

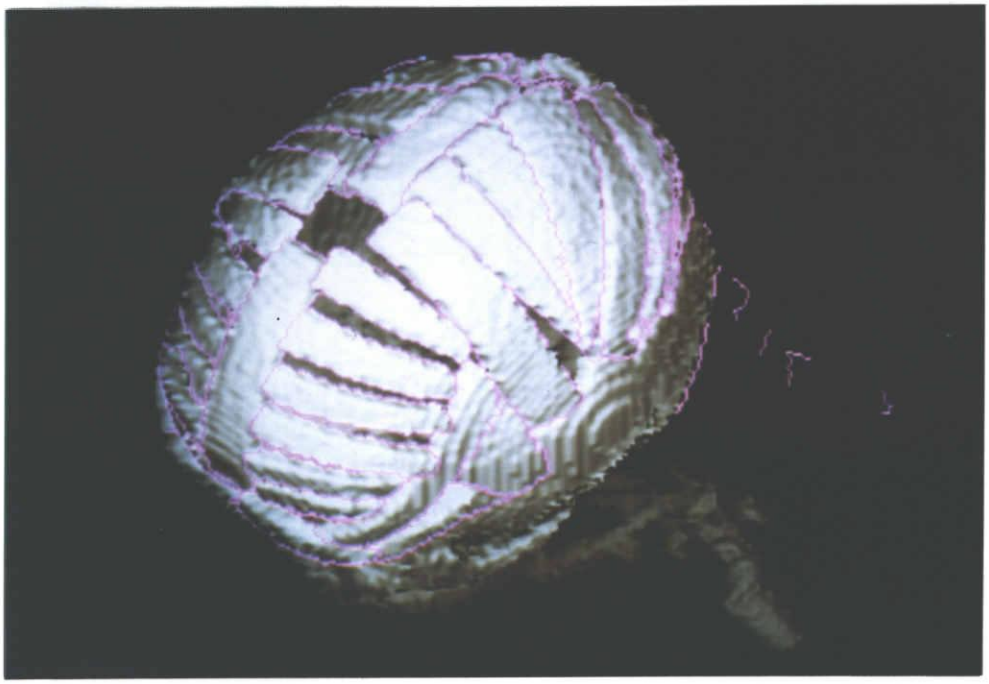

Fig.5.8 The plan for another complex surgery.

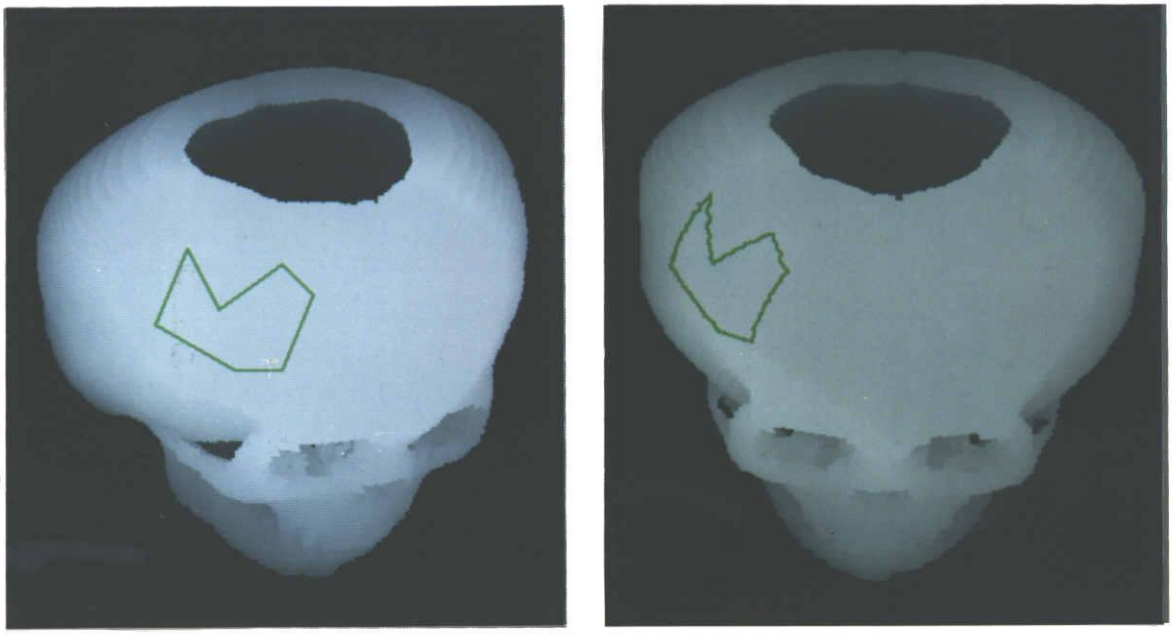

(a) Input a removal region (b) Another view of (b)

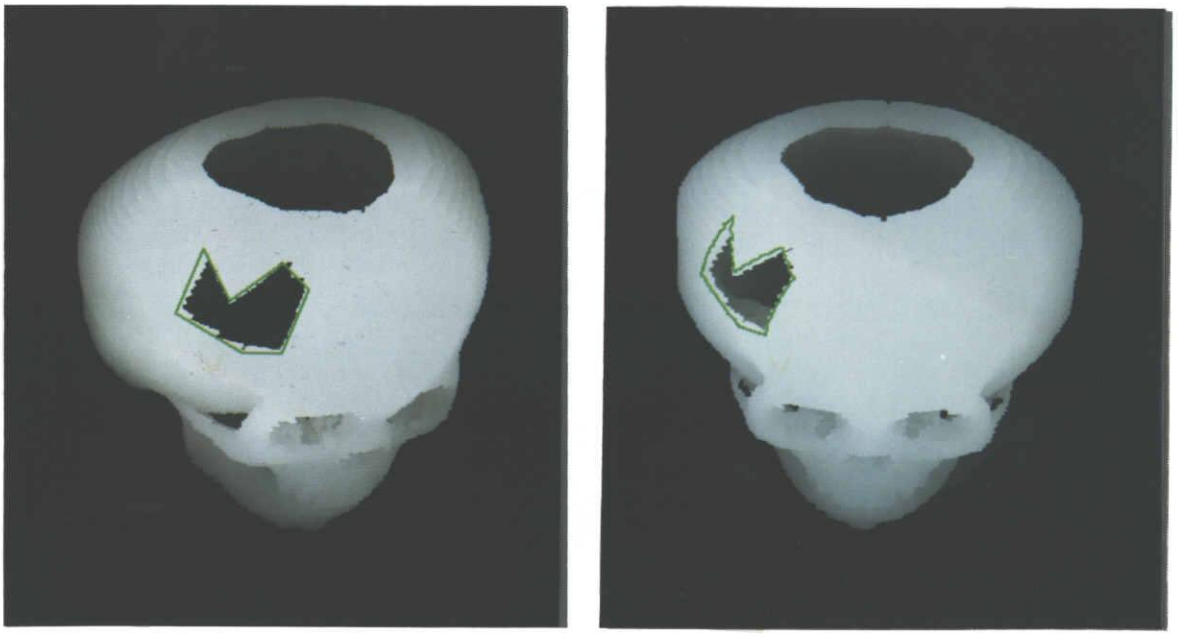

(c) Skull applied removal process (d) Another view of (c)

Fig.5.9 Removal of a polygonal bone region.

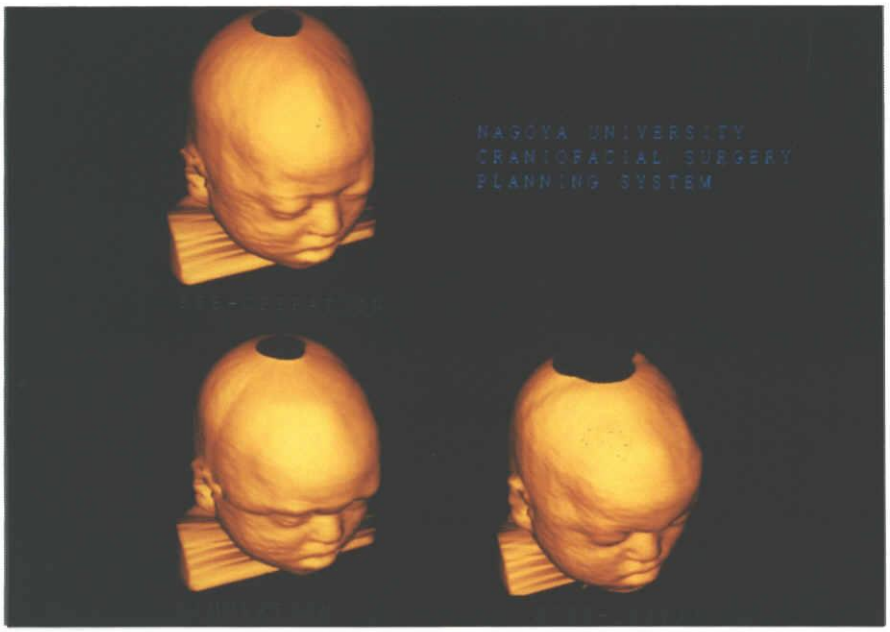

(a) Upper view

(b) Lateral view

Fig.5.10 Predicted face image generated by CCE.

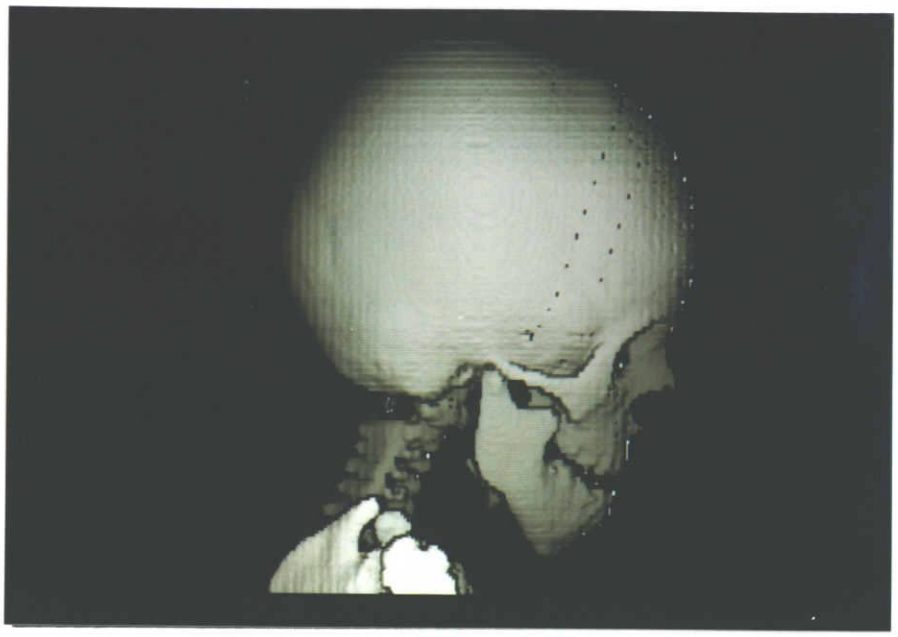

(a) Pre-operation

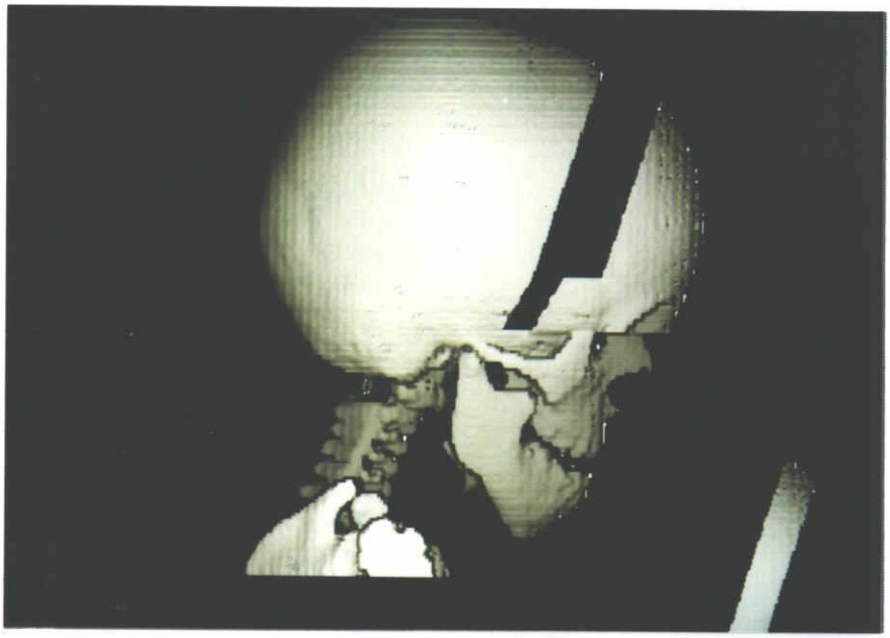

(b) Simulation

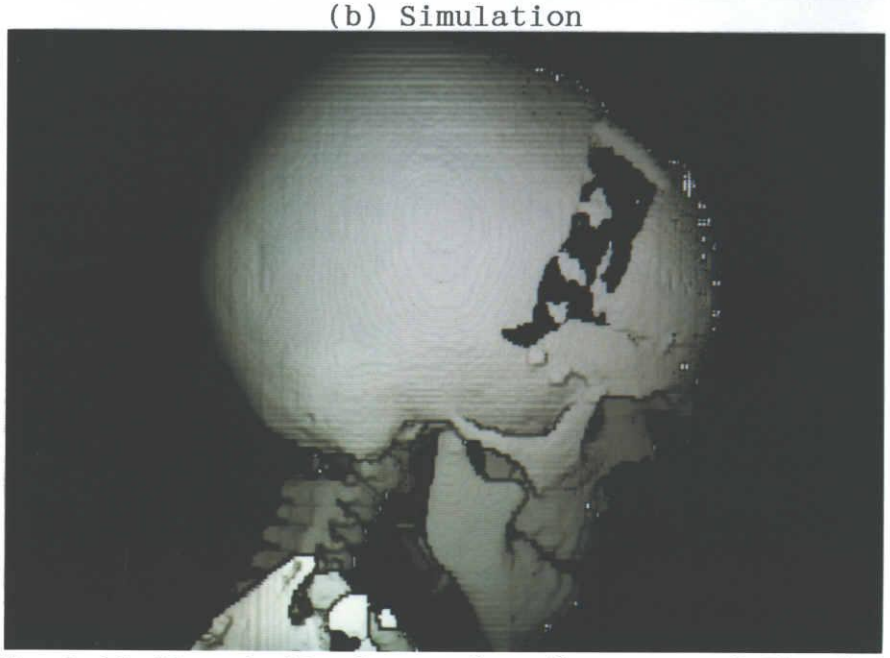

Fig.5.11 The skull shapes for the case of Fig.5.10.

(a) pre-operative(upper left) and simulated(lower left) face are generated by CCE. Voxel expression was used for generation of post-operative face

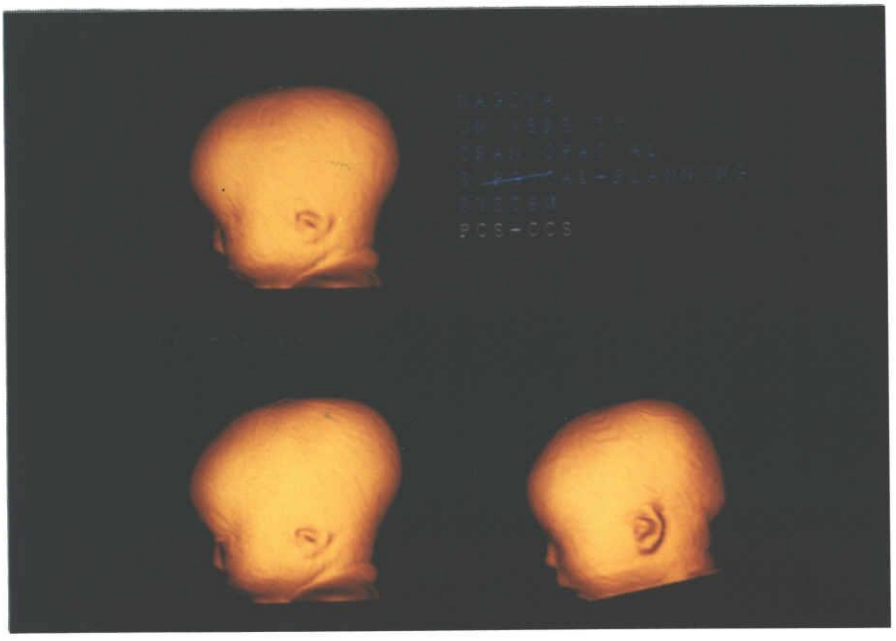

(b) Three images were generated by PCE-CCE method.

Fig. 5.12 Comparison of faces generated by three kinds of method.

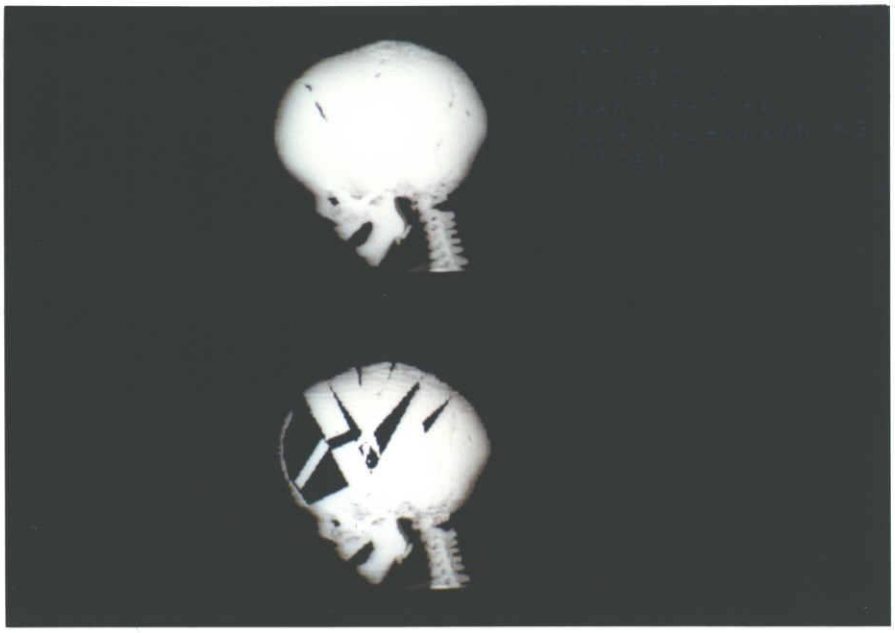

(a) Skulls of pre-operation and the simulation.

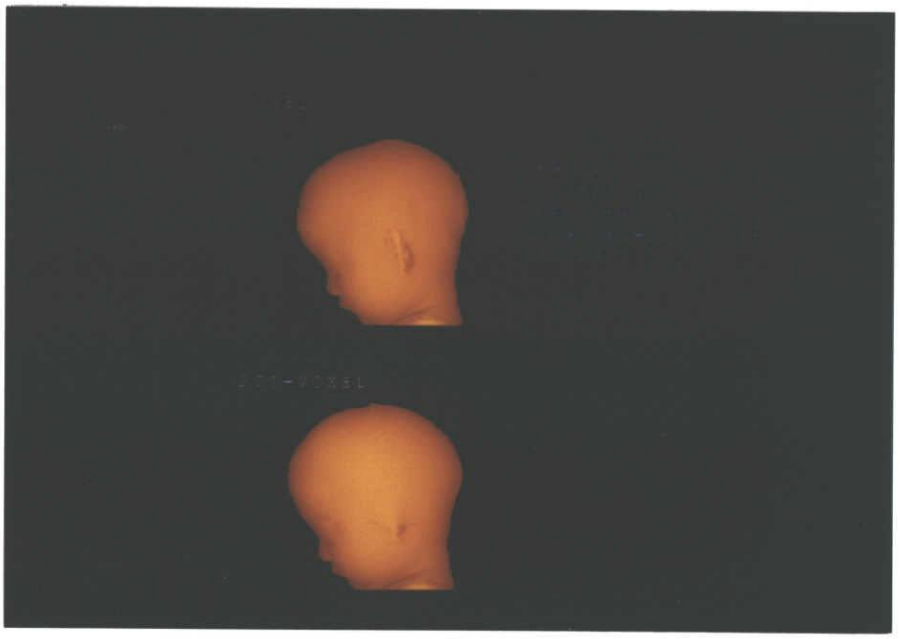

(a) Pre-operative face generated by voxel method (up)
and predicted post-operative face by PCE-voxel(down).

Fig.5.13 PCE-voxel combined method.

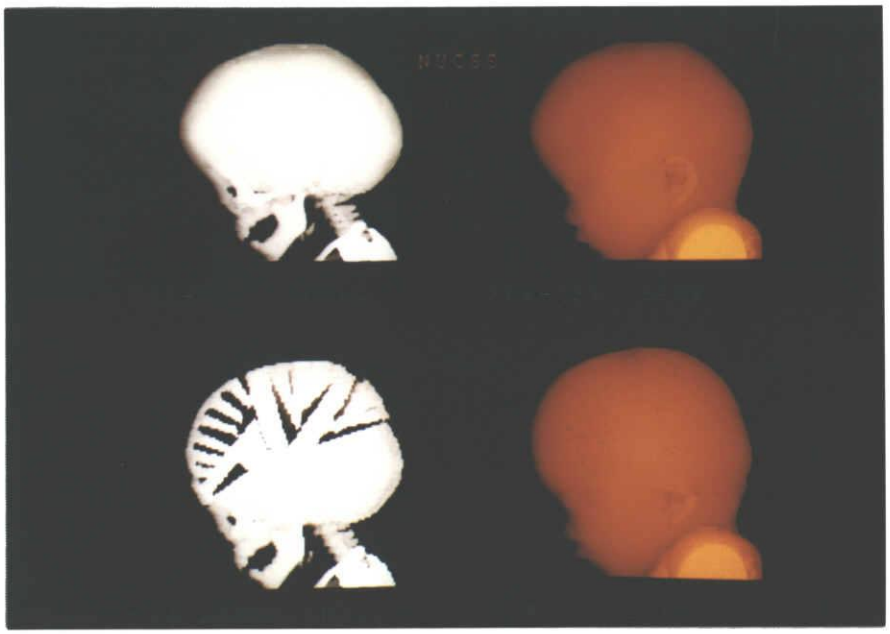

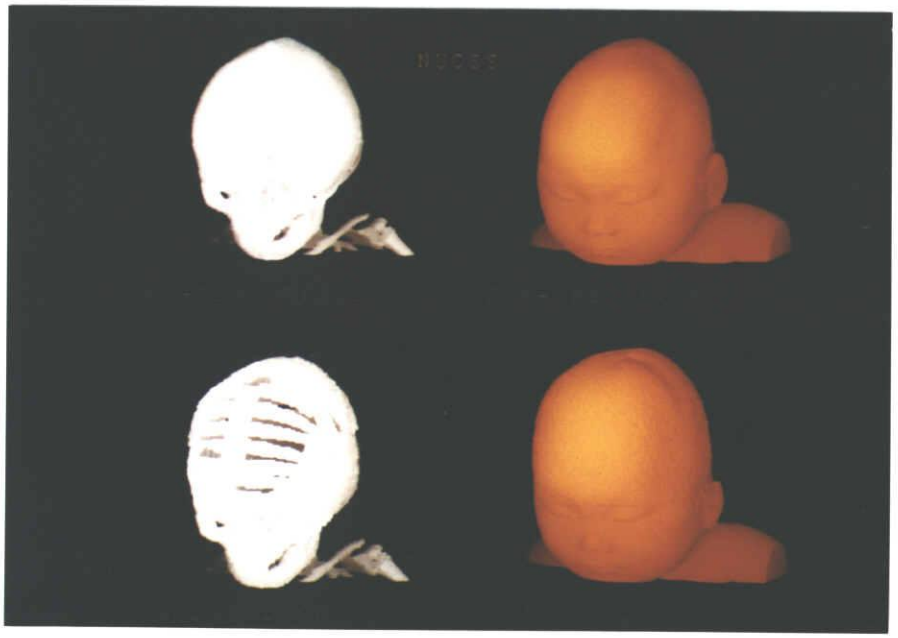

Fig.5.14 Prediction of the post-operative face shape. pre-operative skull and face (up): the simulated skull and face (down).

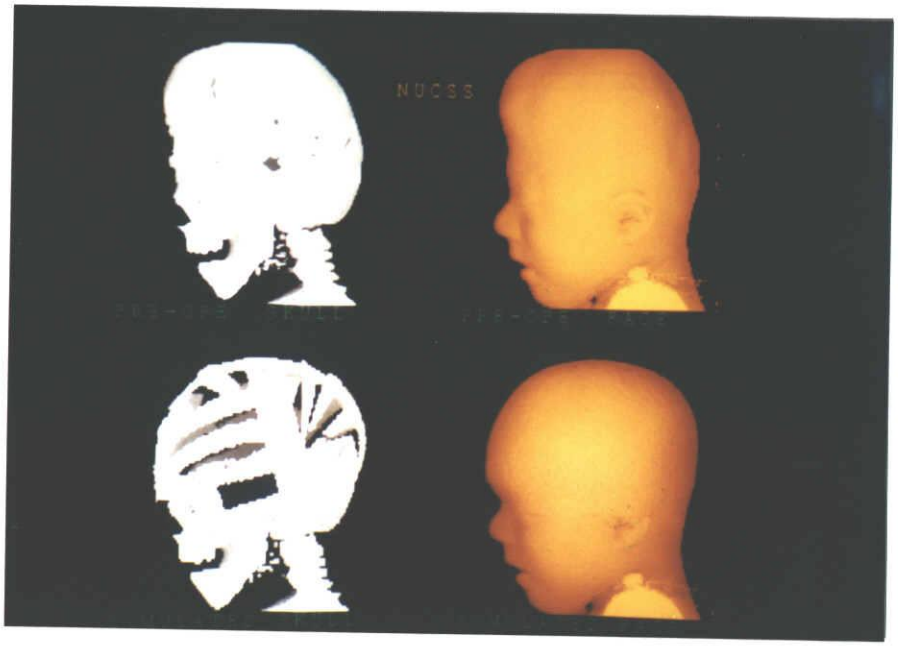

Fig.5.15 Another clinical example of the face prediction. pre-operative skull and face (up): the simulated skull and face (down).

6. CONCLUSION

In this chapter, we will summarize the contents of the paper and present problems remaining to be solved in this field.

The brief survey of the use of 3-D CT images were described in chapter 1. The background of the 3-D image generation from CT slices were also referred. Several applications of this kind of studies made it sure that 3-D reconstructions of CT images had a lot of possibilities to be used in the actual clinical medicine. This chapter also indicated where the studies in the thesis were located in the field of image processing and graphics in medicine.

In chapter 2 and 3, we described a computer system for brain surgical planning and diagnosis. Image processing techniques and computer graphics schemes greatly contributed to the system. The quality of the displayed images were not good due to the restriction of the computer system and CT machine which were available at that time. However, this system could be transfered to the recent computer system and could produce much better performance.

Another application of 3-D CT imaging to craniofacial surgery was presented in chapters 4 and 5. The simulation system NUCSS discussed there has already been proved to be quite effective in the clinical usage by surgeons who used this system to make surgical plans for about 10 cases. In NUCSS, several functions were developed to be used in routine works. In section 4.2, we showed an accelerated projection method to reduce the computation time required to generate 3-D images, since the response time of the system was one of the most important factors for making a suitable surgical plan. The prediction of the post-operative shape of the soft tissues is necessary in order to evaluate the decided plan. This kind of function was also developed in NUCSS, and the detail of the scheme was described in this chapter.

In chapter 5, we explained the function for making surgical plans by manipulating the 3-D image on the screen. Finally, in section 5.5, the experimental results on the screen were presented by showing pictures observed.

By using 3-D images reconstructed from CT slices, it is now possible to visualize human internal organs in three dimensions, to interactively manipulate them just as a surgeon would do during a surgery, and to obtain vital quantitative information about them. This dissertation described computer systems for simulation of brain surgery and craniofacial surgery. We feel the system for brain surgery would not be able to be used immediately in clinical routine works. However, it is valuable to understand the whole brain structures in three dimensions and could be used for precise diagnosis in the hospital.

For the craniofacial surgery, according to experimental usage by surgeons, the system was considered to be applicable for real operation. Especially, the followings were pointed: (1)the fundamental functions of planning in the system are enough for most of ordinary craniofacial surgeries such as the "fan technique" which enlarges the back of the head, and (2)the 3-D display of the skull transformed by the decided plan is especially useful, when surgeons can not imagine the frontal shape of bony blocks on the lateral view in the planning stage.

Possibility to apply 3-D medical images generated by computer to surgical planning as well as diagnosis was made clear in this thesis. Still, the requirements of improved techniques suitable for surgical planning exist.

First of all, it is necessary to cope with more complex surgical procedures. At the present time, manipulations are restricted to cut the image by the plane perpendicular to the screen from one direction, mainly the lateral view, or move the bony pieces on the screen plane. It could be a reasonable method to combine several manipulations which are specified from various viewing directions to make the plan for complex

surgeries.

Secondary, effective tools to manipulate 3-D data set via a view space are required. It is hard to imagine the whole shape of a 3-D. object and its location from a projected image. We are planning to develop a new software to generate two or three images viewed from different directions on the same image plane to help surgeons imagine the shape and the location of a 3-D object easily.

Finally, general sophisticated method for soft tissue prediction after bony structure correction should be developed. Although the precise prediction of. the face is difficult, a general scheme could be realized to predict the soft tissue especially for the upper part of the head. It is necessary to analyze the elastic features of muscles in order to predict the post-operative shape more exactly.

REFERENCES

Chapter 1

[1]G.N.Hounsfield , " Computerized transverse axial scanning (tomography) Part I Description of the system " , Brit. J. Radiol. , Vol.46 , pp.1016-1022 (1973).

[2]G.T.Herman and H.K.Liu , " Three-dimensional display of human organs from computed tomograms ", Computer Graphics and Image Processing , Vol.9 , pp.1-21 (1979).

[3]T.Yasuda , J.Yorozu , S.Yokoi , J.Toriwaki , and K.Katada , " Application of 3-D display of brain CT images to operation planning " , Japanese Journal of Medical Electronics and Biological Engineering , Vol.24 , pp.22-27 (1986).

[4]H.Suzuki and J.Toriwaki , " Automatic segmentation and 3-dimensional display based on the knowledge of head MRI images " , Japanese Journal of Medical Electronics and Biological Engineering , Vol.25 , pp.1-7 (1987).

[5]N.Niki, K.Higuti, and Y.Takahashi , " High-precision surface formation and the 3-D shaded display of the brain obtained from CT images",Trans. IEICE, Vol.J69-D ,pp.1518-1527 (1986).

[6]H.Oshita, S.Yokoi, J.Toriwaki, and M.Matsuo , "3-D display of magnetic resonance images by use of multiplex holography " , Japanese Journal of Medical Electronics and Biological Engineering, Vol.25, pp.61-68 (1987).

[7]S. Eiho , M. Kuwahara , T. Matsuda , and C.Kawai , " 3 - D reconstruction of the left ventricle from magnetic resonance images " , Proc. the 26th. conference of the Japan society medical electronics & biological engineering, Vol.25, pp.147-148 (1987).

[8]M.Okada , F.Kimura , S.Tsuruoka , Y.Miyake , S.Umaoka , and K.Sekioka , "Local spatial phase analysis of left ventricular wall motion using hilbert transform" , Trans. IEICE, Vol.J69-D, pp.1490-1499 (1986).

[9]M.W.Vannier, J.L.Marsh and J.O.Warren , " Three dimensional computer graphics for craniofacial surgical planning and evaluation " , Computer Graphics , Vol.17, pp.263-273 (1983).

[10]G.T.Herman , " Three dimensional imaging from tomograms ", State University of New York Technical Report No. MIPG8 (1981).
[11]H.K.Tuy and J.K.Udupa , " Representation , manipulation and display of 3 - D discrete objects " , Proc. 16th. Hawaii International Conference on System Science , Vol.II, pp.397-406 (1983).
[12]L.J.Brewster , S.S.Trivedi , H.K.Tuy , and J.K.Udupa, " Interactive surgical planning", IEEE Computer Graphics and Application, Vol.4, pp.31-40 (1984).
[13]L.L.Fellingham , J.Vogel , C.Lau , and P.Dev , " Interactive graphics and 3-D modelling for surgical planning and prosthesis and design " , Proc. NCGA , pp.132-142 (1986).
[14]T.Yasuda, Y.Hashimoto, S.Yokoi , and J.Toriwaki , " Planning support system for craniofacial surgery using CT images ", Trans. IEICE , Vol. J70-D , pp.2134 - 2140 (1987).
[15]Y.Soyama, T.Yasuda, S.Yokoi, and J.Toriwaki, " Separation of pelvis and femur in a hip joint 3-dimensionalCT image", Proc. the 27th. conference of the Japan society medical electronics & biological engineering, Vol.26 , p.427 (1988).
[16]J.W.Granholm , D.D.Robertson , P.S.Walker , and P.C.Nelson , " Computer design of custom femoral stem prostheses ", Computer Graphics & Applications , Vol.7 , pp.26-35 (1987).
[17]T.Kuno, S.Yokoi, J.Toriwaki, and S.Yasuba , " Manufacturing artificial bone model using CT image data " , IEICE Tech. Report, IE87-117, pp.1-8 (1988).
[18]N.Suzuki, M.Ito, and T.Okamura , " Morphological database of human body by computer graphics system " , Proc. the 26th. conference of the Japan society medical electronics & biological engineering , Vol.25 , p.427 (1987).

Chapter 2

[1]A.Sunguroff and D.Greenberg , " Computer generated images for medical applications " , Computer Graphics , ACM SIGGRAPH'78 Proc., pp.196-202 (1978).
[2]J.K.Udupa , " Display of 3D information in discrete 3D scenes produced by computerized tomography " , Proc. IEEE, Vol.71, 3 , pp.420-431 (1983).
[3]S.Yokoi, T.Yasuda, Y.Hashimoto and J.Toriwaki , " A

craniofacial surgical planning system " , Proc. NCGA Computer Graphics, pp.152-161 (1987).
[4]J.Toriwaki and S.Yokoi , " Algorithms for skeltonizing three-dimensional digitized binary pictures " , Proc. SPIE, Vol. 435, pp.2-9 (1983).
[5]H.Suzuki and J.Toriwaki , " Derivation of edge detection operators for 3-dimensional digital images and evaluation of their performance " , Trans. Information Processing Society, Japan, Vol. 25 , 2, pp.243-250 (1984).

Chapter 3

[1]A.Rosenfeld and A.C.Kak , " Digital picture processing, 2nd. edition " , Academic Press (1982).
[2]H.N.Christiansen and T.W.Sederberg , " Conversion of complex contour line definitions into polygonal element mosaics", Computer Graphics, Vol.12, pp.187-192 (1978).
[3]T.Yasuda , J.Toriwaki , S.Yokoi and K.Katada , " A three-dimensional display system of CT images for surgical planning " , Proc. IEEE MIII'84 , pp.322-328 (1984).
[4]H.K.Huang and R.S.Ledley , " Three - dimensional image reconstruction from in vivo consecutive transverse axial sections " , Comput. Biology Med., Vol.5 , pp.165-170 (1975).
[5]S.J.DwyerIII , " Texture analysis in diagnostic radiology ", in Digital processing of Biomedical Images , K.Preston Jr. and M.Onoe (eds.) , Univ. of Tokyo Press , pp.203-226 (1976).
[6]C.H.Lee , P.C.Hsi and J.Mozley , "Curvelinear view generation from CAT scanned data " , Proc. 6th. CCAR. , pp.81-85 (1979).
[7]M.E.Newel , R.G.Newel and T.L.Sancha , " A solution to the hidden surface problem " , Proc. ACM National Conference , pp.443-456 (1972).
[8]A.Sunguroff and D.Greenberg , " Computer generated images for medical applications " , Computer Graphics , ACM SIGGRAPH'78 Proc., pp.196-202 (1978).
[9]G.T.Herman and J.K.Udupa , " Display of 3-D digital images: computational foundations and medical applications " , IEEE Computer Graphics and Applications , Vol. 3 , 5 , pp.39-46 (1983).
[10]L.T.Cook , S.J.DwyerIII , S.Batnitzky and K.R.Lee , " A three-dimensional display system for diagnostic imaging

applications " , ibid , pp.13-19.
[11]S.Yokoi , J.Yorozu, S.Tsuruoka and Y.Miyake , " A method for three - dimensional display of CT image sequence " , Proc. MEDINFO'83 , pp.385-388 (1983).

Chapter 4

[1]M.W.Vannier , J.L.Marsh and J.O.Warren , " Three dimensional computer graphics for craniofacial surgical planning and evaluation " , Computer Graphics , Vol.17, pp.263-273 (1983).
[2]G.T.Herman , " Three dimensional imaging from tomograms " , State University of New York Technical Report No. MIPG 8 , (1981).
[3]H.K.Tuy and J.K.Udupa , " Representation , manipulation and display of 3-D discrete objects " , Proc. 16th Hawaii In ternational Conferece on System Science , II , pp. 397 - 406 , (1983).
[4]L.J.Brewster , S.S.Trivedi , H.K.Tuy and J.K.Udupa , " Interactive surgical planning" , IEEE Computer Graphics & Applications , Vol.4 , pp.31-40 (1984).
[5]L.L.Fellingham , J.Vogel , C.Lau and P.Dev , " Interactive graphics and 3 - D modeling for surgical planning and prosthesis and implant design " , Proc. NCGA Computer Graphics , pp.132-142 (1986).
[6]G.T.Herman and K.Liu , " Three dimensional display of human organs from computed tomograms ", Computer Graphics and Image Processings , Vol.9 , pp.1-21 (1979).
[7]D.Gordon and R.A.Reynolds , " Image space shading of 3-dimensional objects " , Computer Vision, Graphics & Image Process, Vol.29 , pp.361-376 (1985).
[8]S.Yokoi , J.Yorozu , S.Tsuruoka and Y.Miyake , " A method for three-dimensional display of CT image sequence ", MEDINFO-83, IFIP , pp.385-388 (1983).
[9]E.Artzy , " Display of three dimensional information in computed tomography " , Computer Graphics and Image Processing , Vol.9 , pp.196-198 (1979).
[10]G.T.Herman and J.K.Udupa , " Display of 3D discrete surfaces " , Proc. SPIE , 283 , pp. 90 - 97 (1981).
[11]G.Frieder, D.Gordon and R.A. Reynolds , " Back - to - front display of voxel-based objects " , IEEE Computer Graphics

& Appl. , Vol.5 , pp.52-60 (1985).
[12]L.Chen , G.T.Herman , R.A.Reynolds and J.K.Udupa , " Surface shading in the cuberille environment",IEEE Computer Graphics & Applications , Vol.5 , pp.33-43 (1985).
[13]S.Yokoi,T.Yasuda,Y.Hashimoto and J.Toriwaki," A craniofacial surgical planning system " , Proc. NCGA Computer Graphics , pp.152-161 (1987).
[14]M.Nagao and T.Matsuyama , " Edge preserving smoothing ", Computer Graphics and Image Processing , Vol.9 , pp.394-407 (1979).
[15]A.Rosenfeld and A.C.Kak ," Digital picture processing, 2nd. Edition. Academic Press (1982).

Chapter 5

[1]T.Yasuda, Y.Hashimoto, S.Yokoi , and J.Toriwaki , " Planning support system for craniofacial surgery using CT images ", Trans. IEICE , Vol. J70-D , pp.2134 - 2140 (1987).
[2]S.Yokoi,T.Yasuda,Y.Hashimoto and J.Toriwaki, " A craniofacial surgical planning system " , Proc. NCGA Computer Graphics , pp.152-161 (1987).
[3]T.Yasuda , S.Yokoi , J.Toriwakim M.Fujioka and H.Nakajima , " Application of 3-D brain CT image display for craniofacial operation planning ", Proc. NICOGRAPH'85 , pp.189-196 (1985).
[4]T.Yasuda , Y.Hashimoto , K.Kato , S.Yokoi and J.Toriwaki , " Advanced craniofacial surgical planning support system using computer graphics " , Proc. NICOGRAPH'88 (1988).
[5]S.S.Trivedi, G.T.Herman, J.K.Udupa P.Margasahayam and L.Chen, " Measurements on 3-D displays in the clinical environment ", Proc. NCGA Computer Graphics , pp.93-100 (1986).
[6]D.Gordon and R.A.Reynolds , " Image space shading of 3-dimensional objects " , Computer Vision , Graphics & Image Processing , Vol.29, pp.361-376 (1985).
[7]Y.Soyama, T.Yasuda, S.Yokoi and J.Toriwaki , " Development of the planning support system for orthopedic surgery of the hip joint " , Proc. Electric related joint conference at tokai branch, pp.642 (1988).
[8]M.Fujioka , H.Nakajima , S.Yokoi , T.Yasuda and J.Toriwaki , " Computer graphics simulation of craniofacial surgery " , RSNA '86 Science Exhibition (1986).

[9]D.Meagher," Efficient synthetic image generation of arbitrary 3 - D objects " , Proc. IEEE Computer Society Conference Pattern Recognition Image Processing , pp.473-478 (1982).
[10]M.L.Rhodes , J.F.Quinn and B.Rosner , " Data compression techniques for CT image archiving " , J. Computer Assisted Tomogr., Vol.7 , 6 , pp.1124-1126 (1983).
[11]S.S.Trivedi ," Representation of three-dimensional binary scenes " , Proc. NCGA Computer Graphics , pp.132-144 (1985).
[12]R.A.Reynolds , D.Gordon and L.S.Chen , " A dynamic screen technique for shaded graphics display of slice-represented objects ", Computer Vision , Graphics and Image Processing , Vol.38, pp.275-298 (1987).